University of Kerbala

College of Science

Department of Chemistry

New Chitosan and Dopamine / Hexamolybdate Nanostructures for Drug Delivery

A Thesis

Submitted to the Council of the College of Science/University of Kerbala
as a Partial Fulfillment of the Requirements for the Degree of Master of Science in Chemistry

By

Mariam Radhi Kadhim

B.Sc. in Chemistry (2017) / University of Kerbala

Supervised by

Assist. Prof. Dr. Ahmed AL -Yasari
and
Assist. Prof. Dr. Ihsan AL -Dahhan

July 2024 AD **Muharram 1446 AH**

بسم الله الرحمن الرحيم

﴿وَنُرِيدُ أَن نَّمُنَّ عَلَى الَّذِينَ اسْتُضْعِفُوا فِي الْأَرْضِ وَنَجْعَلَهُمْ أَئِمَّةً وَنَجْعَلَهُمُ الْوَارِثِينَ﴾

صدق الله العلي العظيم

سورة القصص الآية (5)

Report of the Head of the Chemistry Department

According to the recommendation presented by the Chairman of the Postgraduate Studies Committee, 1 forward this thesis " New Chitosan and Dopamin / Hexamolybdate Nanostructures for Drug Delivery.

Kerbala University
Science College
Asst. Prof. Dr. Thaer M. M. Al-Rammahi
Head of Chemistry Department

Signature:

Assist. Prof. **Dr. Thaer Mahdi Madlool**

Head of Chemistry Department

Address: University of Kerbala, College of Science, Department of Chemistry

Date: 30 / 6 / 2024

Supervisor Certification

We certify that this thesis " New Chitosan and Dopamin / Hexamolybdate Nanostructures for Drug Delivery " was conducted under our supervision at the Chemistry Department, College of Science, University Karbala, as a partial requirement for the degree of Master of Science in Chemistry.

Signature:
Name:
Assist. Prof. Dr. Ahmed Hadi AL-Yasari
Title:
Assist. Prof.
Address:
University of Kerbala,
College of Sciences ,
Department of Chemistry

Date: / / 2024

Signature:
Name:
Assist. Prof. Dr. Ihsan Mahdi AL-Dahhan
Title:
Assist. Prof.
Address:
University of Kerbala,
College of Sciences ,
Department of Chemistry

Date: / / 2024

Examination Committee Certification

We certify that we have read this entitled " New Chitosan and Dopamin / Hexamolybdate Nanostructures for Drug Delivery " as the examining committee, examined the student "Mariam Radhi Kadhum " on its contents, and that in our opinion, its adequate for the partial fulfillment of the requirements for the Degree of Master in science of chemistry

Signature:
Name: Dr. Eman Talib Kareem
Title: Professor
Address: University of Kerbala, College of Science, Department of Chemistry.
Date: / / 2024
(Chairman)

Signature:
Name: Dr. Sajid Hassan Guzar
Title: Professor
Address: University of Kerbala, College of Science, Department of Chemistry.
Date: / / 2024
(Member)

Signature:
Name: Dr. Hussein Enaya Sharhan
Title: Assistant Prof
Address: University of Al-Mustansiriya, College of Science, Department of Chemistry.
Date: / / 2024
(Member)

Signature:
Name: Dr. Ihsan Mahdi Al-Dahhan
Title: Assistant Prof
Address: University of Kerbala, College of Science, Department of Chemistry.
Date: / / 2024
(Member & supervisor)

Signature:
Name: Dr. Ahmed Hadi Al-Yasari
Title: Assistant Prof
Address: University of Kerbala, College of Science, Department of Chemistry.
Date: / / 2024
(Member & supervisor)

Approved by the council of the College of Science

Signature:
Name: Dr. Hassan Jameel Al-Fatlawy
Title: Professor
Address: Dean of College of Science, University of Kerbala.
Date: / / 2024

Dedication

To who turned adversity into a grant... Allah

To the savior of the world's injustice... Imam Mehdi.

To the holy blood... The martyrs of Iraq.

To our angels in life... our parents.

To the roses blooming in the hardest days... our brothers and sisters.

To encourage us and helped us the length of our life scholastic … All teachers and our friends.

Dedicate this work with our love and gratitude.

Mariam

Acknowledgments

In the name of Allah, the most merciful, the most compassionate, First and foremost, we must acknowledge our limitless thanks to Allah the almighty for his help and blessings, which we are sure that without his guidance this work has never become truth.

We would like to express our special thanks of gratitude to our supervisor Assist. Prof. **Dr. Ahmed AL-Yasari** and Assist. Prof. **Dr. Ihsan AL-Dahhan** for their valuable advances, keen interest, and support during the whole period of the study and especially for their patience and guidance through the writing process. We would like to express ours appreciate to the dean of the college and the head of the department for their support to perform this work.

Mariam

Supervisor Certification

I certify that this thesis was prepared by **Mariam Radhi Kadhum** my supervision at the Chemistry Department, College of Science, University Karbala, as a partial requirement for the degree of Master of Science in Chemistry.

Signature:
Name:
Assist. Prof. Dr. Ahmed AL-Yasari
Title:
Assist. Prof.
Address:
University of Kerbala,
College of Sciences ,
Department of Chemistry

Date: / / 2024

Signature:
Name:
Assist. Prof. Dr. Ihsan AL-Dahhan
Title:
Assist. Prof.
Address:
University of Kerbala,
College of Sciences ,
Department of Chemistry

Date: / / 2024

Abstract

This study examined the self-assembly of organic-inorganic hybrids using polyoxometalate (POM) Lindqvist-type hexamolybdate and dopamine/chitosan to synthesize novel three-dimension (3D) nanostructures. These nanostructures were then investigated for their suitability as nanocarriers for the chemotherapy drug temozolomide (TMZ). The release of TMZ from the nanocarrier was studied under various pH conditions.

This study comprises two practical components. The first part focuses on synthesizing hierarchical nanostructures specifically designed to load TMZ drug. The amount of drug loaded onto the as-prepared nanostructure of POM-Dopamine/Chitosan was determined using high performance liquid chromatography (HPLC) at various loading times The second part of the study investigates the release process of the TMZ drug from the hierarchical nanostructures. This release process is examined in the presence of two buffer solutions with distinct pH values. The buffers utilized are phosphate-buffered saline (PBS) with a pH of 7.4 and glycine-HCl with a pH of 2.8. The surface characteristics, size, chemical composition, and identity of the nanostructures were analyzed using techniques such as high-performance liquid chromatography (HPLC), Fourier Transform Infrared Spectroscopy (FT-IR), X-Ray Diffraction (XRD), Scanning Electron Microscopy (SEM), Atomic Force Microscopy (AFM), X-Ray Photoelectron Spectroscopy (XPS). The nanocarriers demonstrated an intriguing pH-dependent release behavior, suggesting their potential application in drug delivery systems. Finally, this study showed successfully prepared new nanocarriers of dopamine/chitosan and POM loaded with TMZ via self-assembly as a means of oral drug delivery.

Table of Contents

Contents		Pages
Abstract		I
Contents		II
List of Tables		V
List of Figures		VI
List of Abbreviations and Symbols		X
CHAPTER ONE: INTRODUCTION		
1.	Introduction	1
1.1.	General Introduction	1
1.2.	Nanotechnology	2
1.2.1.	Approaches for synthesis of nanomaterial	4
1.2.2.	Nanotechnology in medicine	5
1.2.3.	Nanocarrier	6
1.3.	Drug delivery system (DDS)	9
1.4.	Modified drug delivery system	13
1.5.	Drug loading techniques	13
1.6.	Controlled drug delivery system (CDDS)	14
1.7.	Self-assembly method	16
1.8.	Polyoxometalate (POM)	19
1.8.1.	Structures and types of POMs	20
1.8.2.	Review of synthesis of inorganic organic hybrid POM compound	22
1.9.	Dopamine (DA)	24
1.9.1.	Physical and chemical properties of dopamine	26
1.9.2	Application of dopamine	27
1.10.	Chitosan	28

1.10.1.	Physical and chemical properties of Chitosan	30
1.10.2.	Application of chitosan based on nanocomposite	31
1.11.	Temozolomide	32
1.11.1.	Mechanism of Action to Temozolomide	33
1.11.2.	Physical and chemical properties of Temozolomide	34
1.12.	Chromatography	35
1.12.1.	Classification of chromatography	36
1.12.2.	High performance liquid chromatography (HPLC)	37
1.12.2.1.	Instrumentation of HPLC	38
1.12.2.2.	Type of mode in HPLC	40
1.12.2.3.	HPLC description	40
1.13.	The aim of the work	42
CHAPTER TWO: EXPERIMENTAL		
2.1.	Chemicals	43
2.2.	Instruments	44
2.3.	Methodologies	45
2.3.1	Preparation of chemical solution	45
2.3.1.1.	Phosphate buffer saline (PBS)	45
2.3.1.2.	Preparation of Tris-HCl solution	45
2.3.1.3.	Acetic acid solution	45
2.3.1.4.	Chitosan solution	45
2.3.1.5.	Dopamine solution	45
2.3.1.6.	Phospho tungstic acid (PTA)	45
2.3.2.	Synthesis of hierarchical nano-structure	45
2.3.2.1	Synthesis of A, as -Prepared nanostructure	46
2.3.2.2.	Synthesis of B, as- Prepared nanostructure	47
2.3.3.	Drug loading into as-prepared nano-structure	48

2.3.4.	In vitro release of temozolomide loaded on as-prepared nanostructures	49
CHAPTER THREE: RESULTS AND DISCUSSION		
3.1.	Characterization of nanostructures before and after drug loading	51
3.1.1.	Fourier Transform Infrared Spectroscopy (FTIR)	51
3.1.1.1.	Fourier Transform Infrared (FTIR) Spectra of DA, POM, Chitosan and Temozolomide	51
3.1.1.2.	Fourier Transform Infrared (FTIR) Spectra of POM -dopamine nano-composite prior and after loaded with TMZ	54
3.1.1.3.	Fourier Transform Infrared (FTIR) Spectra of POM -Chitosan nano-composite prior and after loaded with TMZ	55
3.1.2.	X-Ray Diffraction (XRD)	57
3.1.2.1.	X-Ray Diffraction (XRD) for compound A	57
3.1.2.2.	X-Ray Diffraction (XRD) for compound B	61
3.1.3.	Scanning Electron Microscopy (SEM)	64
3.1.3.1	Scanning Electron Microscopy (SEM) and (EDX) analysis of the POM – DA as-prepared nano-structures prior and after loading with TMZ	64
3.1.3.2.	Scanning Electron Microscopy (SEM) and (EDX) analysis of the POM – Chitosan as-prepared nano-structures prior and after loading with TMZ	66
3.1.4.	Atomic Force Microscopy (AFM)	69
3.1.4.1	Atomic Force Microscopy (AFM) of the POM – DA as-prepared nano-structures prior and after loading with TMZ	69
3.1.4.2.	Atomic Force Microscopy (AFM) of the POM – Chitosan as-prepared nano-structures prior and after loading with TMZ	71
3.1.5.	X-Ray Photoelectron Spectroscopy (XPS)	72

3.1.5.1	X-Ray Photoelectron Spectroscopy (XPS) for POM – DA as-prepared nano-structures prior and after loading with TMZ	72
3.1.5.2	X-Ray Photoelectron Spectroscopy (XPS) for POM – Chitosan as-prepared nano-structures prior and after loading with TMZ	74
3.2.	Calibration curve of temozolomide	75
3.3.	Optimization of HPLC	76
3.4.	Release behavior of TMZ loaded onto as-prepared nanostructures	77
3.4.1	Release behavior of TMZ loaded onto POM – DA as-prepared nanostructures	77
3.4.2.	Release behavior of TMZ loaded onto POM -Chitosan as-prepared nanostructures	79
3.5.	Conclusion	81
3.6.	Future Works	82
3.7.	References	83

List of Tables

No.	*List of Tables*	Pages
1-1	provides the terminology related to nanomaterials with their definitions and explanations	3
2-1	The chemicals that used in this work	43
2-2	illustrated the instruments that used in this study	44
3-1	The difference in the interplanar spacing (d) before the process of loading and after using for TMZ	58
3-2	The difference in the interplanar spacing (d) before the process of loading and after using for TMZ3	61
3-3	demonstrated the major surface characteristics of the as-prepared nanostructures POM-DA prior and after loaded with TMZ	70

3-4	demonstrated the major surface characteristics of the as-prepared nanostructures POM-Chitosan prior and after loaded with TMZ	71
3-5	Chromatographic conditions	77
3-6	Result of drug loading	77

List of Figures

No.	List of Figures	Pages
1-1	Approach of synthesis of nanomaterials by top-down and bottom-up methods	4
1-2	The benefit of nano-technology in the medical field	5
1-3	targeted nanodrug delivery systems	6
1-4	Some common examples of nanocarriers in drug delivery system	7
1-5	The advantages of nanocarriers	8
1-6	Features taken into consideration when constructing nanocarriers	8
1-7	The history of medication delivery technology from 1950 to the present and the technologies that will be needed in the future	12
1-8	Advantages of controlled drugs delivery system	15
1-9	drug concentration in blood in (a) traditional drug dose, and (b) control drug delivery dose	16
1-10	The forces which involve in self-assembly	17
1-11	Conceptual scheme indicating the main stages of the self-assembly process in nanoscience	18
1-12	Structures of some archetypical POM clusters	19
1-13	Structure of hexamolybdate	21
1-14	The chemical structure of dopamine	24

1-15	Dopaminergic routes the dopamine biosynthesis, metabolism, and redox pathways	25
1-16	diagrammatic illustration of chemical and physical properties of dopamine	26
1-17	The possible application of dopamine	27
1-18	show (A) Chitosan chemical structure. (B) Chitosan from chitin by deacetylation	28
1-19	Explained the functional groups in chitosan's structure that are able to be chemically modified	29
1-20	diagrammatic illustration of chemical and physical properties of chitosan	30
1-21	Application of chitosan based on bio nano-composites	32
1-22	Chemical structures of temozolomide	33
1-23	Schematic representation of mechanisms of cytotoxicity of temozolomide	33
1-24	diagrammatic explanation of physical and chemical properties of temozolomide	35
1-25	Schematic representation of some types of chromatography	36
1-26	Diagram showing components of a typical apparatus for HPLC system	39
2-1	schematic diagram of synthesis of A, nano-structure	46
2-2	schematic diagram of synthesis of B nano-structure	47
2-3	The UV-Visible scan for temozolomide.	48
2-4	Temozolomide drug loading on nano composite (A , B)	49

2-5	In vitro release of temozolomide loaded on as prepared nanostructures	50
3-1	FTIR spectrum of dopamine	51
3-2	FTIR spectrum of hexamolybdate	52
3-3	FTIR spectrum of chitosan	53
3-4	FTIR spectrum of Temozolomide	53
3-5	The FTIR spectra of POM-dopamine nano-composite (A) prior to loaded with TMZ, and (B) after loaded with TMZ	55
3-6	The FTIR spectra of POM-Chitosan nano-composite (A) prior to loaded with TMZ, and (B) after loaded with TMZ.	56
3-7	XRD patterns of (1) POM hexamolybedate, (2) dopamine, (3)the as-prepared nanostructure prior to loading with TMZ and (4) the as-prepared nanostructure after loading with TMZ	60
3-8	XRD patterns of (1) POM hexamolybedate, (2)chitosan, (3)the as-prepared nanostructure prior to loading with TMZ and (4) the as-prepared nanostructure after loading with TMZ	63
3-9	SEM images of the POM-DA as-prepared nanostructures prior to loading with TMZ.	65
3-10	SEM images of the POM-DA as-prepared nanostructures after loading with TMZ	65
3-11	the EDX analysis of the (A) POM-DA as-prepared nanostructures prior to loading with TMZ (B) POM-DA as-prepared nanostructures after loading with TMZ	66
3-12	SEM images of the POM-Chitosan as-prepared nanostructures prior to loading with TMZ	67

3-13	SEM images of the POM -Chitosan as-prepared nanostructures after loading with TMZ	68
3-14	the EDX analysis of the (A) POM-Chitosan as-prepared nanostructures prior to loading with TMZ (B) POM- Chitosan as-prepared nanostructures after loading with TMZ	69
3-15	AFM images of (A) the POM-DA as-prepared nanostructure before loading with TMZ (B) The POM-DA as-prepared nanostructure after loading with TMZ	70
3-16	AFM images of (A) the POM-chitosan as-prepared nanostructure before loading with TMZ (B) The POM-chitosan as-prepared nanostructure after loading with TMZ	72
3-17	X-Ray photoelectron spectra of: (a) the as-prepared POM-DA nanostructure prior to loading with TMZ; and (b) the as-prepared POM-DA nanostructure after loading with TMZ	73
3-18	X-Ray photoelectron spectra of: (a) the as-prepared POM-Chitosan nanostructure prior to loading with TMZ; and (b) the as-prepared POM-Chitosan nanostructure after loading with TMZ	75
3-19	HPLC Calibration curve of Temozolomide	76
3-20	Release behavior of TMZ loaded onto nanostructures at pH 7.4 (blue) and pH 2.8 (black)	78
3-21	Release behavior of TMZ loaded onto nanostructures at pH 7.4 (blue) and pH 2.8 (black)	80

List of Abbreviations and Symbols

List of Abbreviations and Symbols	
Abbreviations and Symbols	The Meaning
AFM	Atomic Force microscopy
A	Nano-composite (hexamolybedate + dopamine)
ACN	Acetonitrile
Abs	Absorbance
B	Nano-composite (hexamolybedate + chitosan)
Chit	Chitosan
CDDS	Controlled Drug Delivery system
DA	Dopamine
DDS	Drug Delivery system
D.W	Distal Water
EDX	Energy Dispersive X-Ray Spectroscopy
FTIR	Fourier Transformation Infrared
FDA	Food and Drug Administration
HPLC	High Performance Liquid Chromatography
HCL	Hydrochloric Acid
NP-HPLC	Normal Phase High Performance Liquid Chromatography
POM	Polyoxometale
PBS	Phosphate Buffer Saline
PTA	Phosphotungstic Acid
RP-HPLC	Reverse phase High Performance Liquid Chromatography
SEM	Scan electron microscopy
TMZ	Temozolomide
T%	Transmission
UV-Vis	Ultraviolet Visible
XRD	X-Ray Diffraction
α	Absorbance Coefficient

β	Full Half-Maximum Intensity Width (FWHM) in Degrees
θ	Bragg Angle
λ	Wavelength in nm

Chapter One
Introduction

1. Introduction

1.1 General Introduction

In the past few decades, there have been improvements in delivery of medically important drugs ,through the development of controlled release dosage forms. There are two different types of medication release patterns: those with a rapid initial dose preceded by a gradual zero or first-order maintained component release. Controlled release systems are designed to maintain medication levels in the bloodstream or target tissues for as long as possible.[1] . This is possible by using nanotechnology to build new nanostructures with a variety of improved features. Due to their distinct characteristics and myriad possible uses, nanostructures have gained increased attention in recent years. Materials that are biological, electrical, magnetic, opto-electronic, and catalytic [2] .

Nanotechnology has the potential to create superior medicine delivery methods for disease prevention and treatment by modifying the characteristics of substances like polymers and creating nanostructures. Drug delivery methods made of nanostructures have a number of advantages over conventional delivery systems. There has been discussion on the benefits of nanostructures in drug delivery. Drug delivery nanostructures such as liposomes, nano capsules, nano emulsions, solid lipid nanoparticles, dendrimers, and polymeric nanoparticles have yielded numerous benefits. The materials used to generate nanostructures dictate the type of nanostructures that are developed, and these nanostructures determine the many attributes that are created as well as the characteristics of how pharmaceuticals placed within them are released [3] .

Self-assembly is gaining popularity as an effective bottom-up technique in advanced nanotechnology for developing new useable nanomaterials by connecting multiple components[4]. Electrostatic interactions between cations and anions, often known as ionic self-assembly (ISA), are common and essential for the development of distinctive nanostructures[5] .

Electro-optical materials, nano-reactors, and catalysis science, hybrid nanomaterials, have been intensively researched and used in drug and gene delivery due to their well-controlled shapes, well-defined sizes, and promising capabilities[6]. Because of their diverse electrical, magnetic, photochemical, biological, and catalytic capabilities, they have received interest as ideal inorganic precursors and are widely utilized in the construction of hybrid materials. Controlled drug release systems provide numerous benefits over commercial or traditional methods, including a developed efficient medication, reduced toxicity, and increased patient appropriateness. The primary goal of drug release control is to provide patients with the best chance of recovery feasible [1] .

1.2 Nanotechnology

Nanotechnology is a branch of science concerned with the manufacture of nanoparticles ranging in size from 1 to 100 nm using various synthetic methodologies, particle structure, and size change [7] . It is the scientific process of manipulating and controlling matter on a nano scale for variety of industrial and therapeutic purposes [2] . Nanotechnology has demonstrated the ability to close the gap between biological and physical sciences by employing nano-structures and nanophases in a variety of scientific domains, particularly nanomedicine and nano-based medication delivery systems [3] . Due to its ability to create products that are better made, safer, cleaner, longer-lasting, and smarter for use in industries like medical, communications, everyday life, agriculture, and other fields, nanotechnologies have had a substantial impact on nearly all industries and areas of society [8] . Nanoparticles, nanospheres, or nanocapsules can be produced depending on the technique of preparation [9] . Table (1-1) provides the terminology related to nanomaterials with their definitions and explanations.

Table (1-1) the terms related to nanomaterials and their definitions and explanations.

Term	Description	References
Nanoscale	Approximately 1 to 1000 nm size range.	[2]
Nanotechnology	The science and technology that have made it possible to examine, create, and control structures and devices with nanometer size tolerances.	[10]
Nanoscience	The study of nanoscale systems.	
Nanoparticles	Are microscopic materials with sizes ranging from 1 to100nm.	[11]
Nano capsules	Drug-contained vesicular systems in which the medication is contained within a chamber that is encircled by using a polymer membrane	[12]
Nano spheres	Are matrix systems where the medicine is physically and evenly distributed.	
Nanocarriers	Are nanomaterials of 10–200 nanometers in diameter which consider as potential vehicles for drug delivery system	[13]
Nanomedicine	the area of medicine that applies the science of nanotechnology to the prevention and treatment of different illnesses by employing materials at the nanoscale level	[14]

1.2.1 Approaches for the synthesis of nanomaterials:

Top-down techniques and bottom-up approaches are the two basic approaches employed for nanomaterial production as shown in Fig. (1-1).

1- In the "top down" synthesis (physical methods), nanoparticles are created by shrinking macroscopic systems to nanoscale. Particle size reduction can be accomplished through a variety of physical means [15] .

2- Bottom-up techniques (chemical methods), as opposed to top-down production, depend on transferring specific bonds between molecules or nanoparticles—often via elementary chemistry—to initiate an independent self-assembly process after the precursors are combined in the right circumstances. For nanofabrication, this is especially attractive because of the vast array of possibilities available for adjusting the interactions between nanoscale elements (interaction forces, molecular structure, form, size, and surface qualities). One way to create tunable nanostructures is to modify certain process parameters, like the chemistry of sacrificial templates, pH, humidity, and temperature [16].

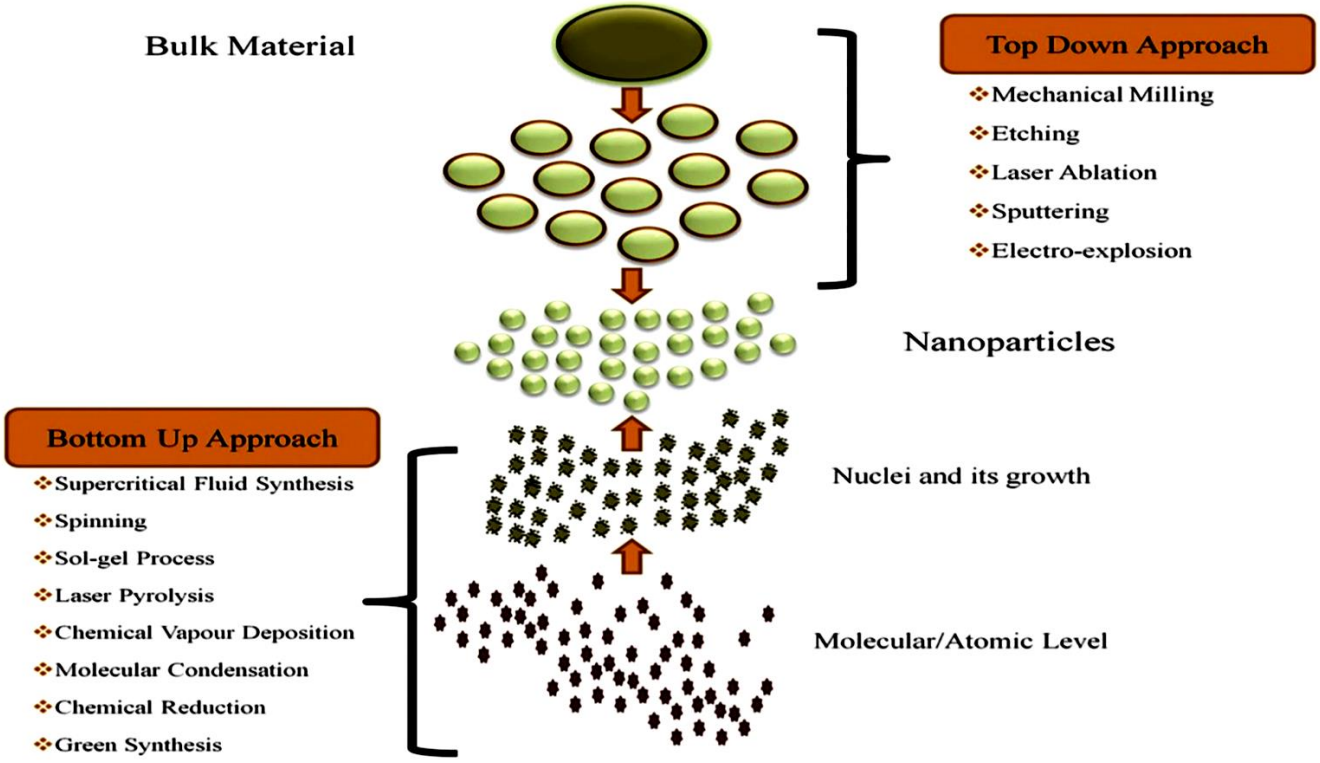

Figure (1-1) Approach of synthesis of nanomaterials by top-down and bottom-up methods [17]

1.2.2 Nanotechnology in Medicine

A new field of research called "nanomedicine" has emerged as a result of the use of nano-technology in medicine. Nano-medicine is the study of nanoparticles to enhance illness detection, control , prevention, and therapy [12] . Nanoparticles can be utilized for gene therapy, radiation therapy, immunotherapy, and chemotherapeutic delivery. Chemotherapy delivery seeks to reduce medication toxicity and enhance pharmacokinetics by selectively targeting and administering chemotherapy to cancer tissues [18] , As mention in Fig (1-2) . The process of developing nanomedicine is complicated and calls for careful consideration of a number of factors, including those relating to chemistry, production, control, as well as economic and legal considerations. The creation of new products and manufacturing scale-up of formulations based on nanomedicine present significant chemical, manufacturing, and control considerations. It is vital to analyze the composition and structure of the early formulation in order to assess the viability of producing nanomedicine. This guarantees reliability for confirmatory investigations and safety and effectiveness for human clinical trials [19] .

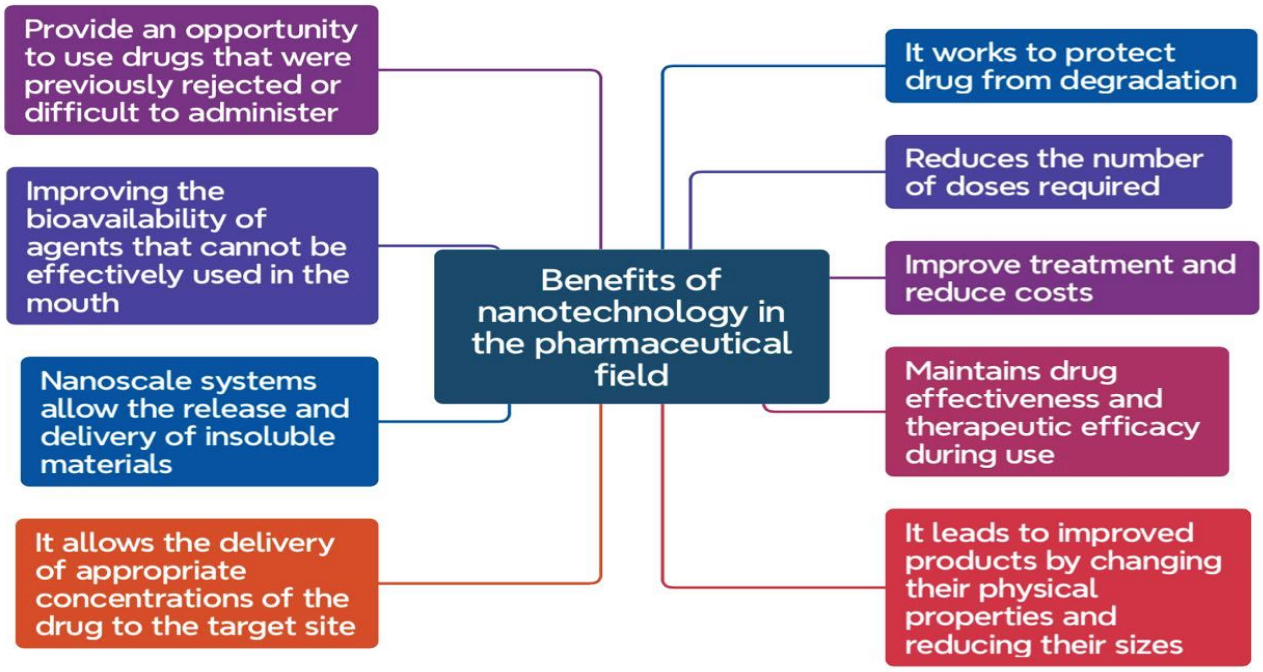

Figure (1- 2) The benefit of nano-technology in the medical field [20] .

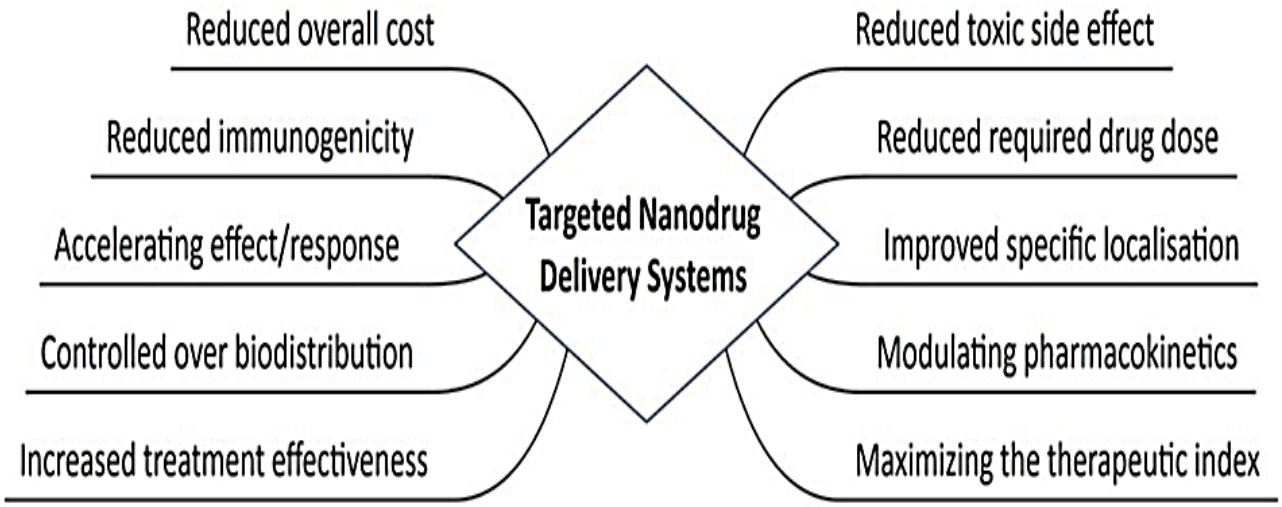

Figure (1-3) Targeted nanodrug delivery systems [21] .

1.2.3 Nanocarriers

Nanocarriers are the colloid drug delivery systems with submicron particle sizes, usually 500 nm or less. Since nanocarriers have shown such promise for medicine delivery over the past two decades, a considerable deal of study has been conducted on them. Because of their large surface area to volume ratio, nanocarriers have the ability to alter the basic properties and bioactivity of pharmaceuticals. [22]. Because of their unique physicochemical and biological properties, which allow them to be absorbed by cells more readily than larger molecules, nanocarriers are useful delivery systems for already recognized bioactive substances. When used in medical applications, nanocarriers need to be nontoxic and biocompatible, meaning they shouldn't damage any specific biological system or trigger an immune reaction [23]. The Fig. (1-4) demonstrates the commonest example of nanocarrier.

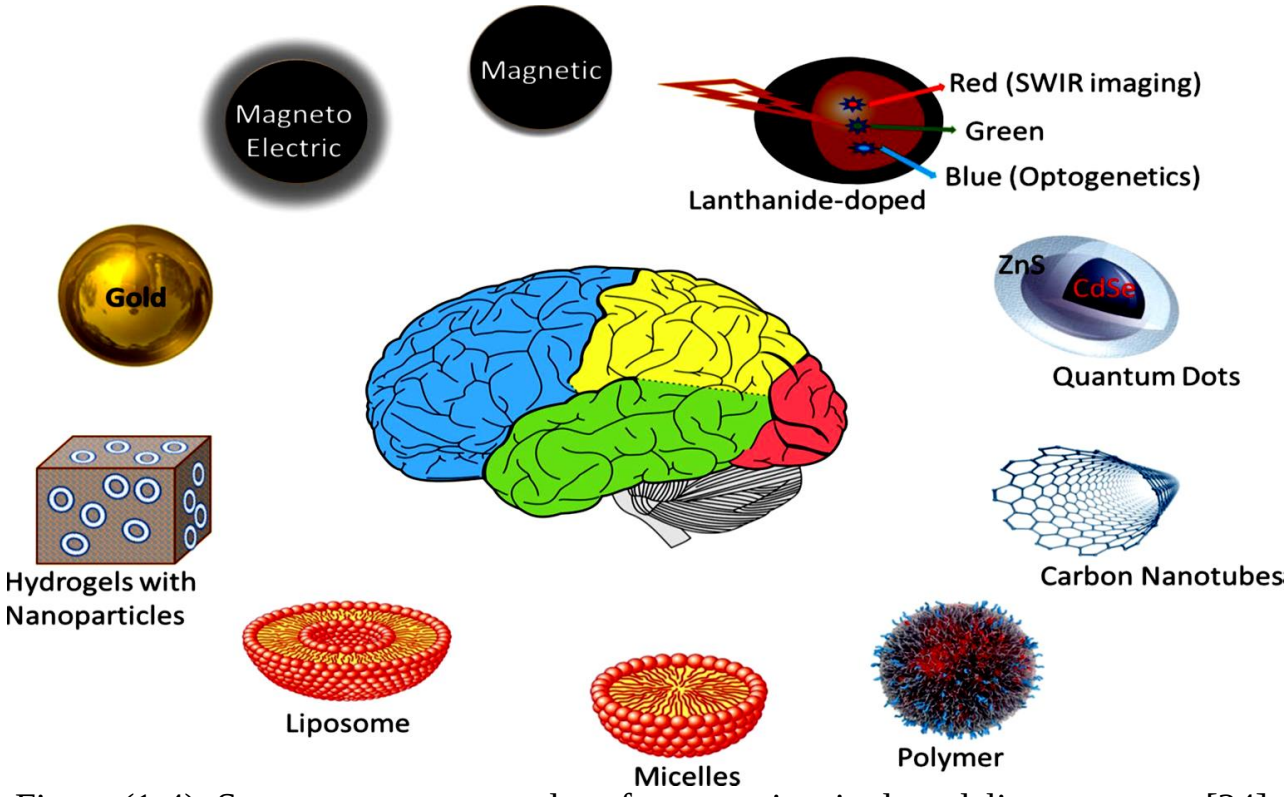

Figure (1-4): Some common examples of nanocarriers in drug delivery system [24].

Using nanoparticles as drug delivery systems has several benefits as mention in Fig. (1-5) , high drug loading capacity controlled , sustained drug release during transportation and at the target site, and the use of multiple administration routes, such as parenteral, intraocular, oral, and intravenous. Additionally, nanoparticles can easily be modified in terms of size of particles and surface properties to achieve both active and passive drug targeting. Keeping drug molecules from coalescing decreases their mobility, which increases stability and lowers drug leakage. [25]

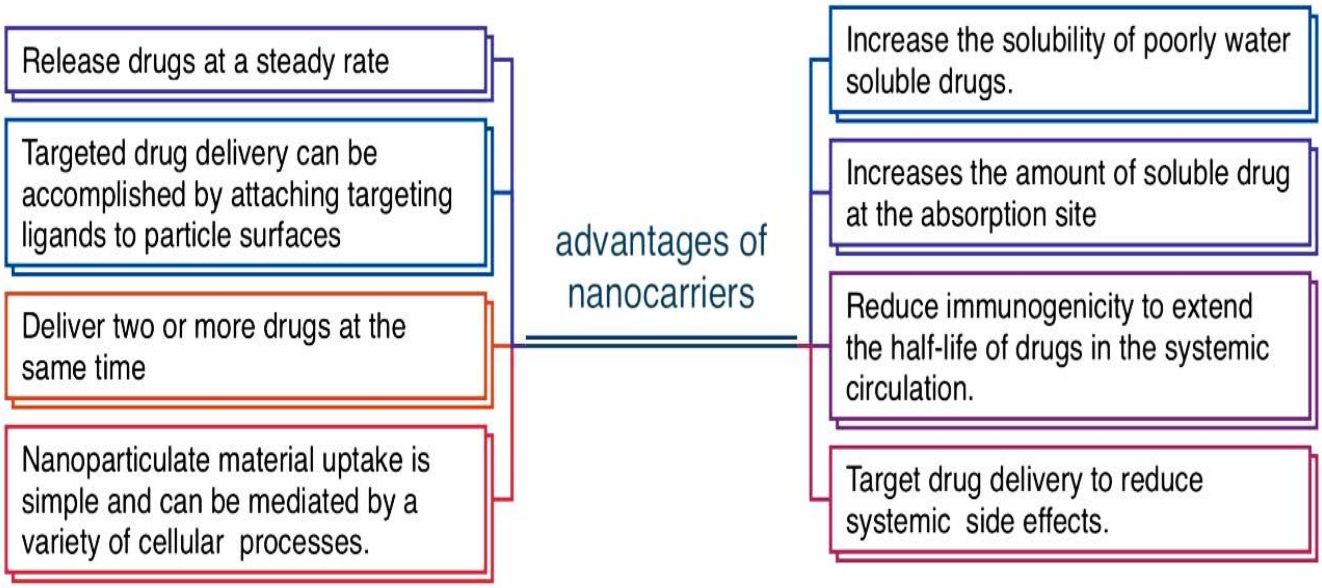

Figure (1-5) The advantages of nanocarriers [26] .

Ideally, Nanocarriers manufactured from synthetic or natural polymers, which are inexpensive, biodegradable, nontoxic, nonthrombogenic, nonimmunogenic, noninflammatory, and have a particle diameter of 100 nm. They also prevent platelet aggregation. [27] . The properties that are to be considered while designing and formation of nanocarriers are expressed in Fig. (1- 6) .

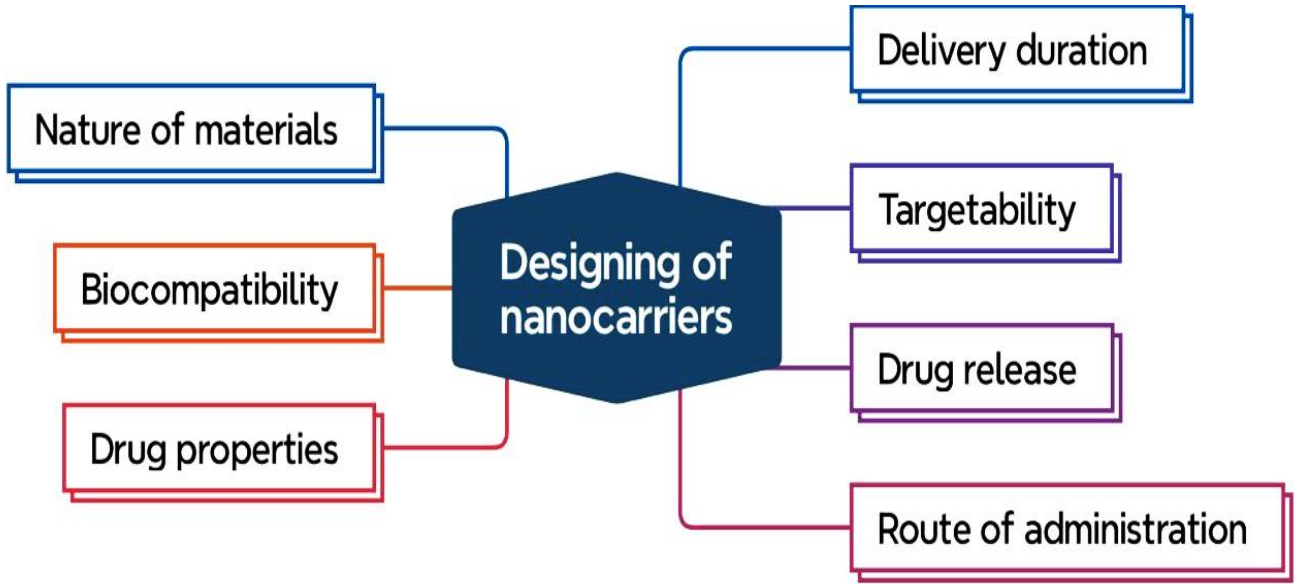

Figure (1-6) Features taken into consideration when constructing nanocarriers [28] .

1.3 Drug Delivery System (DDS)

Drug delivery sciences are primarily concerned with delivering the prescribed bioactive molecules to the patient's body in the most appropriate spatial and temporal patterns to meet therapeutic needs. Since its inception, research in this field has attempted to solve the issues caused by frequent dose. To combat elimination half-life of drug that would attach to more closely recurrent administration, a large number and variety of prolonged-release dosage forms have been proposed over the last fifty years, which retain the bioactive molecule slowly accessible for absorption over a long period of time [29]. Drug delivery methods based on nanotechnology start with nanoparticles that include adsorbed polymer matrices and one or more therapeutic medications that have the ability to bind or disperse. Considerable advancements in imaging, therapy, and diagnostics have been made in the field of nano-drug production in recent years. The main objectives of nano-drug systems are to extend the half-life of injectable medications, enhance the bioavailability of targeted tissue delivery, and deliver pharmaceuticals orally. Because nanomedicines are delivered at lower levels, their pharmacological effects have advanced significantly and their risk to health and side effects has decreased [30].

The usage of nanoscale drug delivery systems dates back more than 60 years in the medication delivery industry. The liposome was created in 1964, and in 1976 the word "nanoparticle" was first used to refer to 100 nm polymer particles. As a result, the concept of employing nanoparticles for drug administration first surfaced approximately 40 years ago, and drug delivery scientists were already aware of the nanoparticles' special capabilities. To increase drug bioavailability, drug delivery researchers began utilizing the special qualities of drug nanocrystals about 30 years ago [31] . There have been many different drug delivery systems created during the past 60 years. For therapeutic uses, the first generation (1950–1980) produced a large number of controlled release formulations for oral and transdermal delivery [32] .

The development of clinical products, however, has not been as successful for the second generation (1980–2010). The type of issues that must be solved is mostly to blame for this. The physicochemical issues were addressed by the first generation of drug delivery methods, but biological barriers were a challenge for the second [33] .

The third generation of drug delivery devices (starting in 2010) must overcome both physicochemical and biological obstacles. Drugs' poor solubility in water, the high molecular weight of peptide and protein medications, and the challenge of regulating drug release kinetics are the root causes of the physicochemical issues [34] .

The body distributes medication delivery systems, not the formulation features that limit administration to a specific target in the body, and this is one of the biological barriers to overcome. Their efficacy in vivo is further limited by the way the body reacts to formulations. The effectiveness of medication delivery systems in the future will depend on whether new systems can overcome the physical limitations placed on them by humans and whether new methods of thinking can speed up the development process [35]. Fig. (1-7) shows a list of the development of drugs delivery technology from 1950 to the present.

i. First Generation (1G)

Throughout the first generation (1G) of development, that lasted from 1950 to 1980 , the majority of the essential knowledge regarding the drug release mechanisms, particularly with regard to transdermal and oral administration rout , was attained. This time period led to the discovery of four drug release mechanisms, which sped up the creation of several oral and transdermal controlled release formulations [36] .

Systems controlled by diffusion and dissolution were the most often used methods. Osmosis-based formulations briefly enjoyed prominence, although there are orders of magnitude less osmosis-based goods available than there are the other two. The ion-exchange process is unique compared to other mechanisms, although it has not shown to be efficacious on its own.

The diffusion-controlled mechanism is necessary for it. Dissolution or diffusion controlled manufacturing processes are still widely used in the creation of oral once daily formulations [37] .

ii. Second Generation (2G)

Second generation (2G) drug delivery formulations have been less successful than first generation (1G) drug delivery formulations, according to how many clinical goods are produced. 2G technologies handle more difficult formulations, which is one of the causes of this. One way to distribute peptide and protein drugs for at least a month is by injectable depot formulations made of biodegradable poly (lactic-co-glycolic acid) (PLGA). Typically, the first burst release of a depot formulation releases half of the drug during the first day or two, and most formulations fail to control this [38] .

iii. Third Generation (3G)

To get through physicochemical and biological limitations, the 3G drug delivery technologies will have to be developed much farther than the 2 G methods. The key to success is realizing and overcoming biological constraints in addition to physicochemical hurdles, as can be seen from the brief examination of the 2G technologies. During the 3G era, there are numerous different medication delivery systems that need to be created [39] .

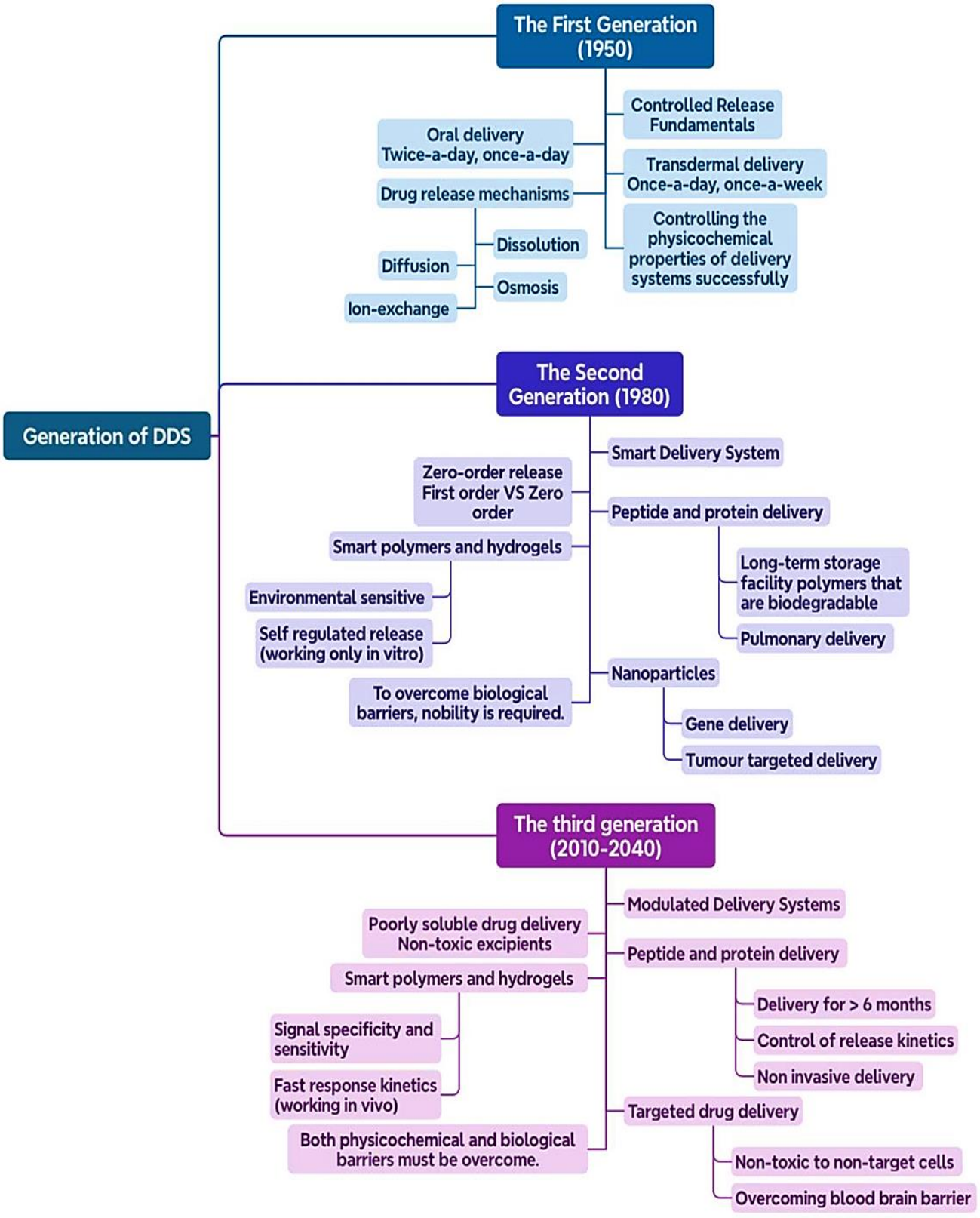

Figure (1-7) : The history of medication delivery technology from 1950 to the present and the technologies that will be needed in the future [40] .

1.4 Modified Drug Delivery Systems

Drug delivery systems are created to increase drug effectiveness and reduce negative effects. As drug delivery systems advance, patients can consume drugs in a more secure and comfortable manner. A remarkable amount of development has been made in drug delivery technology over the past seven decades, including systems for long-term distribution across months and years, localized delivery, and tailored delivery [41] .

Today, one of the most serious diseases and one of the deadliest diseases on the planet is cancer. In past times, the only cancer treatment options were chemotherapy and surgery. Chemotherapy and other forms of radiation are unable to distinguish between self and non-self - cells, which is the main drawback of the conventional approach [42] .

In order to limit the medicine's toxicity and focus its effects as specifically and directly on the tumor as feasible, many trials have been conducted to establish particular drug delivery systems. To increase the efficacy, specificity, and general effect of the anti-neoplastic drugs, the utilization of various drug delivery systems is regularly evaluated and enhanced [43] .

Drugs that are encapsulated in polymeric drug carriers such liposomes, hydrogels, nanoparticles, surfactants, colloidal cells, and viral drug delivery systems are among the current drug delivery technologies that show significant potential [44] .

1.5 Drug Loading Techniques

In order to decrease the number of materials that are required for drug administration, an effective nanoparticulate suspension should ideally have a high drug loading capacity. The two approaches listed below can be used to load a medication into a nanoparticle system: Drug absorption can occur in two ways: (a) at the moment nanoparticles are created (incorporation approach), or (b) after the carrier has been incubated with a concentrated drug solution [45] .

Drug solubility in the solid state in the matrix material or polymer (solid dissolution or dispersion) is a major factor in drug loading and entrapment effectiveness. This solubility is correlated with the molecular weight, composition, drug polymers interaction, and presence of end functional group (ester or carboxyl) in the polymer. The macromolecule has the maximum loading efficiency when loaded at or around its isoelectric point, where it has greater adsorption and less solubility. Research indicates that increasing the drug loading for smaller molecules can be achieved by the effective use of ionic interaction between the drug and matrix materials [46] .

1.6 Controlled Drug Delivery System (CDDS)

Controlling drug releases is a developing field with numerous hurdles to overcome. Because many medications are hydrophobic, their bioavailability is limited. Other medications, such as chemotherapy drugs, are extremely hazardous and should preferably only be administered once, at the tumor site [47] . Applications for controlled drug delivery include both target delivery (e.g: to a tumor, sick blood vessel, etc.) on a one time or ongoing basis as well as improved delivery through days, weeks, months, or years. The amount of medication required to have the same therapeutic impact on patients can be decreased by using controlled release formulations. Patient compliance is also improved by the ease of using fewer, more powerful doses [48] . For predesigned release profiles, Over the years, controlled release research has explored a variety of systems, including coated tablets and gels, biodegradable microspheres, and osmotic systems, both computationally and empirically [49] . Wide varieties of formulations for prolonged action that continuously release their active components at a set pace and for a set amount of time fall under the category of controlled release dosage forms. The bulk of these formulations are intended to be taken orally, but recently, parenteral administration, ocular insertion, and transdermal application have also been made possible with similar devices. Providing a longer duration of action and ensuring improved patient compliance is the

system's primary goal in the development process [50] . A control drug delivery system have many advantages listed in fig.(1- 8) [51] .

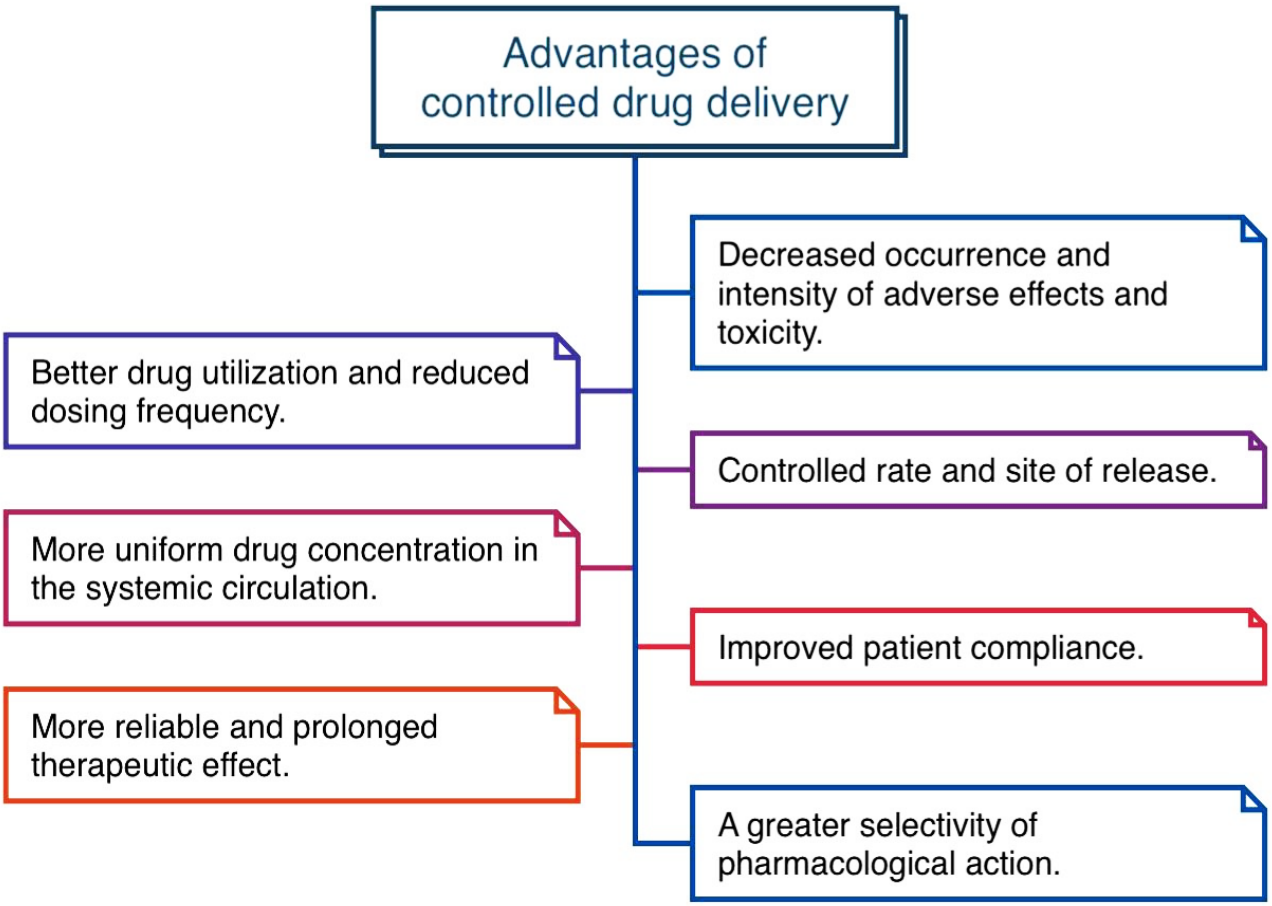

Figure (1-8) Advantages of controlled drugs delivery system.

The goal of many controlled-release systems was to establish a delivery profile that would result in a high blood level of the drug for an extended length of time. With conventional drug delivery methods, the amount of medication in the blood rises following each injection and then falls until the subsequent dose which is explained in Fig. (1-9). Traditional medicine administration's key problem is that the agent's blood concentration needs to be kept between a minimum value, at which the medicine loses its effectiveness, and a highest value, which may indicate a dangerous level [52] .

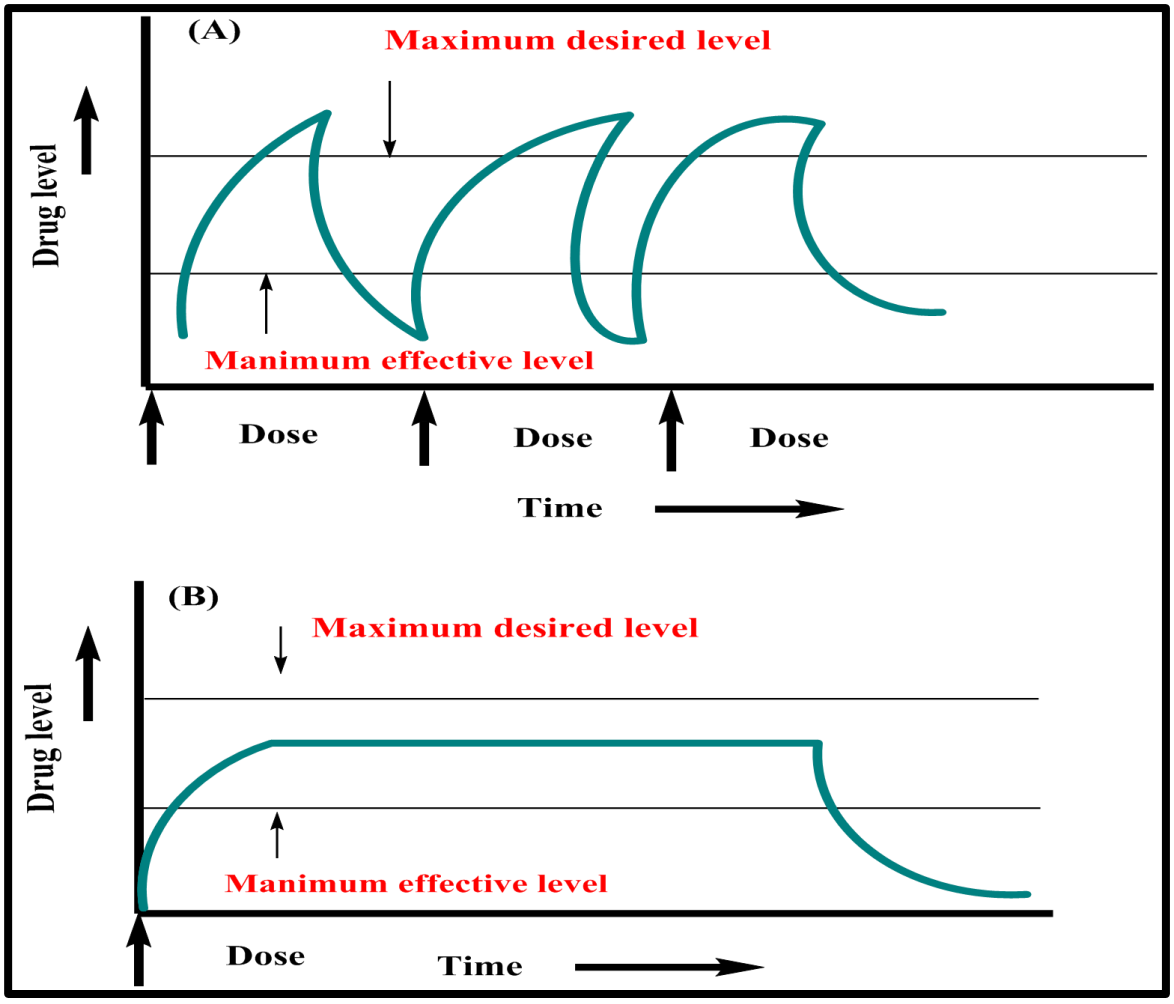

Figure (1-9) drug concentration in blood in (a) traditional drug dose, and (b) control drug delivery dose [53] .

1.7 Self-assembly Method

It is a technique whereby, in the absence of outside direction, local interactions affect the preexisting components, especially in a disordered system, to produce orderly structures or patterns. The self-assembly approach functions as a link in between two ways of material production and manufacture [54] . The majority of biological nanostructures are created through self-assembly. Examples include folding polypeptide chains, building cell membranes from phospholipid bilayers, and DNA's helical helix. Self-assembly is also thought to be responsible for how a ligand interacts with its receptor. Additionally, It describes the formation of phase-separated polymers, colloids, self-assembled monolayers, and molecules [55] .

In contrast to chemical forces, the types of contacts involved in self-assembly processes happening at the colloidal, molecular, or atomic length scale are typically fragile and long range [56] . These are mostly non-covalently linked via hydrophobic, electrostatic, van der Waals forces, hydrogen bonding, p-p aromatic stacking, metal coordination, and other mechanisms. These linkages are typically weaker (2–250 kJ/mol) than covalent linkages (100–400 kJ/mol), but when present in sufficient quantities , they form very stable self-assembled structures , with the final assembly's shape , size , and functionality being controlled by their delicate balance [57] .

Molecular units that connect with one another through a balance of weak, non-covalent intermolecular forces undergo self-assembly. When molecular units align in an ordered structure, these interactions play a significant role. The mechanism underlying unit self-assembly is these interactions. Additionally , different functional connections or forces govern the directionality and utility of self-organized structures which mention in Fig. (1-10) [58] .

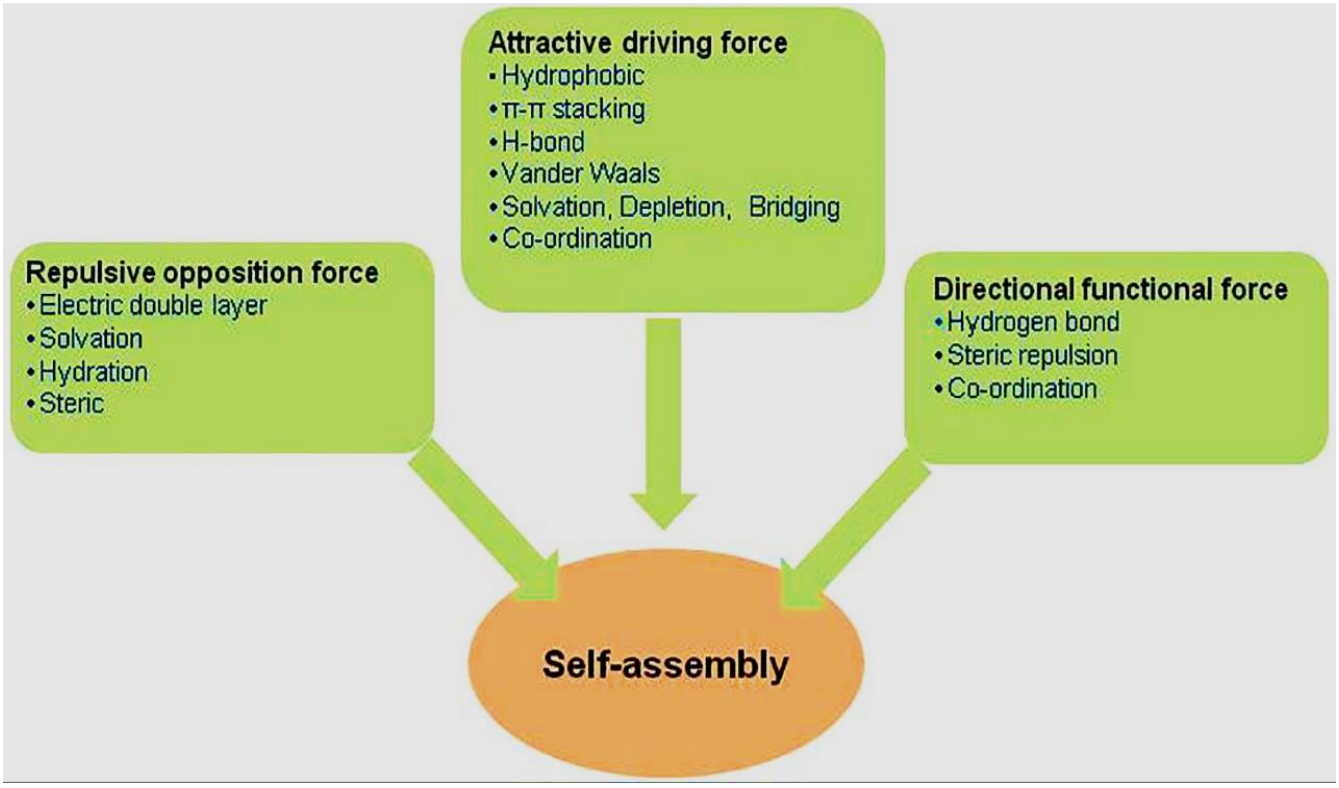

Figure (1-10) The forces which involve in self-assembly [59] .

Building blocks, or fundamental units, interact cooperatively in nanotechnology self-assembly processes to form multicomponent systems that spontaneously organize into new equilibrium states. This allows for appropriate control over the formation processes , as explain in Fig. (1-11) [60] .

These cooperative relationships start out as a (disordered) arrangement of construction pieces. The combination of multifunctional building blocks and cooperative (noncovalent) forces offers a great method for creating novel, complex nanomaterials [61] .

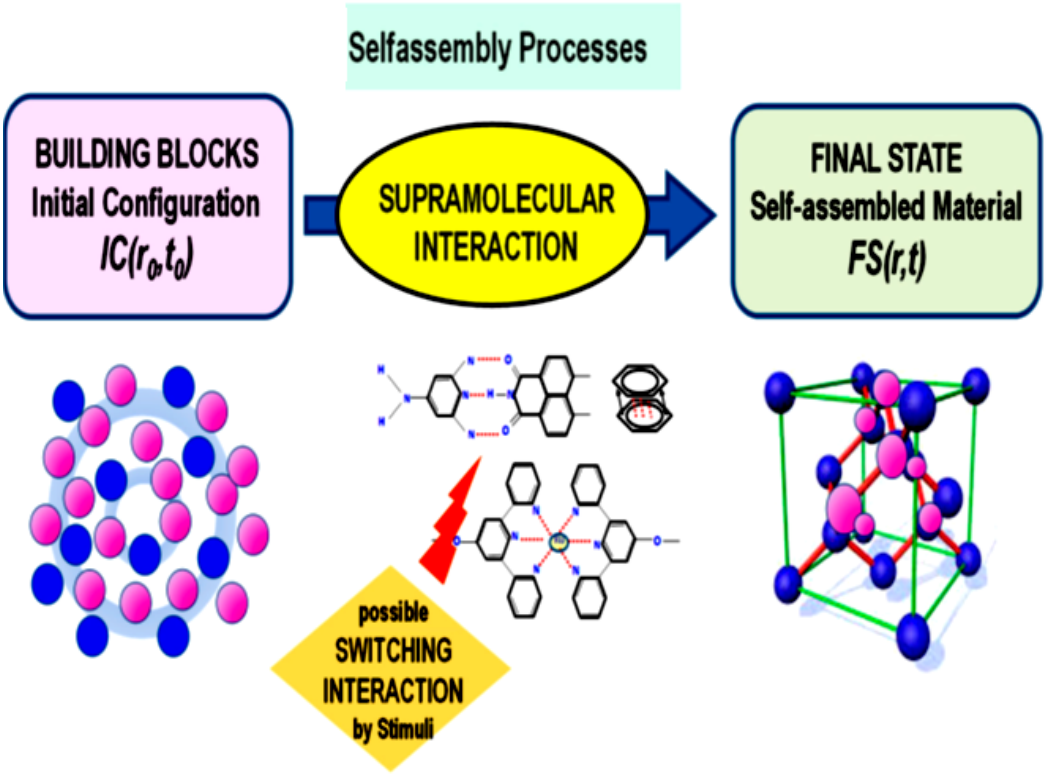

Figure(1-11): Conceptual scheme indicating the main stages of the self-assembly process in nanoscience [4] .

1.8 Polyoxometalate (POM)

The anionic metal-oxides known as polyoxometalates (POMs) are distinct compounds that may be used in medicine, material science, and catalysis [62] . The architecture of polyoxometalates (POMs) consists of oxygen atoms and primary transition metals, such as Ta, Nb, W, V, and Mo at their maximal oxidation state. They also contain a considerable number of heteroatoms such As, Si, P, and Ge [63] . POMs have a three-dimensional structure that is mostly made up of corner sharing (one bridging 2-oxo group) or edge sharing (two bridging 2-oxo groups) MO_6octahedra [64] , the Fig. (1-12) demonstrate various structure of POM .

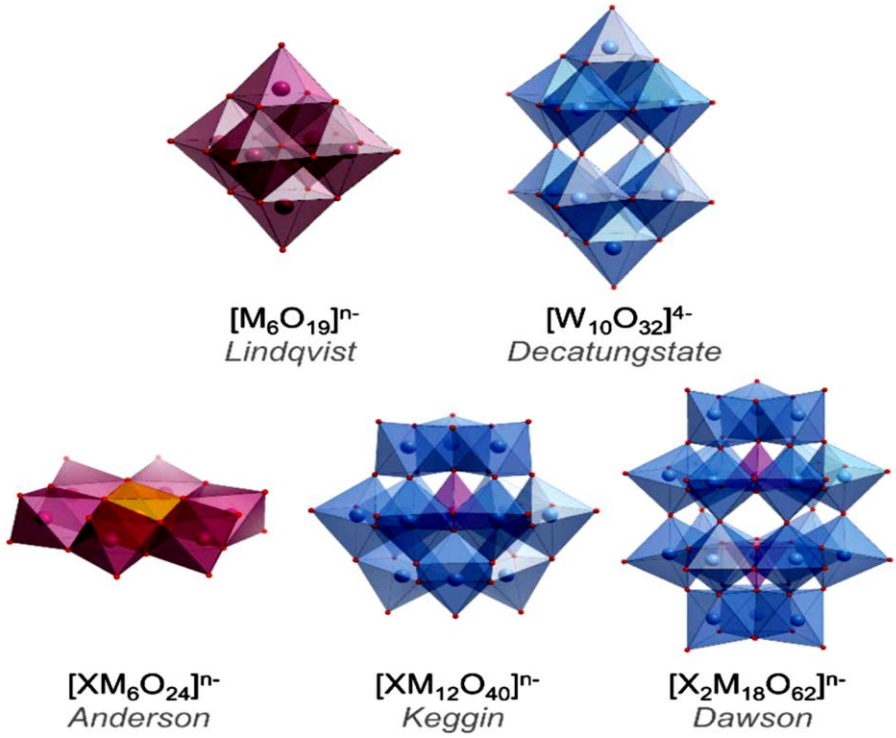

Figure (1-12) Structures of some archetypical POM clusters [65] .

Intriguingly, various elements could be easily added into the POM frameworks, resulting in remarkable structural diversity and diverse characteristics. It is hardly surprising, then, that POMs have a wide range of uses [66] . POMs are particularly useful in the treatment of diabetes and illnesses caused by bacteria, viruses, and leishmania parasites. POMs have a high potential for use in the treatment of nearly all malignancies [67] .

POMs can generate derivatives with various structures by coupling with organic or metal groups since they have excellent electron acceptance and transfer properties and are generally stable. The primary advantage of programmable POMs is their ability to generate and update metal oxide cluster anions' structure in a way that facilitates the easy integration of many elements into the POM framework [68]. POMs' unique characteristics allow them to display an astounding diversity of sizes, structures, and physicochemical characteristics, including as shape, redox potential, surface charge distribution, polarity, and acidity [69] .

It is anticipated that derivatization of POMs with organic partners including synthetic compounds and native bio species via covalent bonding will have a synergistic impact and provide the POM hybrid with new functions or features. Additionally, the conjugation of an organic ligand onto the POMs provides other benefits like improved stability and preferred ligand orientation [70] . The attachment of more physiologically logical organic ligands to POMs has the potential to increase their biocompatibility, enable the selective recognition of biological targets, and modify the bioactivity and cytotoxicity [71].

1.8.1 Structures and Types of POMs

POMs can be classified into various categories based on their composition and structure. POMs exhibit a wide variety of structures, with the Keggin, Dawson, Lindqvist, Anderson, sandwich, and Preyssler structures being among the most common. One common group of POMs is known as iso-polyoxometalates. These POMs, represented by the generic formula $[M_mO_y]^{n-}$, consist solely of a transition metal and oxygen. The example of iso-polyoxometalate is hexamolybdate, which has the Lindqvist type structure [72] .

Hexamolybdate is a polyoxometalate (POM) compound that consists of oxygen and molybdenum atoms. Specifically, the hexamolybdate denotes the hexamolybdate anion, which has the chemical formula $[Mo_6O_{19}]^{-2}$. It is the example of the hexametalate, which

six molybdenum atoms were surrounded by the oxygen atoms in a special arrangement [73] .

Figure (1-13) Structure of hexamolybdate.

Hexamolybdate compounds show special properties due to their distinctive structure and electronic configuration. Owing to their stability with-stand at high temperatures. They have gained significant attention as inorganic building blocks for applications in high-temperature catalysis. They also have an interesting redox activity, they can accept multi electrons with minimal structural changes making them a good candidate as electron-transfer agents and catalysts in numerals applications. Therefore, several studies have focused on exploring the potential applications and properties of hexamolybdate-based derivatives [74] .

The Lindqvist type structure is made by a hexameric cluster of metal atoms surrounded by oxygen atoms where the resulting six-octahedra are arranged in an octahedral pattern. The metal ions are typically transition metals such as tungsten (W), molybdenum (Mo), or chromium (Cr). One notable feature of the Lindqvist structure is the sharing of edges between adjacent octahedra where each octahedron shares four edges with four of its neighboring octahedra. This arrangement contributes to the overall stability and structural characteristics of the lindqvist POM structure [75] .

POM offers a rich variety of structures and properties. Its study continues to advance our research into understanding inorganic chemistry. New classes of hybrid POM species have been developed through covalent functionalization of conventional POM structures, expanding the range of applications and functions available.

1.8.2 Review of Synthesis of Inorganic Organic Hybrid POM Compounds

One of the critical areas of (POM) chemistry is the study of POM compounds with high-dimensional structures and organic - inorganic hybrid topologies, and the reaction system of organic - inorganic material The most frequently studied hybrid POM compounds are the three-component system that includes POM, metal ions and ligands [76]. For this reason, organic and inorganic materials are produced. Hybrid POM complexes frequently appear as a self-assembly process. The complex nature of POMs, metal ions, and ligands in crystallization makes it difficult to predict the structure and composition of the results. One of the main challenges still facing POM compounds is the logical creation and synthesis of hybrid organic-inorganic molecules [77] .

development of organic-inorganic hybrid polyoxometalate (POM) compounds with time

1. Early Years (20th Century): Firstly, POM compounds were discovered and studied for their exceptional structures and properties in the early to mid-20th century Early research focused on the synthesis and characterization of pure POM clusters, mainly composed of transition metals and oxygen atoms. Example: α-Keggin Structure. The α-Keggin structure is a specific type of polyoxometalate (POM) structure characterized by a central heteropolyanion $[XM_{12}O_{40}]^{n-}$, where X is a heteroatom and M is a transition metal. It represents one of the most common and well-studied POM architectures. [78] , [70].

2. Late 20th Century: Researchers commenced exploring the incorporation of organic ligands into POM structures to alter their properties and extend their applications. New methods for functionalizing organic ligands and linking them to POM clusters were developed, allowing the synthesis of hybrid POM compounds. Example: Hybrid Organic-Inorganic POMs. Hybrid organic-inorganic POMs represent a category of compounds where organic ligands are incorporated into POM structures, leading to materials with enhanced properties compared to pure POMs. [79], [80].

3. At 2000s: As researchers realized the potential of hybrid POM chemicals, the POM-based area grew quickly in various fields, including catalysis, materials science, and medicine. New synthetic strategies were developed to control the size, shape, and composition of hybrid POM structures, leading to enhanced properties and functionalities. Example: Functionalized Hybrid POMs. Special Name: Functionalized hybrid POMs refer to compounds where organic ligands attached to POM clusters are modified or functionalized to introduce specific properties or functionalities, such as improved solubility or biomolecule binding capabilities. [81], [82]
4. At 2010s: Many studies focused on the design of organic ligands and optimizing synthetic protocols to achieve tailored properties in hybrid POM materials. Application-focused studies confirmed the utility of hybrid POM compounds in many areas such as energy storage, sensing, and drug delivery. Computational modeling also played a significant role in predicting the behavior of hybrid POM materials and motivating experimental synthesis. Example: Photoluminescent Hybrid POMs. Photoluminescent hybrid POMs are hybrid compounds incorporating organic chromophores or fluorophores into POM structures, resulting in materials with tunable luminescence properties suitable for optoelectronic applications [83], [84].
5. Recent Advances (2020s): Current research continues to drive the boundaries of hybrid POM chemistry, exploring novel ligands, metal clusters, and assembly strategies. Emphasis is placed on sustainable synthesis methods and the development of environmentally friendly POM-based materials. Interdisciplinary collaborations between chemists, physicists, materials scientists, and engineers drive innovation in the field, leading to new applications and discoveries for example: Redox-Active Hybrid POMs. Redox-active hybrid POMs are a category of compounds featuring organic redox-active moieties incorporated into POM clusters, enabling reversible electron transfer processes. These materials hold promise for applications in energy storage, electrocatalysis, and molecular electronics. [85], [86].

1.9 Dopamine (DA)

Dopamine, also known as 4-(2-aminoethyl)-1,2-benzenediol , its structure shows in Fig. (1-14) , is a neurotransmitter found in the mammalian nervous system. It is generated and released by dopaminergic neurons in the brain and spinal column. It is produced in the substantia nigral area of the brain. It is also produced in other parts of the brain, such as the ventral tegmental region and the hypothalamus. $C_8H_{11}NO_2$ is the chemical formula for dopamine [79].

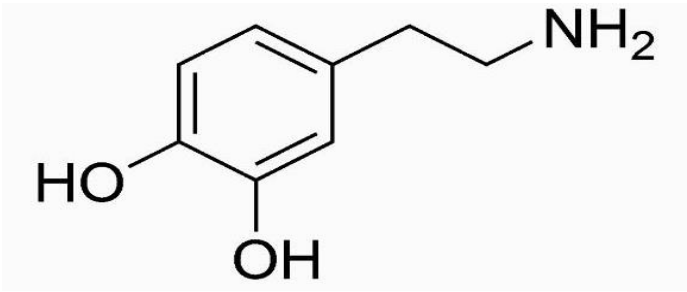

Figure (1-14) The chemical structure of dopamine.

In the cytosol, dopamine is generated from tyrosine through hydroxylation by tyrosine hydroxylase to produce L-DOPA, which is subsequently decarboxylation by aromatic amino acid decarboxylase [80] , such as see in Fig.(1-15) .

Synaptic vesicles, which are present all along the axon, are where dopamine builds up. Ventricular monoamine transporter 2 is responsible for loading synaptic vehicles. The pH gradient that ventricular monoamine transporter 2 depends on is produced by the vesicular membrane's vacuolar ATPase. Monoamine oxidase breaks down dopamine, while the dopamine active transporter accumulates it back into the neuronal cytoplasm. From there, ventricular monoamine transporter 2 can repackage it into synaptic vesicles [81].

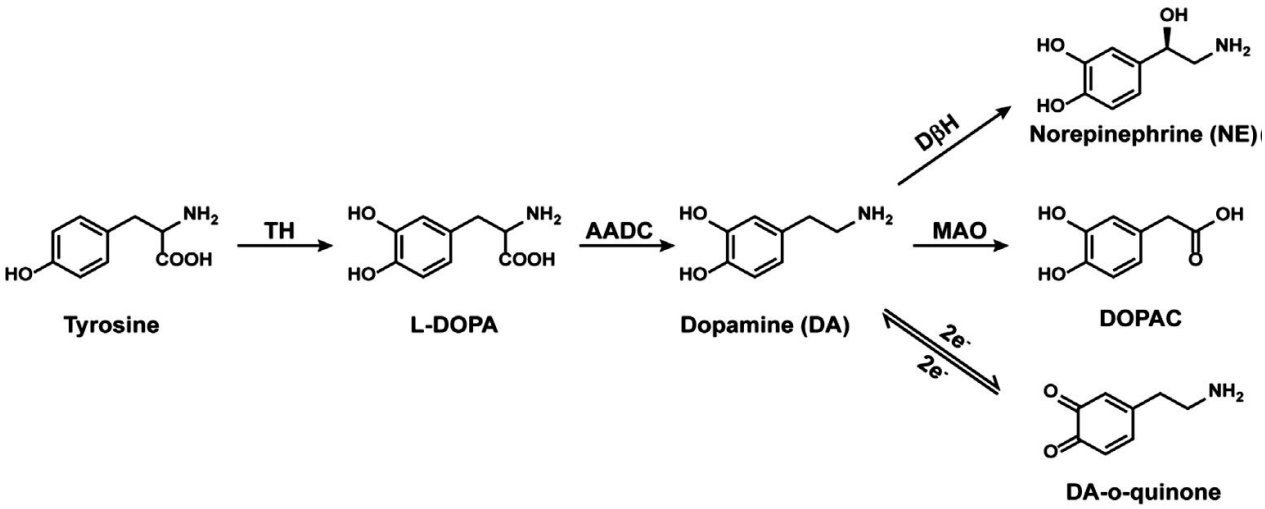

Figure (1-15) Dopaminergic routes The dopamine biosynthesis, metabolism, and redox pathways [86].

Five subtypes of dopamine receptors; D1, D2, D3 , D4 , and D5 are recognized which are a class of G protein-coupled receptors that bind the neurotransmitter dopamine and play a crucial role in various physiological and behavioral processes in brain. More categorization of these subtypes results in two subclasses: D2-like family receptors (including types 2, 3, and 4) and D1-like family receptors (including types 1 and 5). Types 2, 3, and 4 only share structural similarities, whereas types 1 and 5 have equivalent drug sensitivity and configuration [82] .

In contrast to glutamate and GABA, which bind to ionotropic receptors to either excite or inhibit neurons, dopamine modifies neuronal responses via binding to G protein-coupled receptors. The type of receptor that dopamine binds to determines its effects: type 1 receptors are known to be Gs protein coupled, and their increased levels of cyclic AMP, whereas type 2 receptors are known to be $G_{i/o}$ linked [83] .

In order to affect motivated behavior, feelings, and higher-order cognitive functions related to reward processing, the system of dopamine and its projection sites are essential. The functions of reward include approach and consummatory behavior, the capacity to predict the results of potentially rewarding situations, support goal-directed behavior, and offer an evolutionary advantage to species that live in unpredictable environments. The

integrity of the dopamine system is essential for processing reward information correctly. Pathological gambling, drug addiction, Parkinson's disease, schizophrenia, and other disorders have all been linked to this system's malfunction. The effect of genetic predisposition and polymorphism on human reward system activation is yet unknown, despite the fact that there are definite individual genetic variants in sensitivity to and expression of these neuro-psychopathologies [84] .

1.9.1 Physical and chemical properties of dopamine

Dopamine is a neurotransmitter and catecholamine that plays a crucial role in the brain's reward and pleasure centers, as well as in motor control and several other functions. Here are some of its physical and chemical properties shown in Fig.(1-16) [85] .

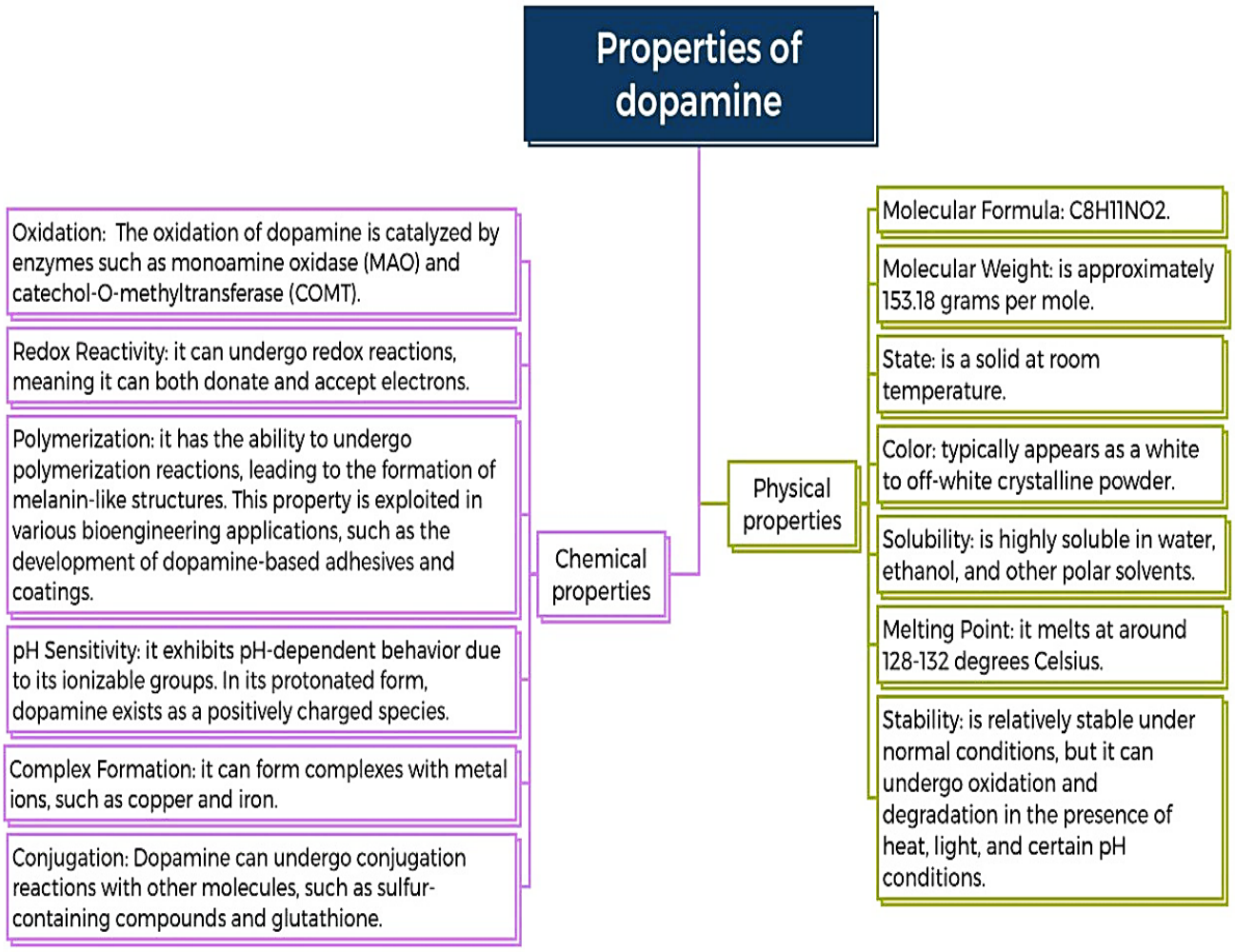

Figure (1-16) diagrammatic illustration of chemical and physical properties of dopamine.

1.9.2 Applications of Dopamine

As mentioned, PDA has a range of intriguing properties and is a potential candidate in a variety of important applications, from biomedical science to energy, as shown in Fig. (1-17).

For example, in energy and environment applications, heterogeneous photocatalysis, which is known as a cost- effective approach for dye degradation and solar water splitting under light irradiation [86].

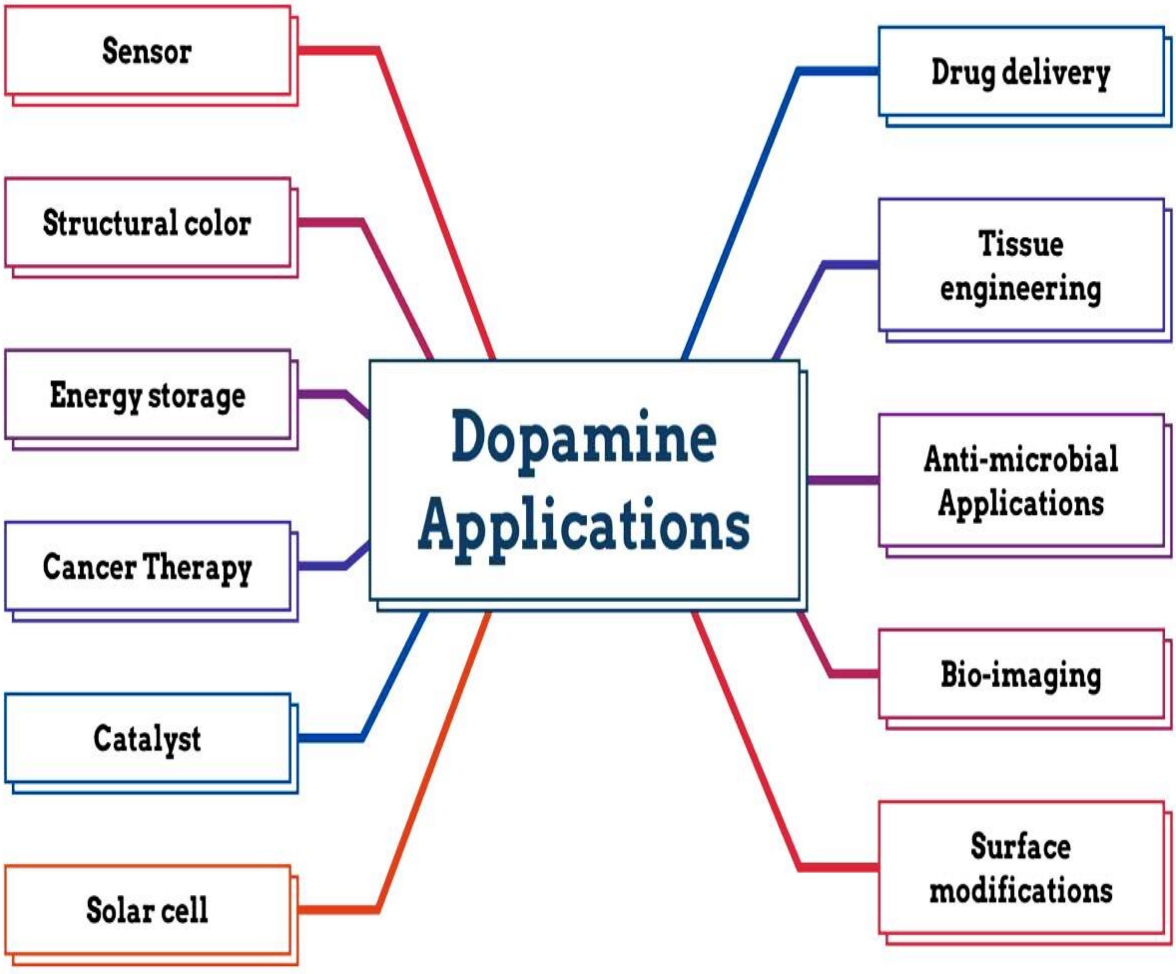

Figure (1-17) The possible application of dopamine.

1.10 Chitosan

Chitosan is a deacetylated derivative of chitin, as shown in Fig. (1-18) a plentiful natural material with less storage capacity than cellulose. Chitosan, a renewable natural alkaline polysaccharide with no toxicity or adverse effects and excellent moisturizing and adsorption characteristics, is a copolymer made up of repeating units of 2-amino-2-deoxy-D-glucopyranose and residual 2-acetamido-2-deoxy-D-glucopyranose. Chitosan is produced by alkaline hydrolysis (deacetylation) of chitin and is also naturally present in certain fungal cell walls [87] .

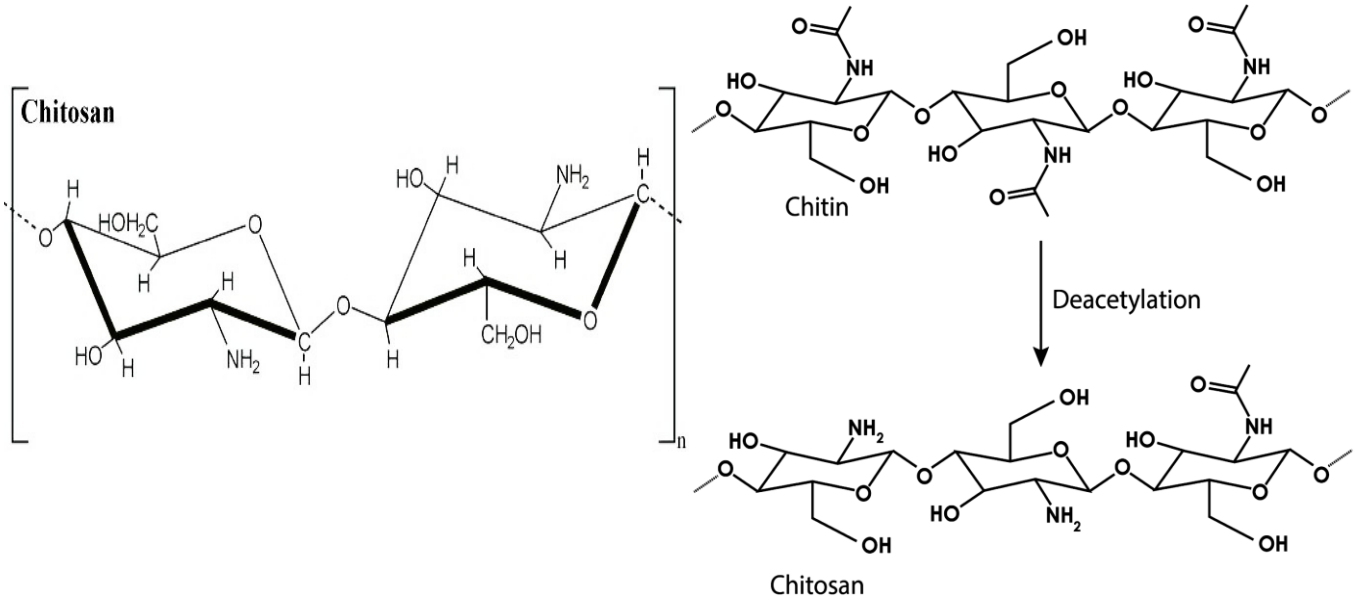

(A) (B)

Figure (1-18): shows (A) Chitosan chemical structure. (B) Chitosan from chitin by deacetylation [88] .

C_3-OH, C_6-OH, C_2-NH_2, acetyl amino and glycoside linkages, and other functional groups are present in chitosan molecules. A difficult bond to break is the glycosidic bond, and the acetyl amino link is just as strong among them. Second hydroxyl C_3-OH has a large steric barrier and is unable to rotate freely, which makes it challenging to react. With the application of different forms of molecular design, the active chemical properties of

C_6-OH and C_2-NH_2 allow these groups to incorporate additional groups into chitosan molecules [89].

These functional groups enable a wide range of alterations, as shown in Fig. (1-19), which produce polymers with novel characteristics and behaviors. Chitosan derivatives have been developed in order to improve the qualities of chitosan, such as solubility or biodegradability, or to incorporate new functions or properties. Deacetylation, depolymerization, and quaternization, among other techniques, have enhanced solubility in water watery conditions [90] .

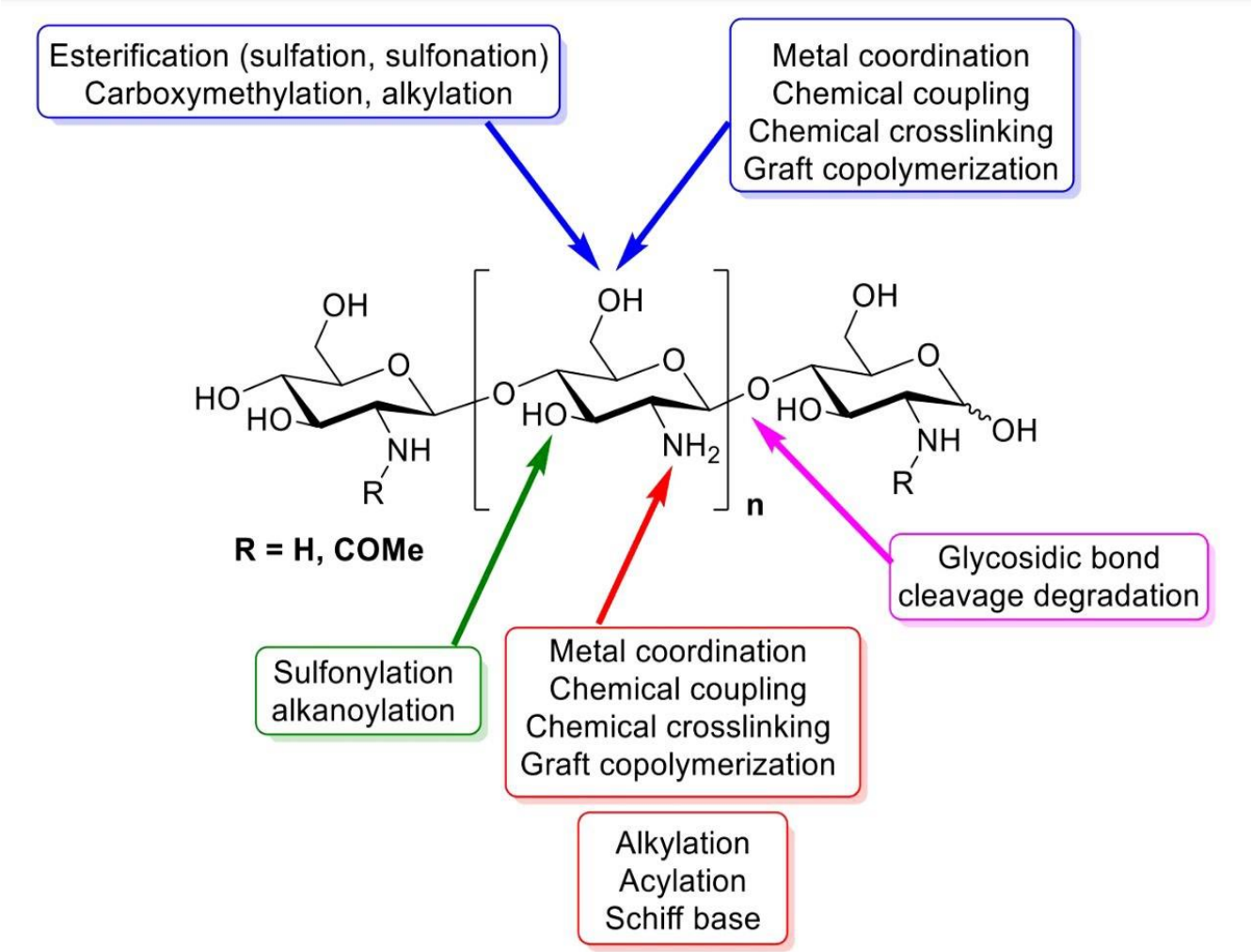

Figure (1-19) Explained the functional groups in chitosan's structure that are able to be chemically modified [90] .

1.10.1 Physical and chemical properties of chitosan.

Chitosan is a biopolymer derived from chitin, found in the exoskeletons of crustaceans like shrimp and crabs, there are some of its physical and chemical properties that shown in Fig.(1-20) .

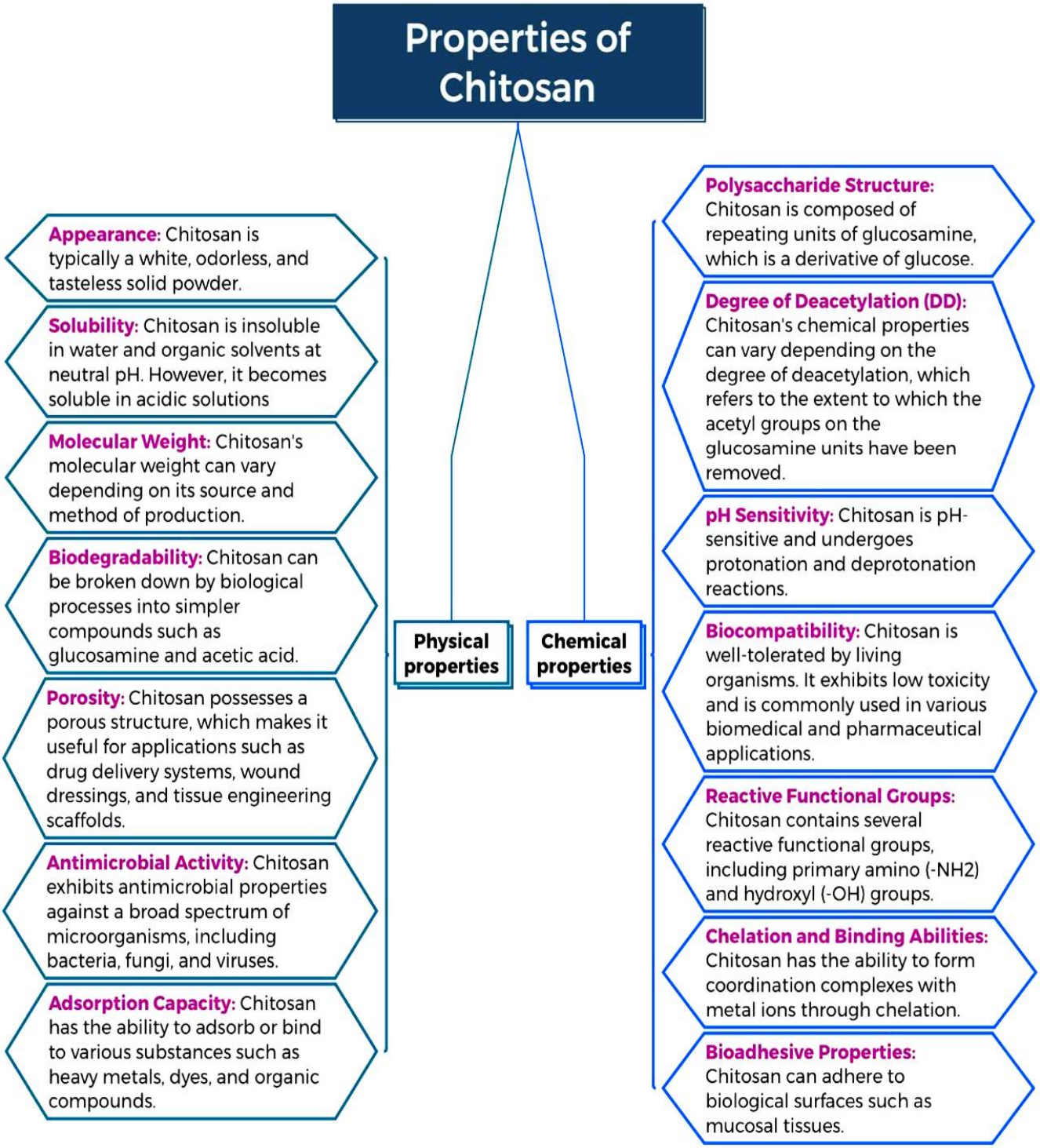

Figure(1-20) The diagram illustrated chemical and physical properties of chitosan [91] .

1.10.2 Applications of chitosan-based bio nanocomposites.

The use of chitosan in advanced wound care, pharmaceuticals and beauty products, agriculture, and the processing of food has revolutionized these industries due to its distinctive qualities. As the most important polysaccharide for the delivery of medications, chitosan is cationic due to its primary amino group content.

They are in charge of their many characteristics, including regulated drug release, permeability enhancement, muco-adhesion, and in situ gelation. Improved hemostatic potential can be achieved by adding biomolecules or biopolymers with a size of 100 nm when creating bio nanocomposites based on chitosan. While retaining the proper concentration level, biopolymer-clay composites can deliver the medicinal element to the intended location [92] .

Bio nanocomposites based on chitosan, that explain in Fig (1-21), possess the capacity to specifically penetrate the membranes of cancerous cells and impart anti-tumor action through several enzymatic, antiangiogenic, immune-stimulating, and apoptotic mechanisms. The anticancer impact of chitosan-metal complexes is due to their ability to scavenge free radicals and interact with cellular DNA. It has been demonstrated that soluble forms of low-MW chitosan oligosaccharides can stop the growth of tumors [93] **.**

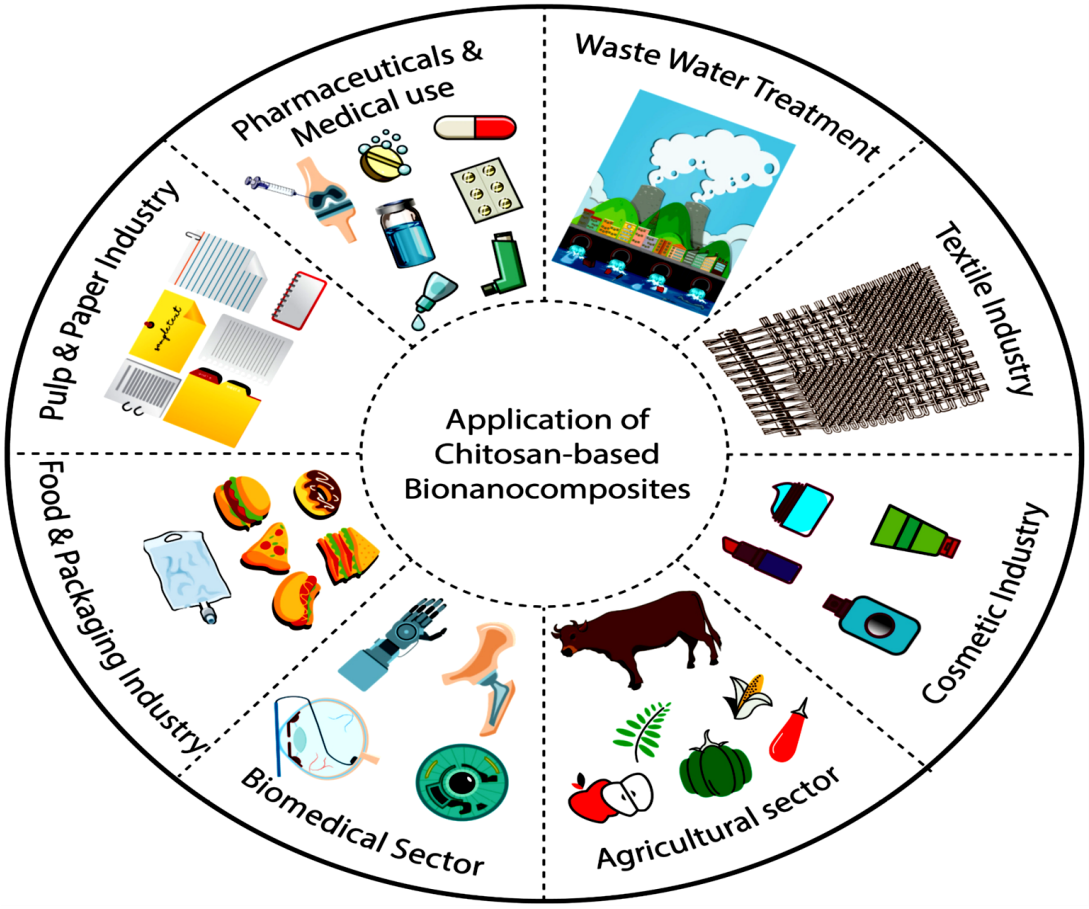

Figure (1-21): Application of chitosan based on bionanocomposites [94] .

1.11 Temozolomide

Temozolomide (3,4-dihydro-3-methyl-4-oxoimidazo-[5,1-d]-as-tetrazine-8-carboxamide TZ), its structure shown in Fig. (1-22) is a imidazotetrazine derivative alkylating drug used to treat primary brain tumors. Temozolomide was approved by the FDA as an oral capsule on the 11th of August 1999, and as an injection via intravenous on February 27, 2009 [95] .

Temozolomide is a prodrug of imidazotetrazine that needs to be hydrolyzed nonenzymatically in vivo at physiological pH in order to carry out the alkylation of adenine/guanine residues. This process damages DNA through cycles of unsuccessful repairing, ultimately leading to cell death [96] .

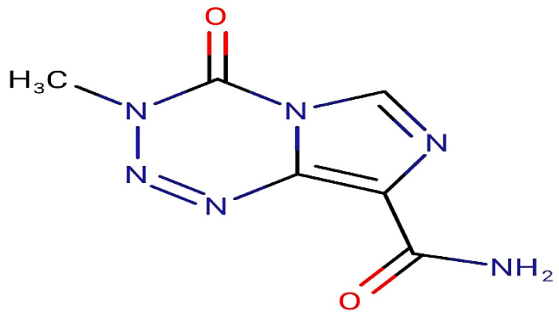

Figure (1-22) Chemical structures of temozolomide [97] .

1.11.1 Mechanism of Action to Temozolomide

Temozolomide is stable at both neutral and acidic pH levels and is quickly and thoroughly absorbed in the digestive system. As a result, temozolomide can be given intravenously and orally. After absorption, temozolomide undergoes a nonenzymatic chemical conversion that results in the active compound 5-(3-methyltriazen-1-yl) imidazole-4-carboxamide (MTIC) + carbon dioxide and a metabolite called temozolomide acid. This process starts at physiological pH but speeds up with increasing alkalinity. When MTIC and water mix to make 5-aminoimidazole-4-carboxamide (AIC) and a highly reactive cation, the result is the active alkylating species known as methyl diazonium cation [98].

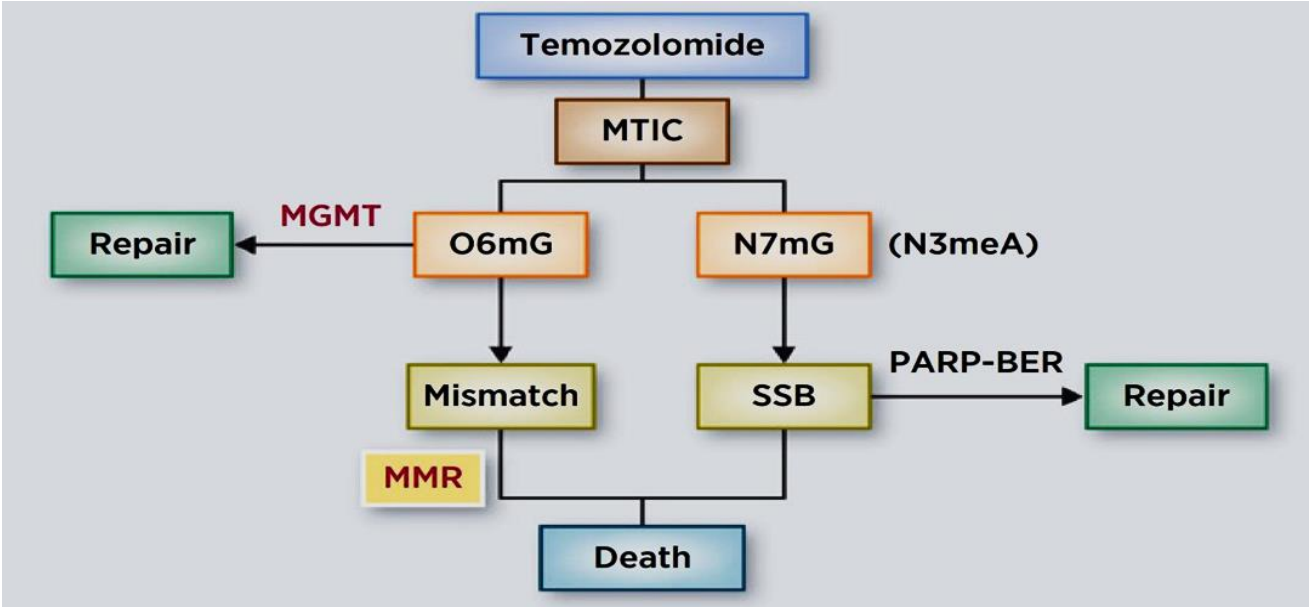

Figure (1-23) Schematic representation of mechanisms of cytotoxicity of temozolomide [99] .

Water reacts with the electropositive C4 atom of temozolomide, producing MTIC and carbon dioxide. MTIC is a reactive methylating chemical that degrades to methyldiazonium ion. Imidazotetrazinones are important DNA-alkylating compounds that work in grooves. They are binding the middle guanine residue of the GGG sequence in a base-selective and preferential manner. DNA methylation occurs at the O3 atoms on adenine, the N7 atoms on guanine, and the O6 atoms on guanine. Despite making up a very small portion of the adducts that temozolomide forms, O6-methylguanine is crucial to the cytotoxic action of the medication. Other active drugs against malignant tumors assault DNA at the O6 atom of guanine [100] .

O6-methylguanine does not interfere with DNA replication or transcription and is not hazardous to cells. On the other hand, thymine rather than cytosine is included in the vicinity of O6-methylguanine as a result of the favored base pairing during DNA replication. The aberrant thymine group in the daughter strand is excised by a cell's mismatch repair system upon recognition of this mismatch. But thymine will certainly be reinserted across from the lesion until the methyl group adduct from the guanine is removed. When O6-methylguanine is present, the mismatch repair pathway's MutS branch is crucial for initiating apoptosis. It is thought that repeatedly failing mismatch repair rounds cause chronic strand breaking, which sets off an apoptotic response [101] .

1.11.2 Physical and chemical properties of Temozolomide.

Temozolomide is a chemotherapy drug that is effective against certain cancers in the central nervous system as well as systemic malignancies. It belongs to the alkylating agent class and is derived from dacarbazine. Its primary mode of action involves interfering with DNA replication, which inhibits the growth of cancer cells. there are some of the key properties of temozolomide that shown in fig (1-24) [102] .

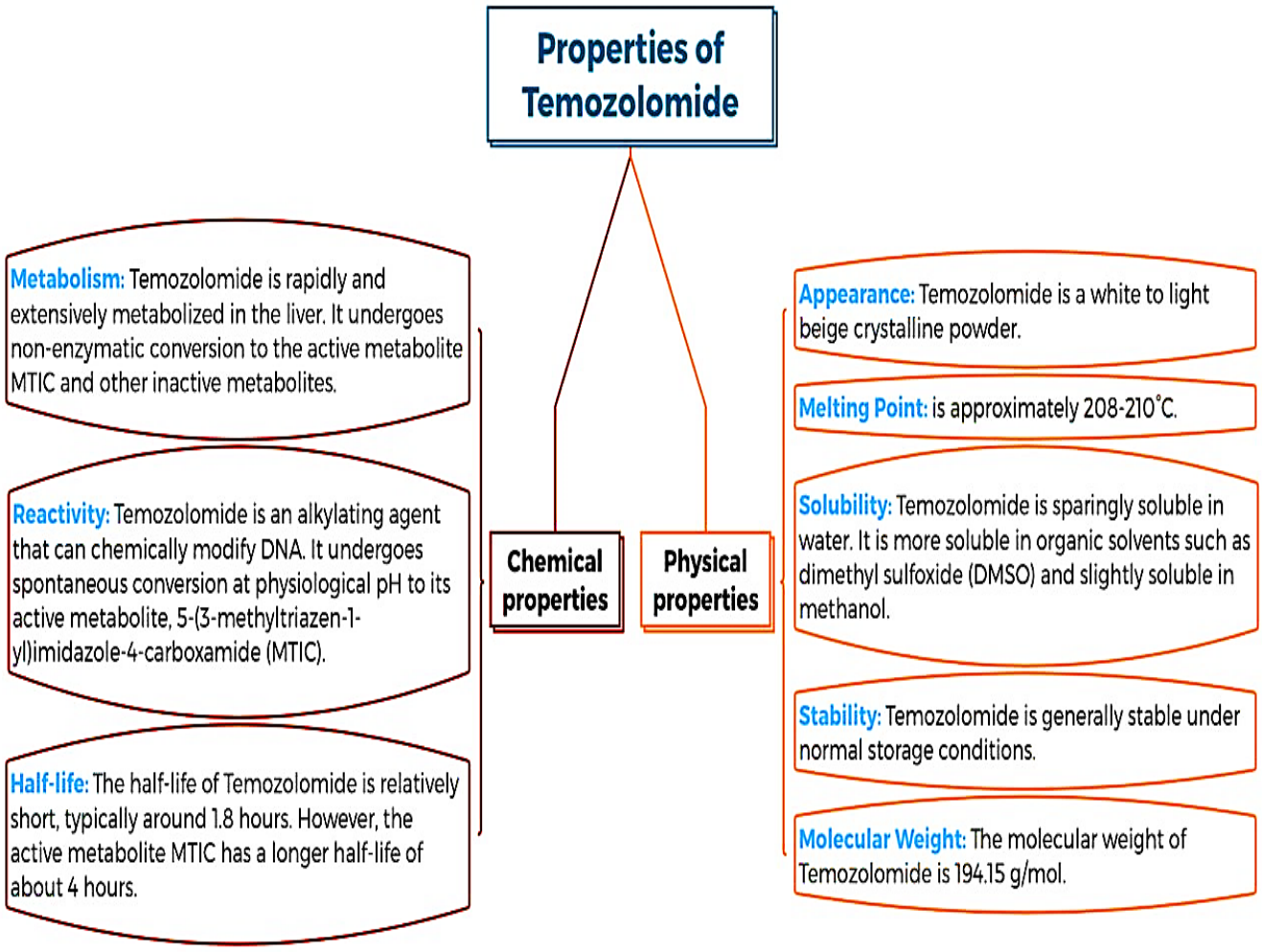

Figure (1-24): Diagrammatic explanation of physical and chemical properties of temozolomide.

1.12 Chromatography

Chromatography is a method for separating a mixture's constituents, or solutes, according to how much of each solute is dispersed between a stationary phase that is continuous and a flowing fluid stream, referred to as the mobile phase. While the stationary phase can be either a solid or a liquid, the mobile phase can be either a liquid or a gas. Chromatography is an important biophysical technique that makes it achievable to separate categories , and remove mixture components for both qualitative and quantitative study. Features

including size and shape, total charge, surface hydrophobic groups, and stationary phase binding capabilities can all be used to refine samples. Ion exchange mechanisms, surface adsorption, partitioning, and size exclusion are the four methods of separation that are based on molecular properties and the type of contact. One of the most used techniques, column chromatography makes use of advanced machinery to produce separations with a high degree of resolution. However, this might not be required for all applications [103] .

1.12.1 Classification of Chromatography

Chromatography is a versatile separation technique used in various scientific fields to separate and analyze complex mixtures. It involves the separation of different components of a mixture based on their physical or chemical properties as they interact with a stationary phase and a mobile phase. Chromatographic techniques can be classified based on several factors, including the nature of the stationary phase, the mode of separation, and the principle of separation. The common classifications of chromatography that explained in Fig. (1-25) [104] .

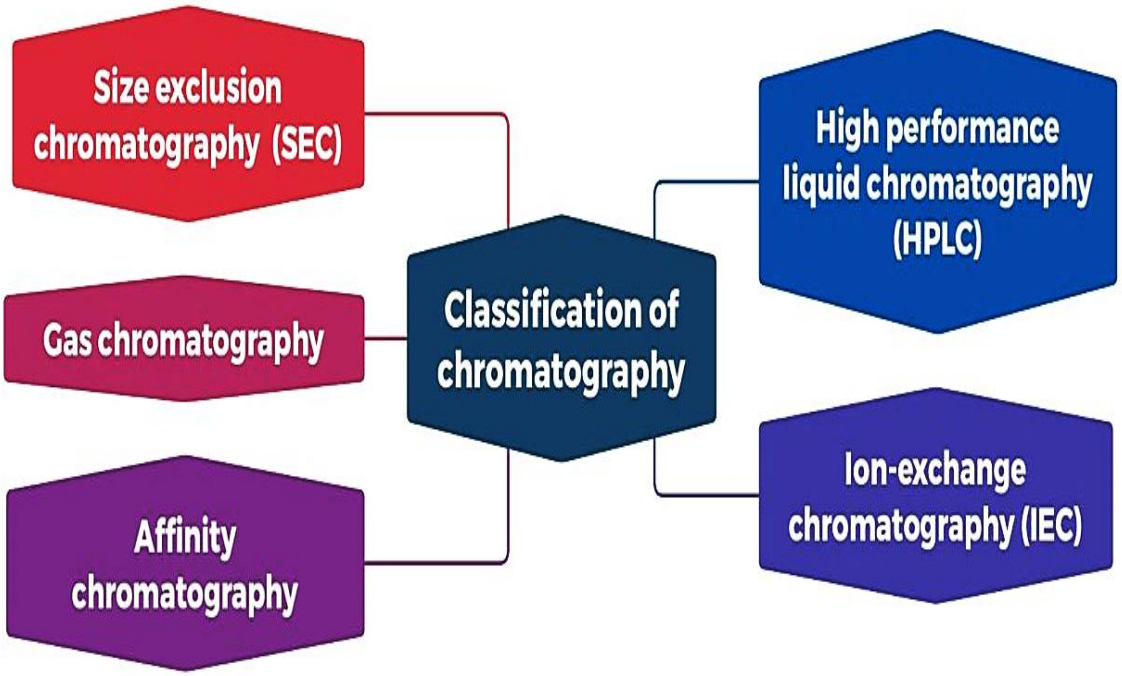

Figure (1-25) Schematic representation of some types of chromatography.

1.12.2 High Performance Liquid Chromatography (HPLC)

Using this chromatography technique it is possible to separation , determine, and purification of many molecules within a short time, This technique yields perfect results in the separation, and identification of amino acids, carbohydrates, lipids, nucleic acids, proteins, steroids, and other biologically active molecules [105] .

HPLC works on the principle of selective partitioning of analytes between a stationary phase (usually a solid or packed particles) and a mobile phase (liquid). The mixture is passed through a column packed with the stationary phase. Components with different affinities for the stationary phase and the mobile phase will move through the column at different rates, causing separation[106].

The HPLC contains two phases, the mobile phase and stationary phase which are crucial components that work together to separate the components of a sample.

A. **Mobile Phase:** The mobile phase is the liquid solvent or mixture of solvents that flows through the column during the chromatographic process. It carries the sample through the column and interacts with the stationary phase to facilitate separation. The choice of mobile phase depends on the nature of the sample and the desired separation mechanism. Common mobile phase solvents include water, acetonitrile, methanol, and mixtures thereof. The composition of the mobile phase can be varied to improve separation such as using gradual elution where the composition changes with time[107] .
B. **Stationary Phase:** The stationary phase is a packed or solid materials that is remain fixed inside the column. The stationary phase reacts with the mobile phase and the components of the sample, leading to separation based on the difference in affinity. The stationary phase can be polar or non-polar, depending on the type of separation required. Common stationary phases include the silica gel phase, revers-phase C18 ,Ion-exchange resins and chiral phases The choice of stationary phase depends on

factors such as the polarity of the sample components and the desired separation mechanism.[108] .

The interaction between the stationary phase, mobile phase, and components of sample is lead to the separation process in HPLC.

1.12.2.1 Instrumentation of HPLC

The HPLC device is designed to control the flow of the mobile phase, introduce the sample into the system, separate the components of the sample, detect the separated components, and collect and analyze the data generated during the analysis [109], the Fig (1-26) explain the components of a typical apparatus for HPLC system . The instrumentation of HPLC typically including many components:

1. **Pump:** The pump is responsible for generating and maintaining the flow of the mobile phase through the system as it delivers the solvent at a constant flow rate to obtain reproducible results.[110] .
2. **Injector:** The injector is used for the purpose of introducing the sample into the HPLC system. The injector measures precise quantities and injects small amounts of the sample into the mobile phase stream. [110] .
3. **Column:** The column is the main separation component of the HPLC system. It consists of a stationary phase packed into a stainless steel or glass tube. The stationary phase interacts with the components of the sample to separate them based on their chemical properties [110] .
4. **Detector:** The detector is used to monitor the eluent leaving the column. It detects the separated components based on their physical or chemical properties and generates signals proportional to their concentration. Common types of detectors include UV-Vis detectors, fluorescence detectors, refractive index detectors, and mass spectrometers [110] .

5. **Column Oven:** The column oven is used to control the temperature of the column. Temperature control can improve separation efficiency and reproducibility by controlling the interactions between the analytes and the stationary phase [110] .
6. **Data System:** The data system collects, processes, and analyzes the signals generated by the detector. It typically includes software for instrument control, data acquisition, and data analysis [110] .
7. **Pressure Regulator:** Since HPLC operates at high pressures (typically between 1000 and 6000 psi), a pressure regulator is used to maintain a constant pressure throughout the system [111] .
8. **Solvent Reservoirs:** These contain the solvents used as the mobile phase. Multiple solvent reservoirs may be used for gradient elution HPLC [111] .
9. **Waste Collector:** It collects the waste from the system, which may include solvent waste and used columns [111] .

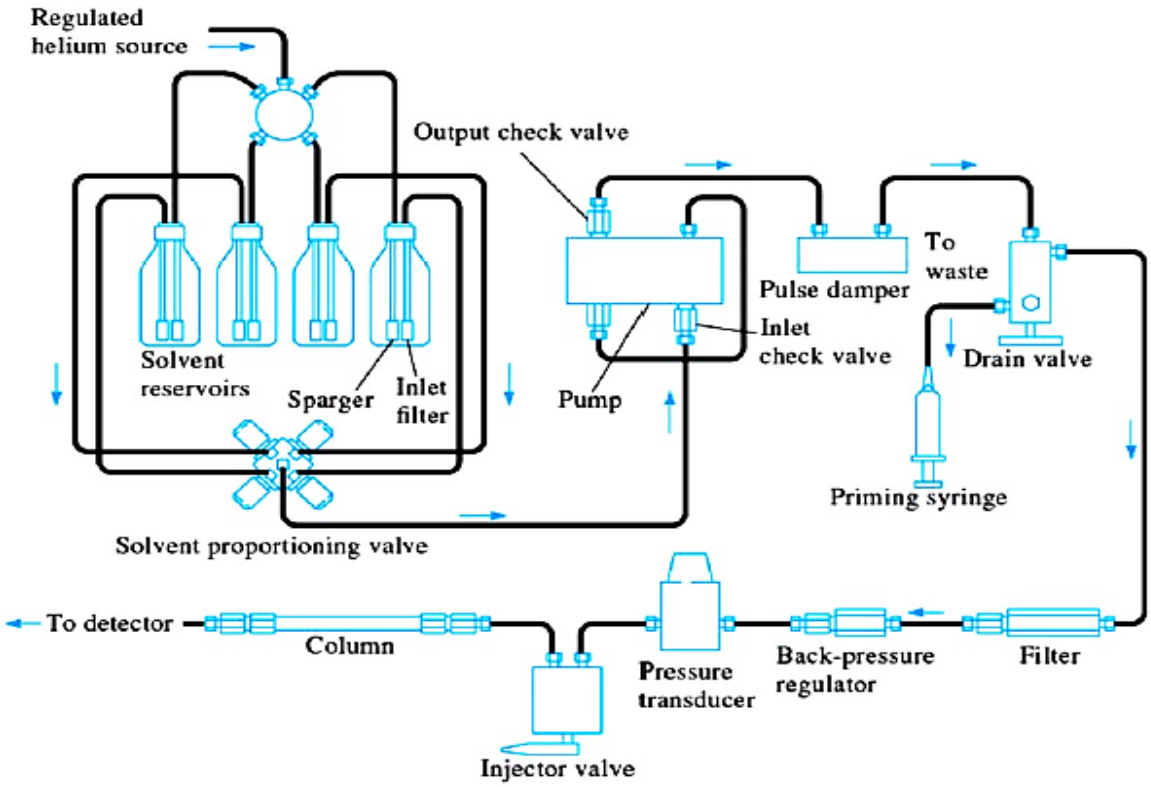

Figure. (1-26): Diagram showing components of a typical apparatus for HPLC system [112]

1.12.2.2 Types of mode in HPLC

A. **Normal Phase HPLC (NP-HPLC):** In NP-HPLC, the stationary phase is polar, such as silica gel, while the mobile phase is non-polar. Separation is based on the polarity differences between sample components and the stationary/mobile phases. It's suitable for separating polar compounds like organic acids, amino acids, and vitamins [113] .

B. **Reverse Phase HPLC (RP-HPLC):** In RP-HPLC, the stationary phase is non-polar, such as C18-bonded silica, while the mobile phase is polar. Separation is based on hydrophobic interactions between the non-polar stationary phase and the sample components. It's widely used for separating non-polar and moderately polar compounds like pharmaceuticals, lipids, and peptides [113] .

1.12.2.3 HPLC Description

These descriptors are essential for method development, optimization, and troubleshooting in HPLC analysis, as they provide insights into the separation mechanism and performance of the chromatographic system.

A. **Retention Time:** The time it takes for a compound to clear from the column after injection. Retention time is affected by multiple factors such as the stationary phase, mobile phase composition, column temperature, and properties of the compound such as size and polarity [107] .

B. **Retention Factor (k):** The retention factor is also called the capacity factor, and it is a measure of the strength of the compound's interaction with the stationary phase relative to the mobile phase which can be calculated from the ratio of the time the compound spends in the stationary phase to the time it spends in the mobile phase [107].

C. **Resolution:** it can be measured as the ability of the chromatography system to separate two adjacent peaks. Column efficiency, operating conditions, and selectivity are factors that are taken into account[107] .

D. **Peak Width:** is the width at the base of the chromatographic peak and is often expressed as full width at half maximum (FWHM) and is affected by factors such as column efficiency, flow rate, and diffusion. [114] .

E. **Selectivity:** is the ability of the stationary phase to distinguish between different compounds depending on their chemical properties and determines the degree of separation between peaks [114] .

F. **Efficiency**: Refers to the ability of the column to resolve individual components of a mixture. It's often quantified using parameters like theoretical plates or plate height [114].

G. **Capacity:** The maximum amount of sample that can be loaded onto the column without overloading it. It's influenced by factors like column dimensions, stationary phase chemistry, and sample properties [114] .

1.14 The Aim of the Work.

This study aims to:

1. Prepare nanostructures via self-assembly of the organic – inorganic hybrid of molecular metal oxides with some coatings such as dopamine, Chitosan and /or conducting polymer nanostructure as drug delivery systems.
2. Investigate the possibility of loading different drugs (such as anticancer treatment drugs) into the as- prepared nanostructure for drug delivery purposes.
3. Study and evaluate how the pH conditions affect the release behavior of the TMZ drug from the hierarchical nanostructures.
4. Investigate the drug release behavior from the nanostructure using HPLC technique and finding the loading weight and the Optimum condition for better loading and control release.
5. Controlled release systems aimed to sustain the desired drug concentration in the bloodstream or specific tissues for an extended duration.

Chapter Two
Experimental part

2.1 Chemicals

The chemicals that used In this work are listed in Table (2-1), used without further purification.

Table (2-1) The chemical use in this work.

No.	Chemicals	Chemical formula	Company supplied	Percentage of Purities/Concentration
1	Dopamine hydrochloride (DP)	$C_8H_{11}NO_2$	Thermo fisher (TMO)	99%
2	Chitosan	$C_6H_{11}NO_4$	Central Drug House (CDH)	99%
3	Temozolomide	$C_6H_6N_6O_2$	Sigma-Aldrich	99%
4	Glycine	$C_2H_5NO_2$	THOMAS BAKER	99%
5	Hydrochloric acid (HCL)	HCL	J.K.Baker Netherlands	36 – 38 %
6	Phosphate buffered saline (PBS)	$Cl_2H_3K_2Na_3O_8P_2$	HiMedia M1452-100G	99%
7	Phosphotungstic acid (PTA)	$H_3[P(W_3O_{10})_4]xH_2O$	HiMedia GRM398-100G	99%
8	Tris (hydroxymethyl) aminomethane	$C_4H_{11}NO_3$	HiMedia TC027-500G	99%
9	Acetonitrile	C_2H_3N	Supelco , Germany	99%
10	Hexamolybedate	Mo_6O_9	U.O.Kerbala	99%

2.2 Instruments

The instruments that used in this work are listed in Table (2-2).

Table (2-2) illustrated the instruments that were used in this study.

No.	Instrument	Places	Company
1	Hotplate Magnetic Stirrer	University of Karbala, College of Science	Heido-MrHei-Standard, Germany
2	Sensitive balance	University of Karbala, College of Science	BL 210 S, Sartorius- Germany
3	Digital pH meter	University of Karbala, College of Science	OAICTON-2100, Singapore
4	Centrifuge	University of Karbala, College of Science	Hettich- Universal II- Germany
5	Oven	University of Karbala, College of Science	Memmert, Germany
6	Ultrasonic	University of Karbala, College of Science	DAIHAN Scientific, Korea
7	High Performance Liquid Chromatography (HPLC)	University of Karbala, College of Science	UFLC-20A, Shimadzu, Japan
8	Double –beam UV-Visible-spectrophotometer	University of Karbala, College of Science	AA-1800, Shimadzu, Japan
9	Fourier-transform infrared spectroscopy (FT-IR)	University of Karbala, College of Science	FT-IR-8400S, Shimadzu, Japan
10	X-Ray Diffraction instrument	University of Tehran	Siemens model D500
11	Scan electron Microscopy (SEM)	University of Tehran	ZEISS model, Oxford instruments, UK
12	Atomic Force Microscopy (AFM)	University of Tehran	DME Denmark
13	X-Ray Photoelectron Spectra (XPS)	University of Tehran	Germany Bes Tek device model

2.3 Methodologies

2.3.1 preparation of chemical solution

A number of solutions was prepared in different pH including:

2.3.1.1 Phosphate buffered saline (PBS)

This solution was prepared by dissolving 0.8035 g of PBS in 100 mL of D.W the pH = 7.4 by using buffer.

3.2.1.2 Tris – HCl solution

Tris – HCl solution was prepared by dissolving a concentrated tris- HCl (10 mM) in 1 L of D.W the pH= 10.5 [115] .

3.2.1.3 Acetic acid solution

A 5 mL of acetic acid solution dissolved 500 mL of D.W.

3.2.1.4 Chitosan solution

Exact 0.2 g from chitosan dissolved in 50 mL of acetic acid solution.

3.2.1.5 Dopamin solution (DA)

A 5 mg from DA dissolved in 5 mL of Tris-HCl solution.

3.2.1.6 Phosphotungstic acid (PTA)

This solution was prepared by dissolving about 5 mg of PTA in 5 mL of Tris-HCl solution.

2.3.2 synthesis of hierarchical nano-structure

A group of hybrid nano composites were prepared by reacting raw materials including dopamine, chitosan, hexamolybedate, phosphotungstic acid, Phosphate buffered saline (PBS), Tris – HCl and Acetic acid with different condition . Only two compounds were use in this study the compound A that result from reaction of hexamolybedate and dopamine at pH 10.5 and compound B that result from reaction of hexamolybedate and chitosan.

2.3.2.1 Synthesis of A (hexamolybedate + dopamine) as-prepared nano-structure

Typically, in this study , synthesis of nano composite A in ratio 1:1 via reacting 1mg of POM (Hexamolypedate) which dissolved in acetonitrile (ACN) and 1mg of DA (Dopamine) which dissolved in 10 mM of Tris-HCl in pH 10.5 at room temperature , the result solution was visible as dark red color. The mixture aging for two hour then the product collected by centrifugation (5000 rpm , for 5 min) after that washing product with D.W for three times [77] the procedure illustrated in Fig. (2-1).

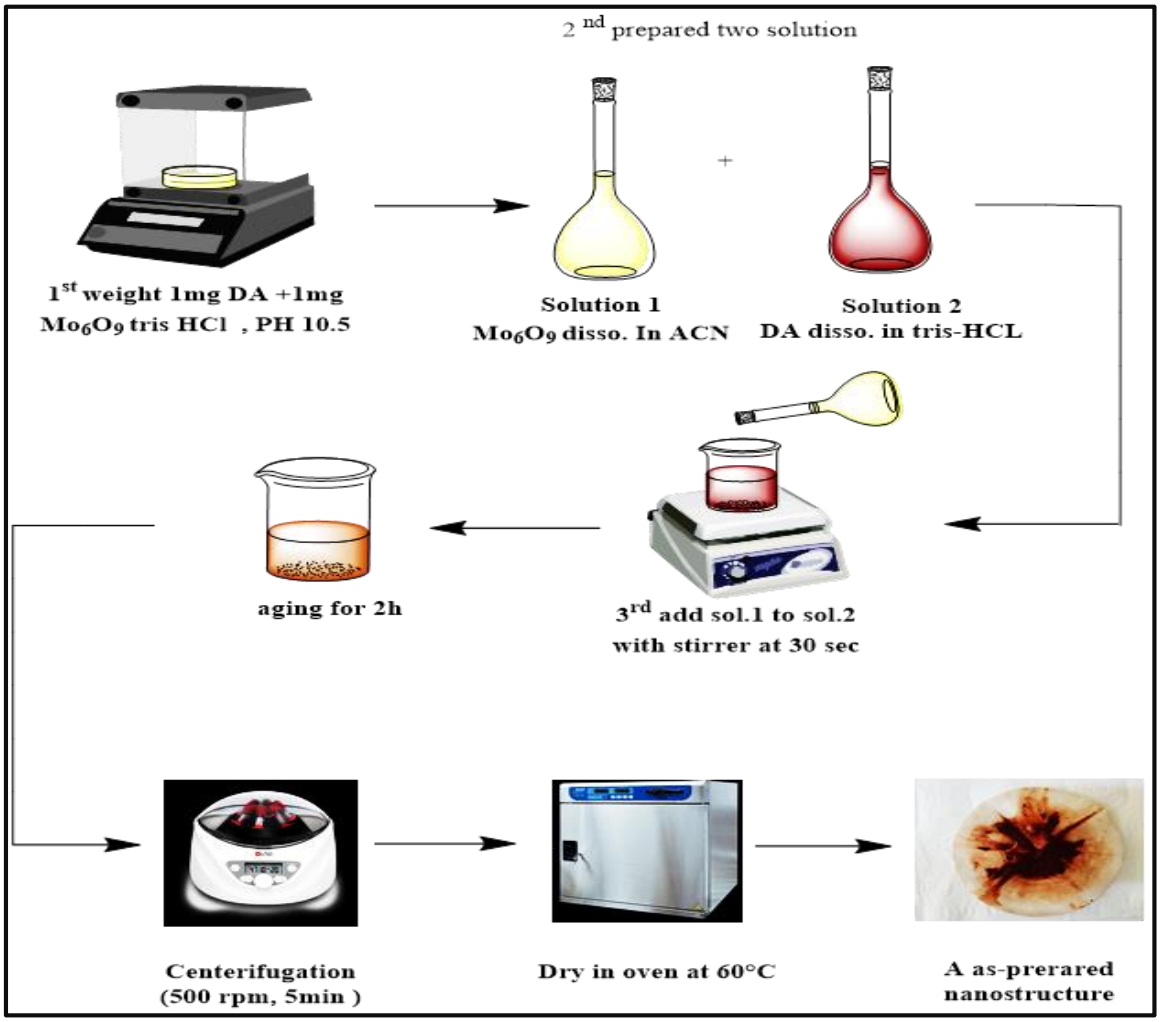

Figure (2-1) Schematic diagram of synthesis of A nano-structure.

2.3.2.2 Synthesis of B (hexamolybedate + chitosan) as-prepared nano-structure

In the same method for synthesis of nano composite A, and B nano-composite was synthesis in ratio 1:1 via reacting 1mg of POM (Hexamolypedate) which dissolved in acetonitrile (CAN) and 1mg of chitosan which dissolved in acetic acid solution , the result solution was visible as faint yellow color. The mixture aging for two hour then the product collected by centrifugation (5000 rpm , for 5 min) after that washing product with D.W for three times [77] the procedure illustrated in Fig. (2-2).

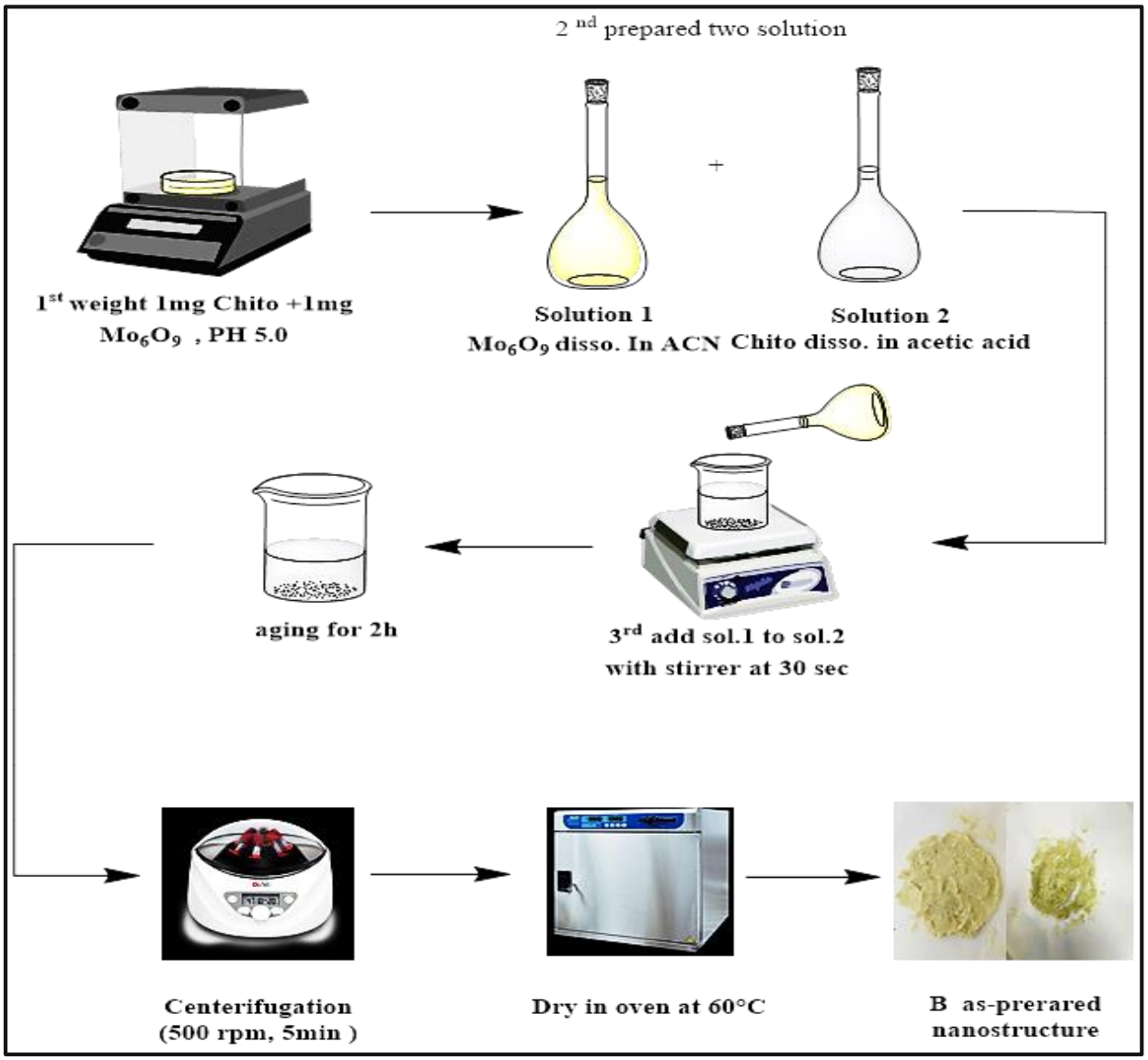

Figure (2-2) Schematic diagram of synthesis of B nano-structure.

2.3.3 Drug loading into as-prepared nano-structures

Temozolomide drug was chosen as model of drug in this study.

A. UV-Visible Measurement

The UV-Visible scan was done for temozolomide drug to determine the λ max that found equal 328 nm**.** That shows in Fig. (2-3).

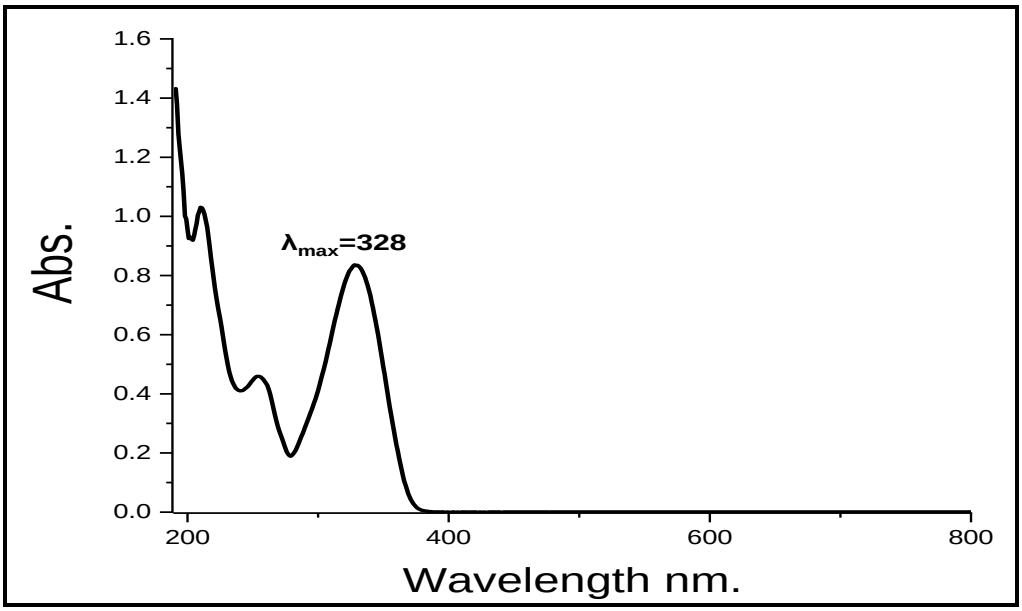

Figure (2-3) The UV-Visible scan for temozolomide.

B. High performance liquid chromatography (HPLC)measurement

HPLC analysis was conducted on Shimadzu system (Shimadzu, Tokyo, Japan) consisted of a binary pump and UV detector. Redone injection valve with a 20 μL loop used for injection of the samples and the chromatographic separation was carried out in C-18 column (μm particle size; Shiseido, Japan). The mobile phase consisted of Acetonitrile and water in ratio (60:40) was used. The freshly prepared mobile phase was filtered through a 0.45 μm pore size nylon membrane filter and pumped in an isocratic mode with a flow rate of 1mL/min. The elution of the analyte was monitored at a wavelength of 328 nm**.**

C. Loading of Temozolomide drug on nano composite

According to the standard method, take (10 mg) from nano particles was immersed in an aqueous solution of drug (0.5 mg/mL, 5 mL). The mixture was then shaken for 12 h at room temperature. Following this process. The sample was washed three times with ultra-pure water and subjected to centrifugation at 5000 rpm for 5 min to remove the unbound drug [116] which was explained in the Fig. (2-4).

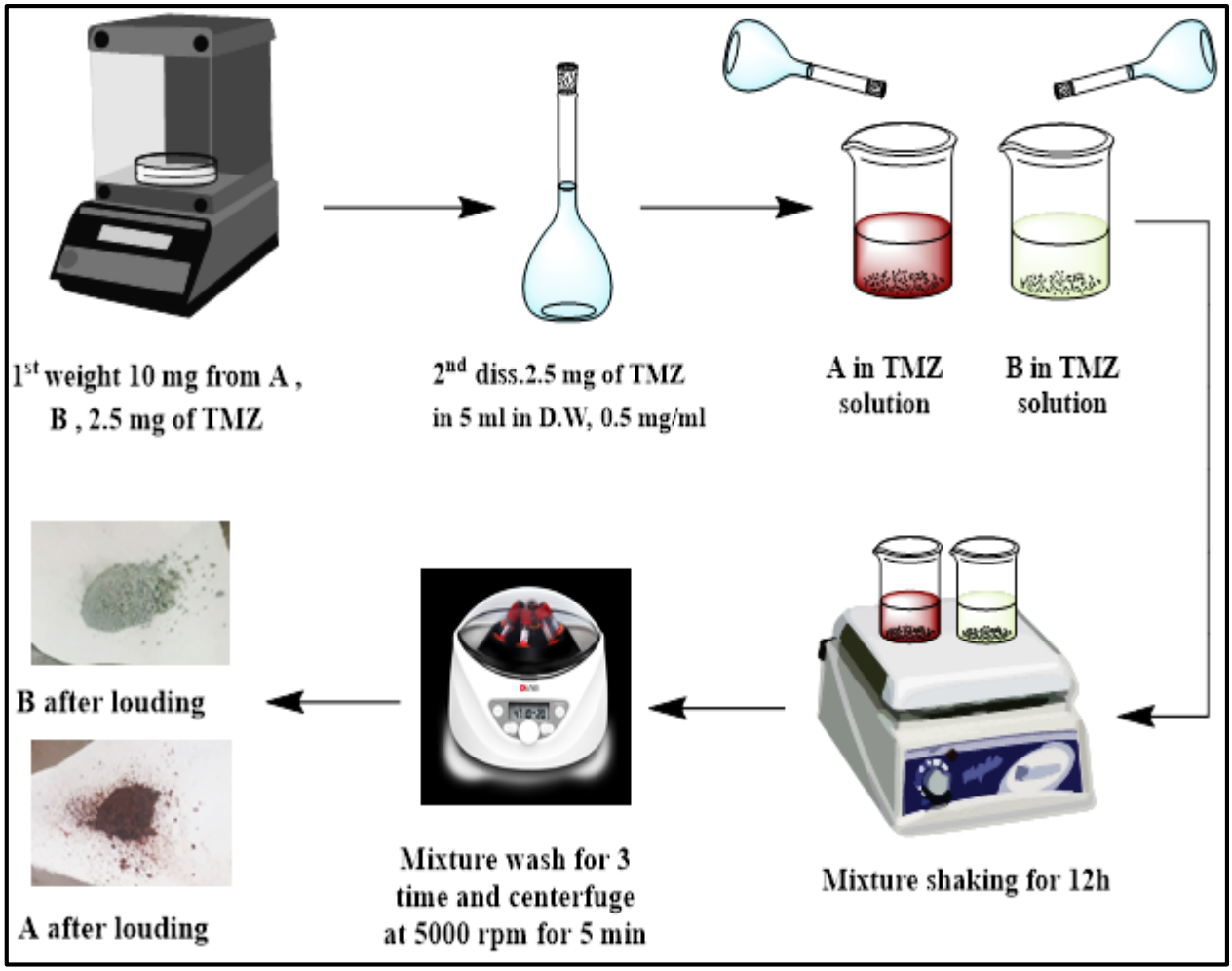

Figure (2-4) Temozolomide drug loading on nano composite (A, B).

2.3.4 In vitro release of temozolomide loaded on as prepared nanostructures.

Temozolomide release was achieved by immersing sample of hierarchical nanostructures loaded with Temozolomide (10 mg) under agitation on shaker plate (500rpm) in two mediums: an acidic medium (pH 2.8 glycine-HCl buffer solution) and neutral medium

(pH 7.4 phosphate buffered saline (PBS) solution) over a period of 24h. The amount of temozolomide release was determined by taking aliquots (0.5ml) of supernatant at timed intervals where same volume of fresh buffer solution was added for replacement. Finally, the amount of temozolomide released was measured on the basis of the HPLC at 328 nm and temperature at 37 C^{o} that is explained in Fig. (2-5).

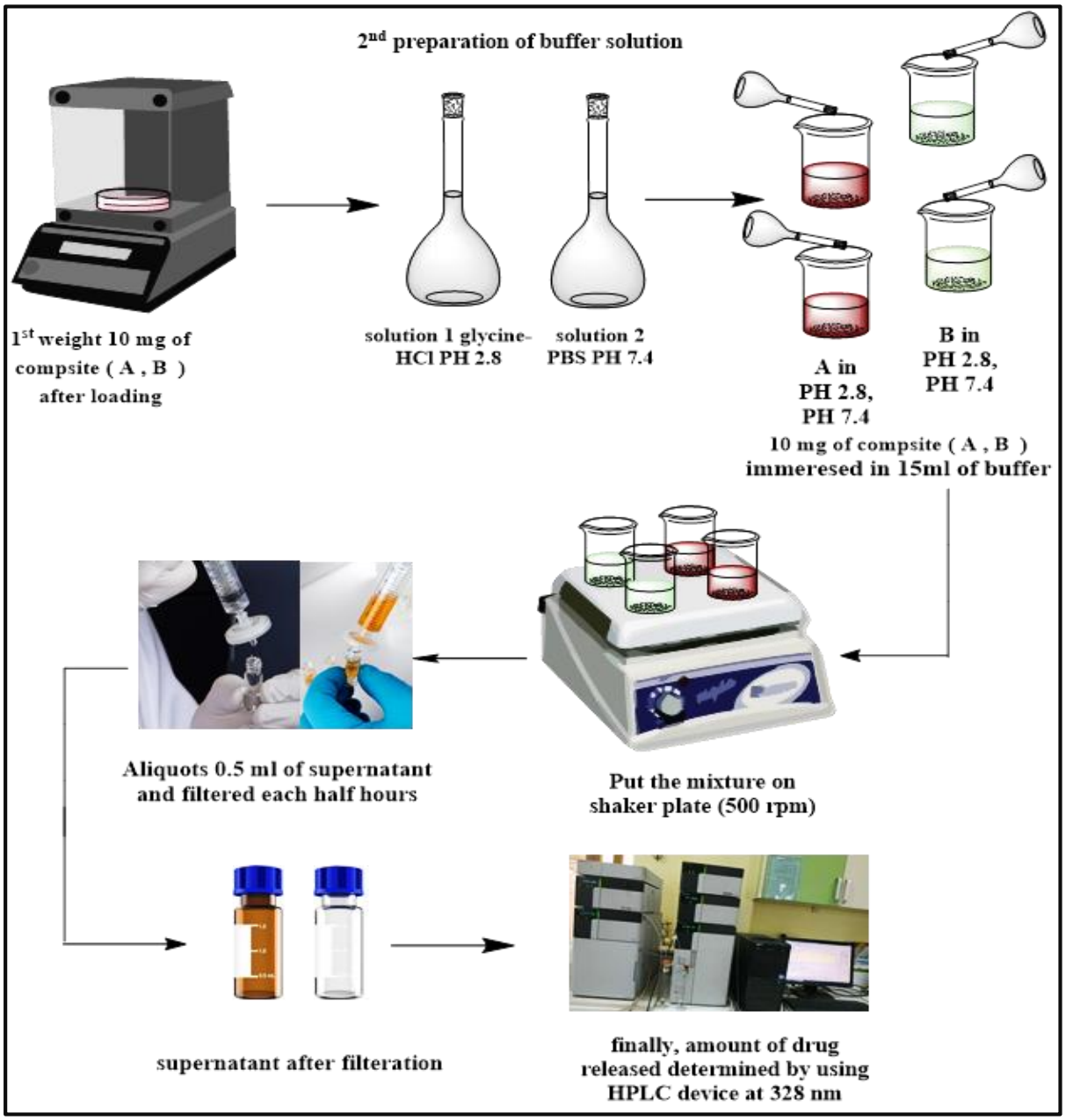

Figure (2-5) In vitro release of temozolomide loaded on as prepared nanostructures.

Chapter Three
Result and Discussion

3.1 Characterizations of nanostructures before and after drug loading

In this work, the studied samples were determined by characterization such as employing XRD, SEM, FTIR, and XPS techniques.

3.1.1 Fourier Transform Infrared Spectroscopy (FTIR)

3.1.1.1 The Fourier transform infrared (FTIR) spectra of DA, POM, Chitosan and Temozolomide.

The FT-IR spectrum of dopamine exhibits several characteristic peaks that correspond to different molecular vibrations as in Fig. (3-1). Based on the observed peaks, there is a wideband at low energy enclosing three important peaks, peak at 3344 cm^{-1} This peak is assigned to the stretching vibration of the hydroxyl group (OH) in dopamine. Peak at 3144 cm^{-1} This peak corresponds to the stretching vibration of the aromatic carbon-hydrogen (CH) group in dopamine. Peak at 2958 cm^{-1} this peak is assigned to the stretching vibration of the NH group in dopamine. Other small peaks in the range of 2723-2642 cm^{-1} correspond to various CH vibrations in aryl or aliphatic CH bonds. These vibrations are associated with the carbon-hydrogen (CH) bonds in the aromatic or aliphatic parts of the dopamine molecule. At higher energies, Peak at 1500 cm^{-1} represents the bending vibration of the CH groups in dopamine. Peak at 1284 cm^{-1} corresponds to the stretching vibration of the aryl oxygen in dopamine .The peak at 1327 cm^{-1} is attributed to the OH groups of the dopamine molecule.[1]

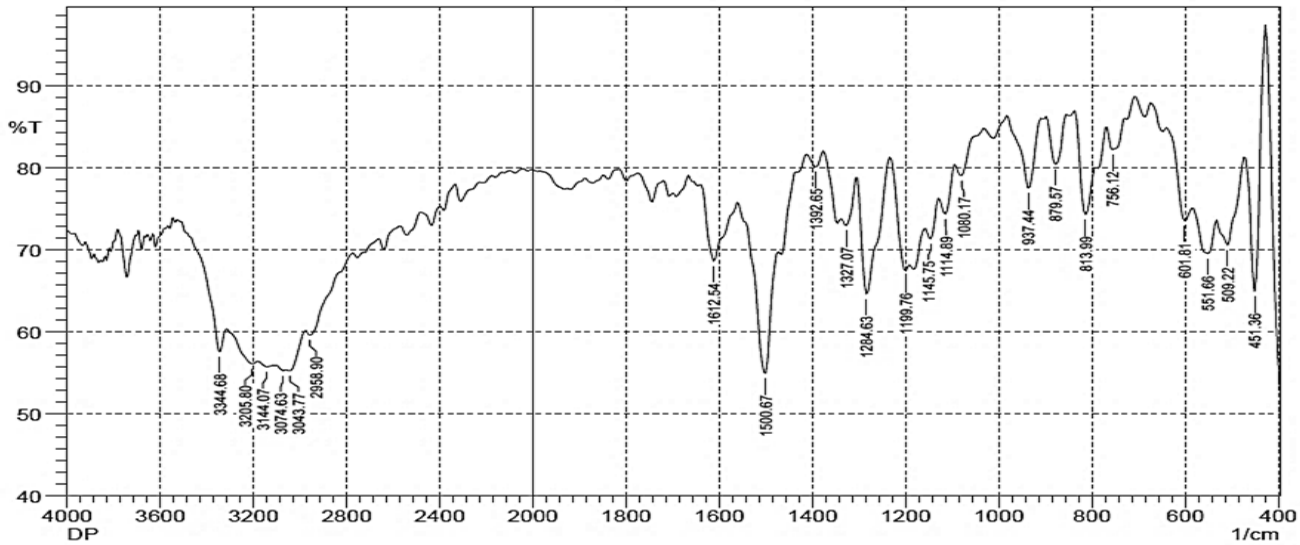

Figure (3-1) FT-IR spectrum of dopamine.

The hexamolybdate compound was analyzed by FT-IR spectrum in Fig. (3-2). The obtained compound appeared as yellow crystals with a characteristic FT-IR spectrum. The spectrum showed strong bands at approximately 956 cm^{-1} and 786 cm^{-1}, which can be attributed to the presence of Mo=O and Mo-O bonds in the compound. These bands provide strong evidence of the formation of hexamolybdate. Additionally, the FT-IR spectrum exhibited bands at 2966 cm^{-1}, 2935cm^{-1} and 2874 cm^{-1}, which can be assigned to the stretching vibrations of C-H bonds. Specifically, these bands are related to the CH2 and CH_3 groups of the tetrabutylammonium cation (counter ion). [117]

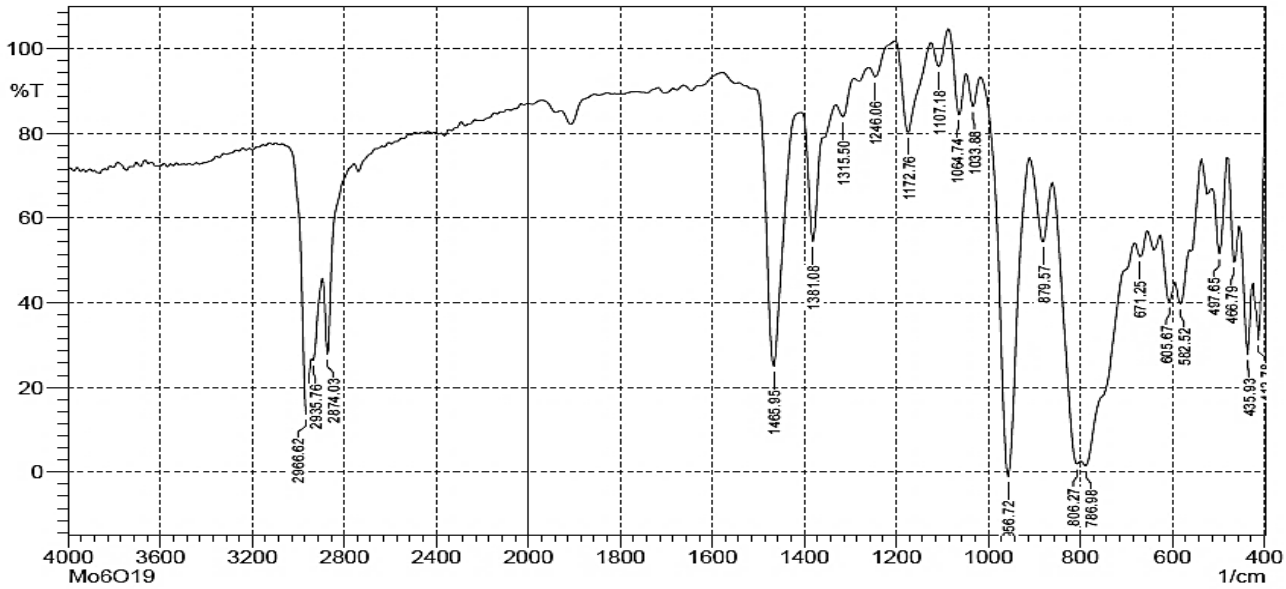

Figure (3-2) FT-IR spectrum of hexamolybdate .

Fig. (3-3) explains FTIR analysis for the chitosan, the FTIR spectrum showed intense broad peak at 3460 cm^{-1} was the characteristic of the hyroxyl-bonded (OH) stretch band. The band at 1643 cm^{-1} belonged to stretch amine group (NH_2) that appears as medium intensity peak. The band at 1516 cm^{-1} arises from presence of amide group (C=O and N-H) which is medium intensity peak. The band was observed between 1072 and 929 cm^{-1}, representing the stretching vibration of the glycosidic linkage (C-O-C) that appears as medium intensity peaks. FTIR spectroscopy measurements are carried out to identify the biomolecules that bound specifically on the given chitosan.[118]

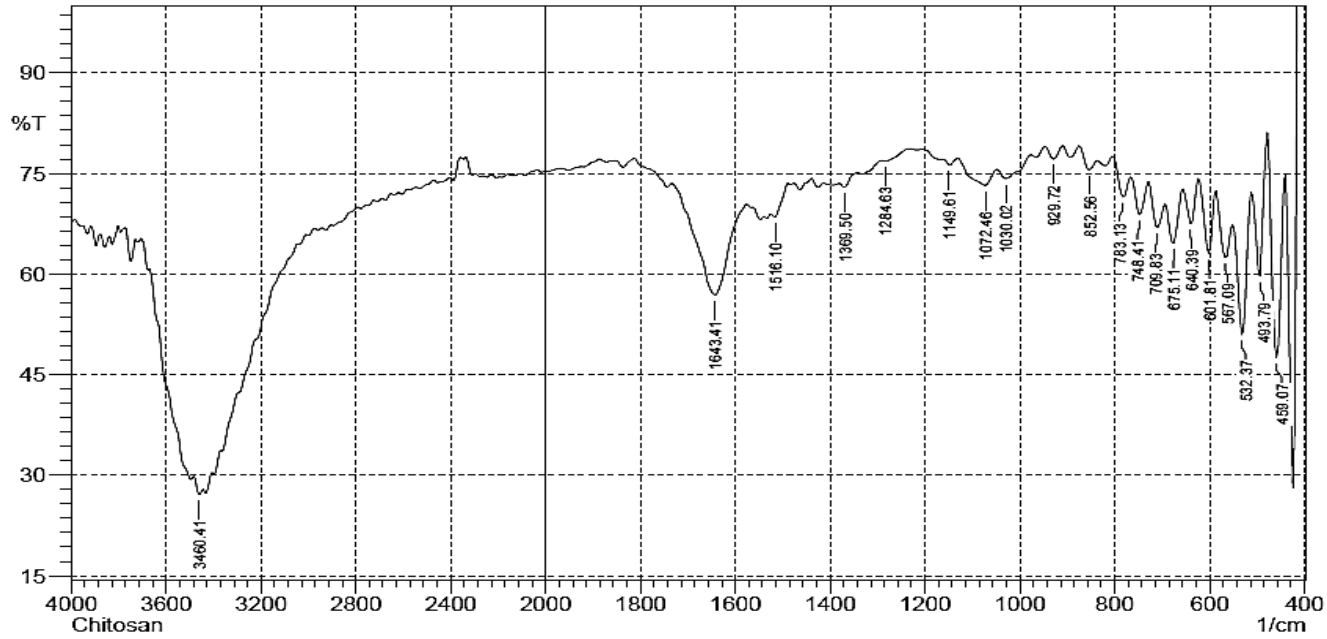

Figure (3-3) FT-IR spectrum of chitosan.

The FT-IR spectrum of TMZ as in Fig. (3-4) provides valuable information about its molecular structure and functional groups. The absorption band at 3387 cm^{-1} matches NH stretching vibrations, while band at 3117 cm^{-1} is attributed to the asymmetric stretching of the alkyl groups. The absorption band at 1732-1678 cm^{-1} is associated with the amide (-NH-C=O) group. These results confirm the chitosan structure.[119]

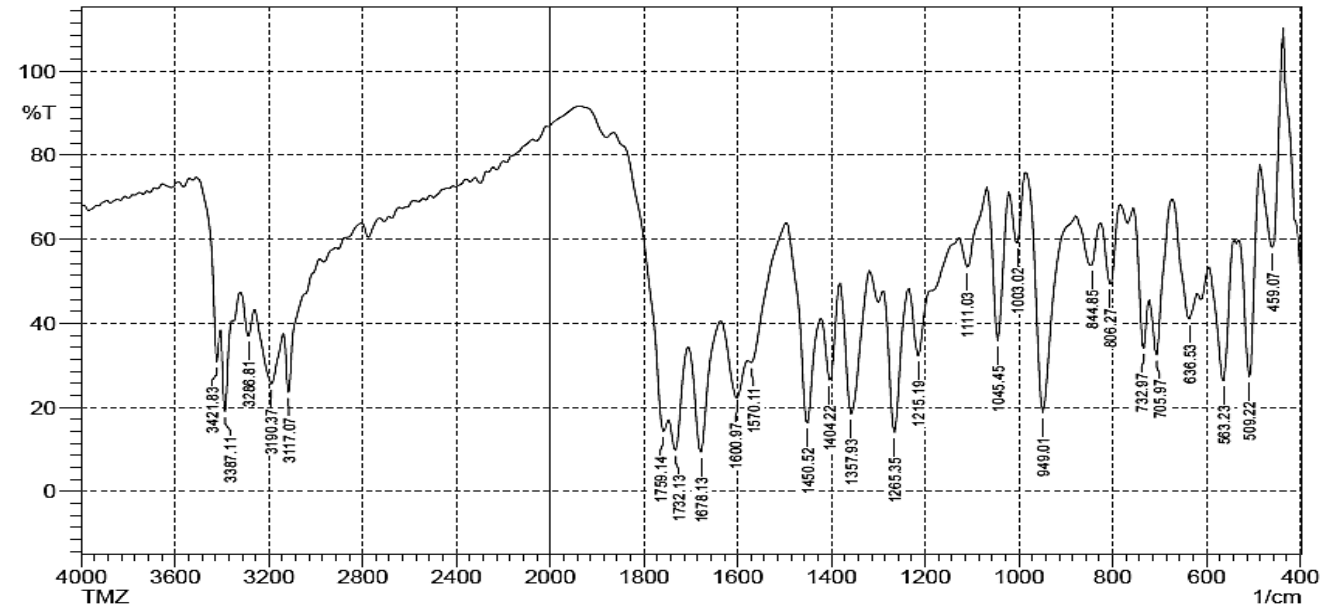

Figure (3-4) The FTIR spectrum of Temozolomide.

3.1.1.2 The Fourier transform infrared (FTIR) spectra of POM-dopamine nano-composite prior and after loaded with TMZ

Fig. (3-5.A) displays the Fourier-transform infrared (FT-IR) spectra of POM-dopamine nanocomposite. From the graph, the most characteristic bands of the precursor with slight shifted can be seen clearly. Band at 2970 cm^{-1} is the POM characteristic band which is shifted to confirm the involvement of dopamine in the complexation process. This shift indicates that dopamine complicates with POM through hydrogen bonding or other intermolecular force. This was also supported by the shifts at 1485 cm^{-1} and 956 cm^{-1} in the POM characteristic bands. On the other hand, two bands at 3047 cm^{-1} and 1593 cm^{-1} in the dopamine characteristic bands are also shifted and further approve the complexation process with POM. According to these data, it can be assuring the alterations in the molecular environment of both POM and dopamine due to the interaction with each other confirm the successful preparation of the POM-DA nano-composite.

In Fig. (3-5. B) the FT-IR spectra for POM-DA-TMZ was explained, in comparison with MTZ and POM, the POM-DA-TMZ showed the most characteristic bands of each of the components (POM and TMZ), though with slight shifts at 3051, 1600, and 945 cm^{-1}. These shifts may be attributed to changes in the molecular environment or interactions between the components, indicating the successful formation of POM-DA-TMZ nanocomposite.

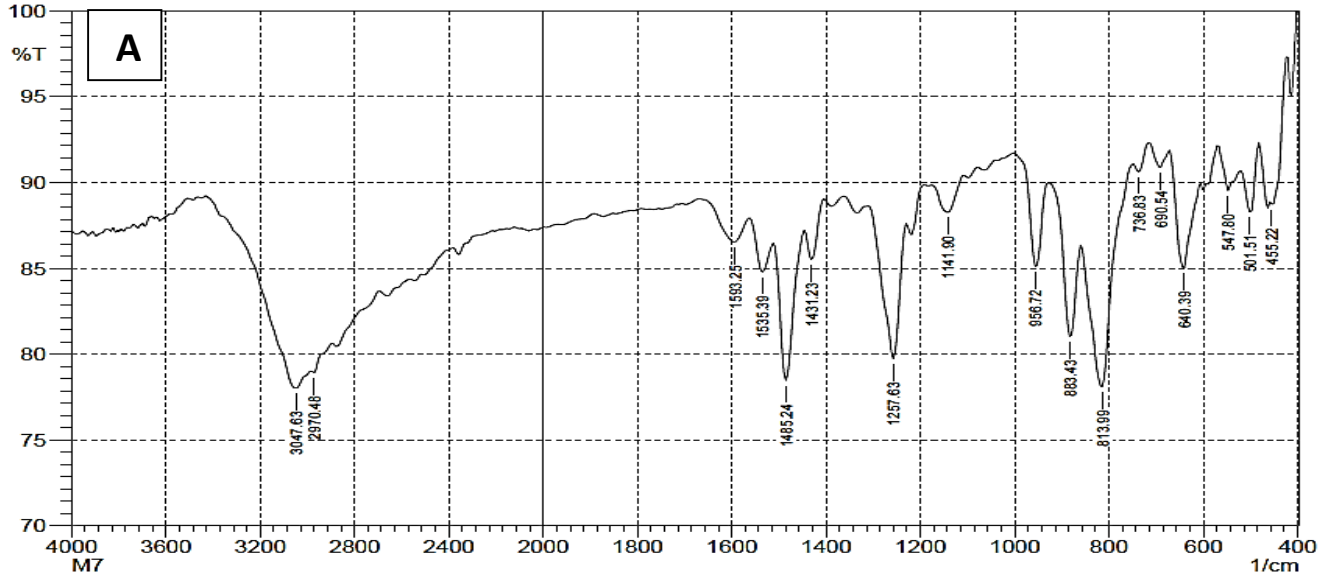

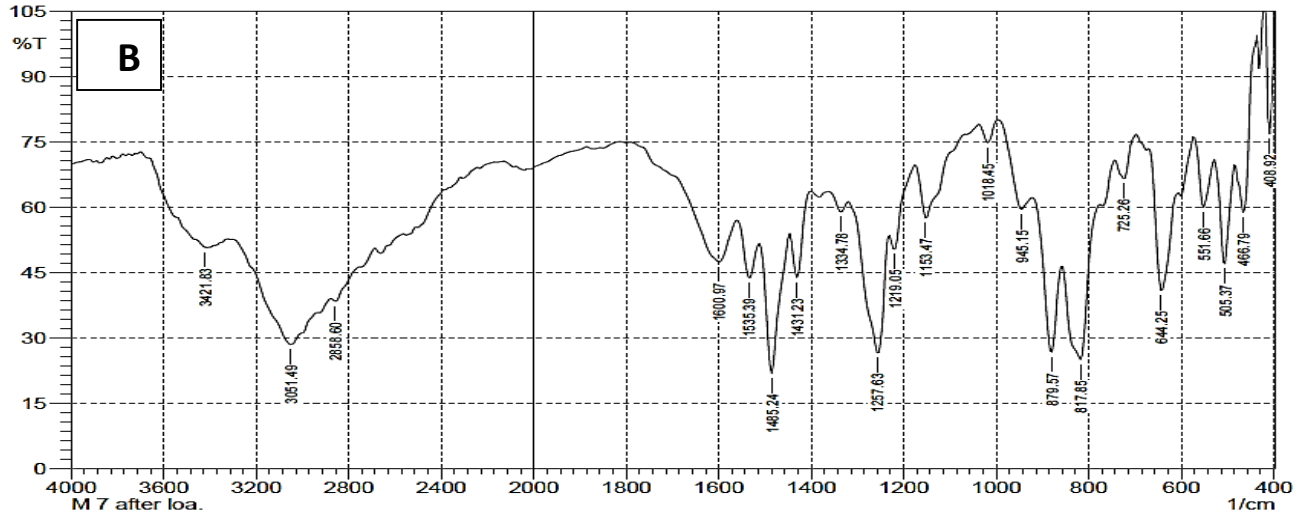

Figure (3-5) The FTIR spectra of POM-dopamine nano-composite (A) prior to loaded with TMZ, and (B) after loaded with TMZ.

3.1.1.3 The Fourier transform infrared (FTIR) spectra of POM-Chitosan nano-composite prior and after loaded with TMZ.

Fig. (3-6. A) show the Fourier-transform infrared (FT-IR) spectra of POM-chitosan nanocomposite that was revealed the most characteristic bands of the precursor with slight shifted. The shift at 2962 cm^{-1} in the POM characteristic band indicates the involvement of chitosan in the complexation process. This shift indicates that chitosan interacts with POM through hydrogen bonding or other intermolecular forces, which leads to modifications in the vibrational characteristics of POM. The shifts at 1465 cm^{-1} and 952 cm^{-1} in the POM characteristic bands also suggested the introducing of chitosan in the complex formation. These shifts refer to modifications in the molecular environment of POM due to the interaction with chitosan, through coordination or other chemical interactions. The shifts at 1519 cm^{-1} and 3429 cm^{-1} in the chitosan characteristic bands further prove the complexation process with POM. The shifts in the characteristic bands of POM in the nanocomposite give evidence of complexation between POM and chitosan these shifts confirm the successful preparation of the POM-chitosan nano-composite.

Fig. (3-6. B) illustrated the FT-IR spectra of POM-Chitosan-TMZ nanocomposites were comparison with those of TMZ and POM individually. This comparison shown the most

characteristic bands of each component, POM and TMZ, with slight shifts observed at 794 cm^{-1}, 891 cm^{-1}, and 1531 cm^{-1} specially for POM. These shifts refer to the complexation between POM and the nano-composite. Depending on the information obtained, the shifts in the characteristic bands of POM in the nano-composite give evidence of complex formation between POM and TMZ. These shifts may be attributed to changes in the molecular environment or interactions between the components, indicating the successful formation of POM-Chitosan-TMZ nanocomposite.

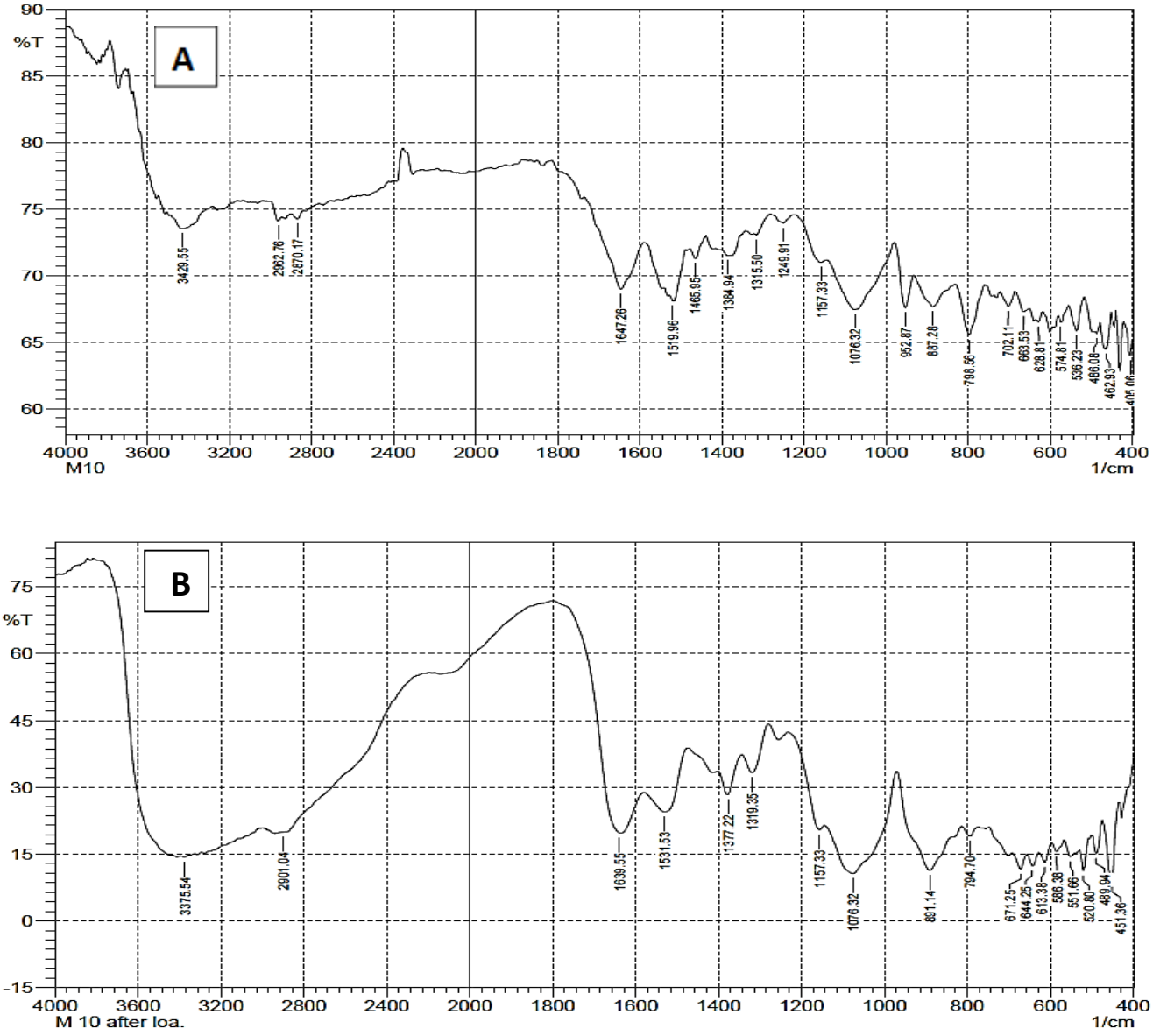

Figure (3-6) The FTIR spectra of POM-Chitosan nano-composite (A) prior to loaded with TMZ, and (B) after loaded with TMZ.

3.1.2 X-Ray Diffraction (XRD)

3.1.2.1 X-Ray Diffraction (XRD) for compound A (POM-DA)

Fig (3-7.1) show The XRD analysis of hexamolybdate which showed the appearance of clear diffraction peaks at angles of (2θ = 15.36°, 23.52°, 25.55°, 25.93°, 26.90°, 31.60°, 34.38°, 35.34°, 44.41°, 46.25°, 56.12°, 65.57°), and the crystal size calculated using the Scherrer's equation [120]

$$L=k\,\lambda / \beta \cos\theta$$

Here: k is the Scherrer's constant based on the dimensionless shape in ranged 0.94-0.85, λ is the wavelength of Cu kα (used 0.15406 nm) as irradiation source, 2θ a Bragg diffraction angle and β is (FWHM) the full half-maximum intensity width in degrees, which must convert to radians by multiplying it by (π/180). The peaks showed that the sample possessed high crystallinity.

Fig. (3-7.2) explains the X-ray diffraction patterns of the DA The mean crystal size (L) was calculated depending on the peaks of angles (25.45°, 34.18°, 52.36°, 25.93°), and found to be (68.56 nm). Well, using Bragg's equation to the same angles, the interplanar spacing (d) of DA was done [121] .

Fig. (3-7.3) explain The X-ray spectrum of the Hexamolybdate - Dopamine composite showed the presence of a broad diffraction peak at (2θ=20°) and this indicates the disappearance of the crystalline nature could clearly be observed, indicating the successful complexation of DA with POM Lindqvist-type hexamolybdates through strong interactions. Compared to its POM and DA precursors, the POM-DA structure showed broader peaks, which can be attributed the smaller crystalline particle size, confirming the nano-character of the resultant POM-DA composite.

After loading TMZ into the POM-DA nanocomposite, the XRD patterns Fig. (3-7.4) showed minimal change compared to the POM-DA composite, though boarder peaks were observed.

Table (3-1). The difference in the interplanar spacing (d) before the process of loading and after using for TMZ

POM-DA nano-composite			POM-DA nano-composite after loading with TMZ		
2θ	d-spacing (A^o)	Intensity (I/I_o) %	2θ	d-spacing (A^o)	Intensity (I/I_o) %
10.084	8.77206	70.08	10.1727	8.6957	28
12.8045	6.91375	16.55	14.1467	6.26068	49.46
14.0076	6.32253	100	15.6653	5.65701	51.72
15.4342	5.74118	87.34	19.9089	4.45975	38.51
17.1453	5.17187	40.85	25.7276	3.4628	100
18.9614	4.68042	45.34	29.9937	2.97928	19.6
19.5801	4.53389	53.51	38.6209	2.33133	11.64
25.2797	3.52312	88.8	40.2593	2.24015	12.84
28.3195	3.15149	18.8	43.3581	2.08696	10.29
29.7736	3.0008	14.52	52.9988	1.72783	6.55
38.6176	2.33151	6.66			
43.1084	2.09847	6.85			
52.6585	1.73819	4.21			

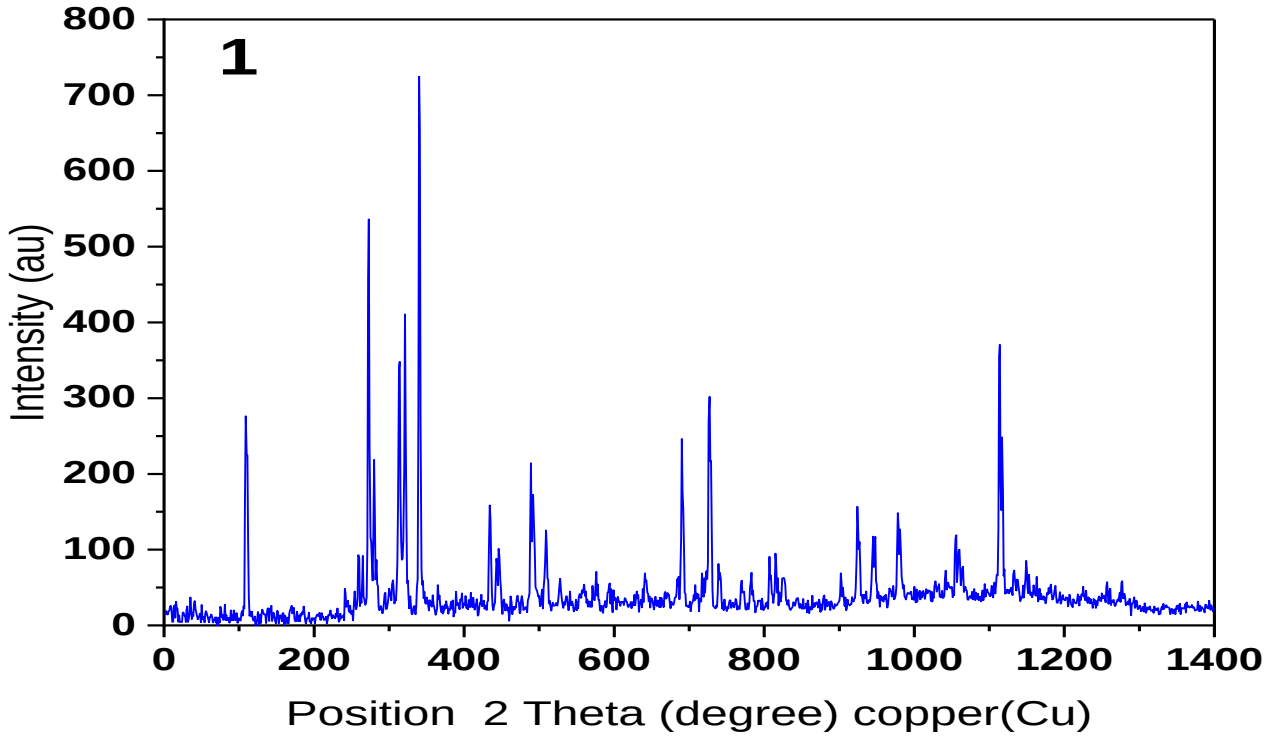
1
Intensity (au)
Position 2 Theta (degree) copper(Cu)

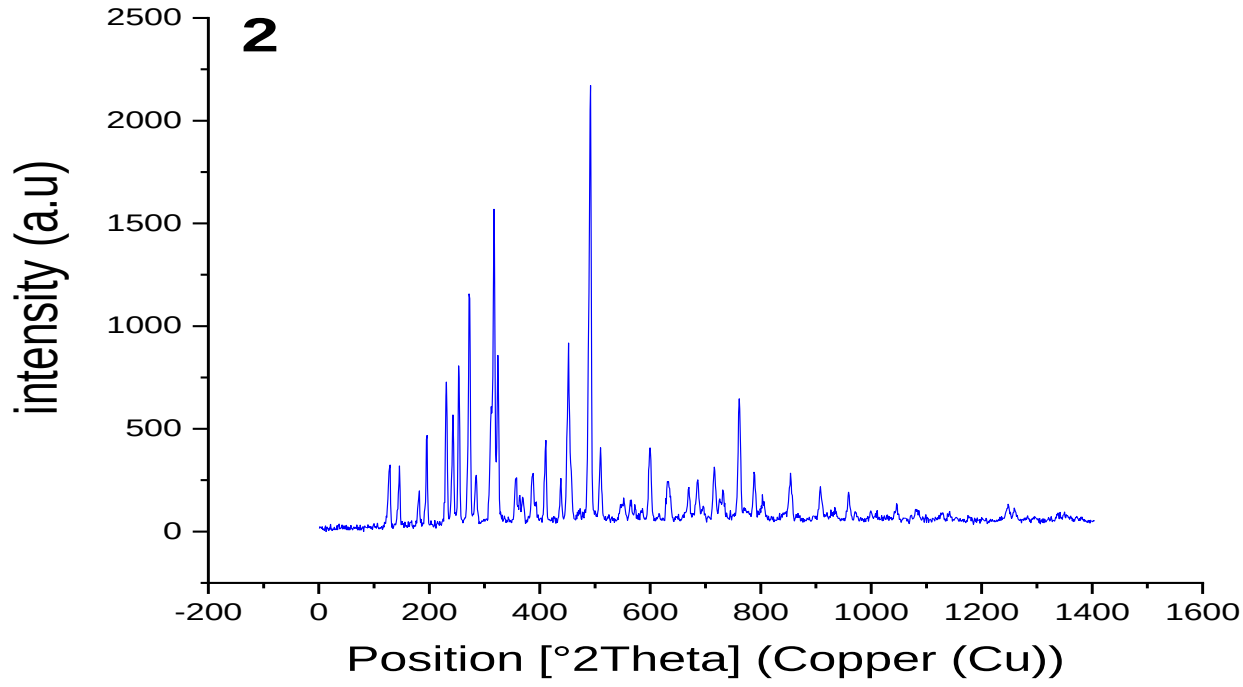
2
intensity (a.u)
Position [°2Theta] (Copper (Cu))

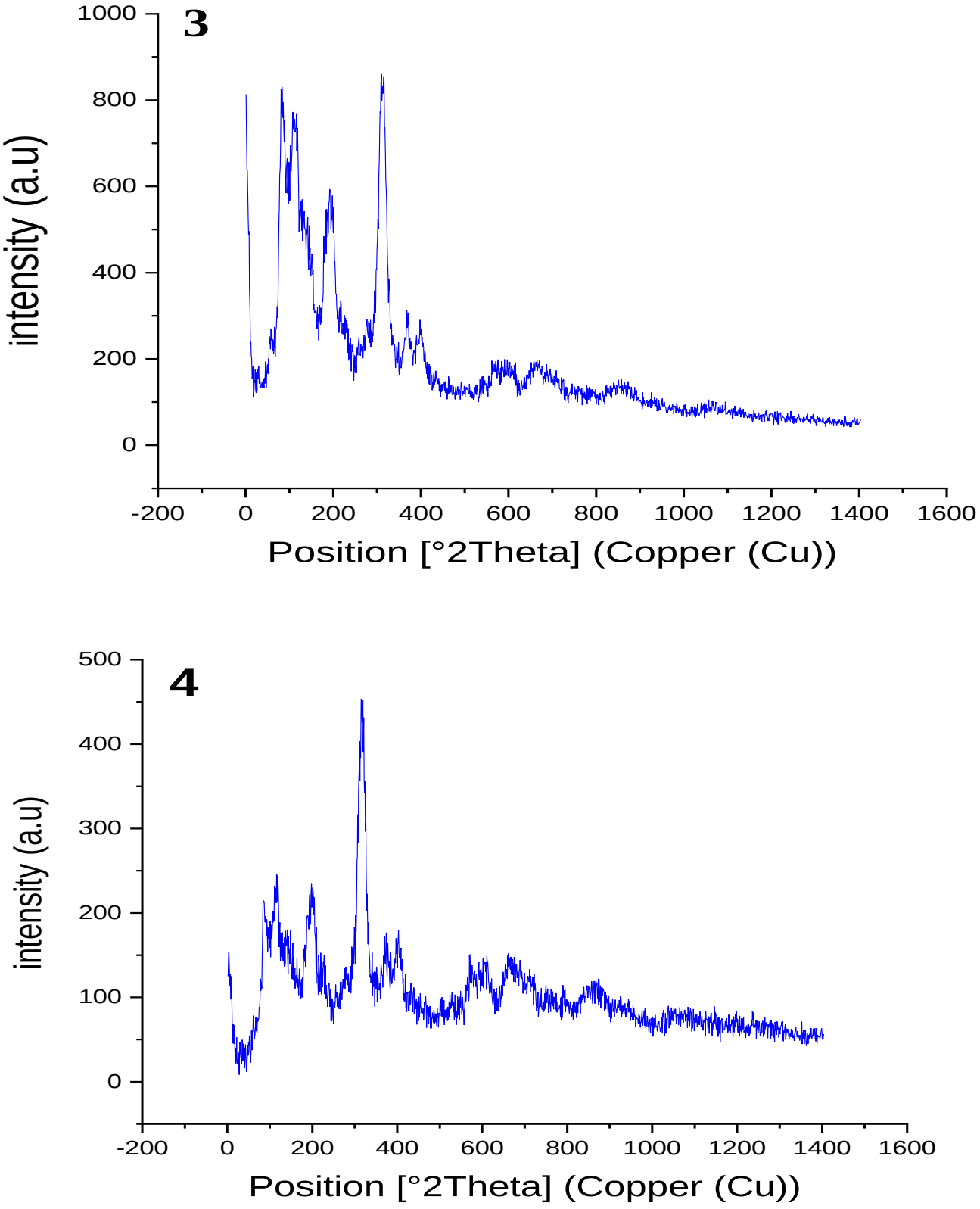

Figure (3-7): XRD patterns of (1) POM hexamolybedate, (2) dopamine, (3) the as-prepared nanostructure prior to loading with TMZ and (4) the as-prepared nanostructure after loading with TMZ.

3.1.2.2 X-Ray Diffraction (XRD) for compound B (POM-Chitosan)

Fig (3-8 .1) shows The XRD analysis of hexamolybdate which showed the appearance of clear diffraction peaks at angles of (2θ = 15.36°, 23.52°, 25.55°, 25.93°, 26.90°, 31.60°, 34.38°, 35.34°, 44.41°, 46.25°, 56.12°, 65.57°), and the crystal size calculated using the Scherrer's equation. The peaks showed that the sample possessed high crystallinity.

The XRD pattern in fig. (3-8.2) of chitosan nanoparticles showed peaks at 2θ = 20.23°, 26.79°, 28.02°, 29.51°, 36.08°, 39.52°, 43.23°, and 48.60°, pointing out the high crystallinity of chitosan. The average size of chitosan nanoparticles was determined to be 6.90 nm utilizing Scherrer's equation.

Fig. (3-8.3) explain the nano-composite of hexamolybdate and chitosan which showed a large diffraction peak at 2θ=27.8° in its XRD spectra, suggesting that its crystalline character had been lost. This implies that strong contacts were formed during the effective complexation of chitosan with POM Lindqvist-type hexamolybdates. The resulting POM-chitosan composite was confirmed to be nanoscale since its structure showed wider peaks than that of the POM and chitosan precursors. This can be explained by the crystalline material's smaller particle size. Although wider peaks were seen, the XRD patterns showed only slight modifications when TMZ was loaded into the POM-chitosan nanocomposite in comparison to the POM-chitosan composite, that demonstrated in Fig (3-8.4) .

Table (3-2). The difference in the interplanar spacing (d) before the process of loading and after using for TMZ

POM-chitosan nano-composite			POM-chitosan nano-composite after loading with TMZ		
2θ	d-spacing (A°)	Intensity (I/I_o) %	2θ	d-spacing (A°)	Intensity (I/I_o) %
15.201	5.339	30.31	15.536	5.235	47.51
20.078	4.054	73.08	20.382	4.011	86.12
25.492	3.222	49.15	25.916	3.150	53.72

29.501	2.805	89.58	29.735	2.731	91.04
34.381	2.463	29.12	34.681	2.388	33.62
39.387	2.196	27.04	39.592	2.127	25.57
44.351	2.011	24.51	44.723	1.927	23.66
56.295	1.671	21.22	56.433	1.651	18.93

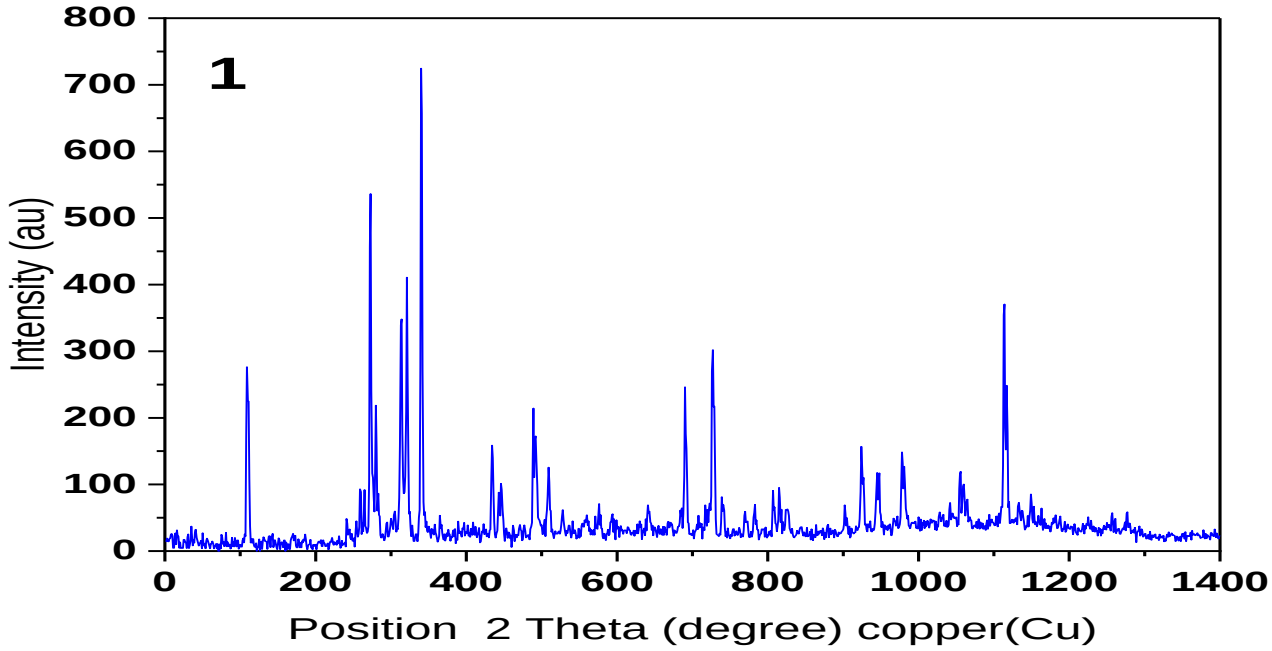

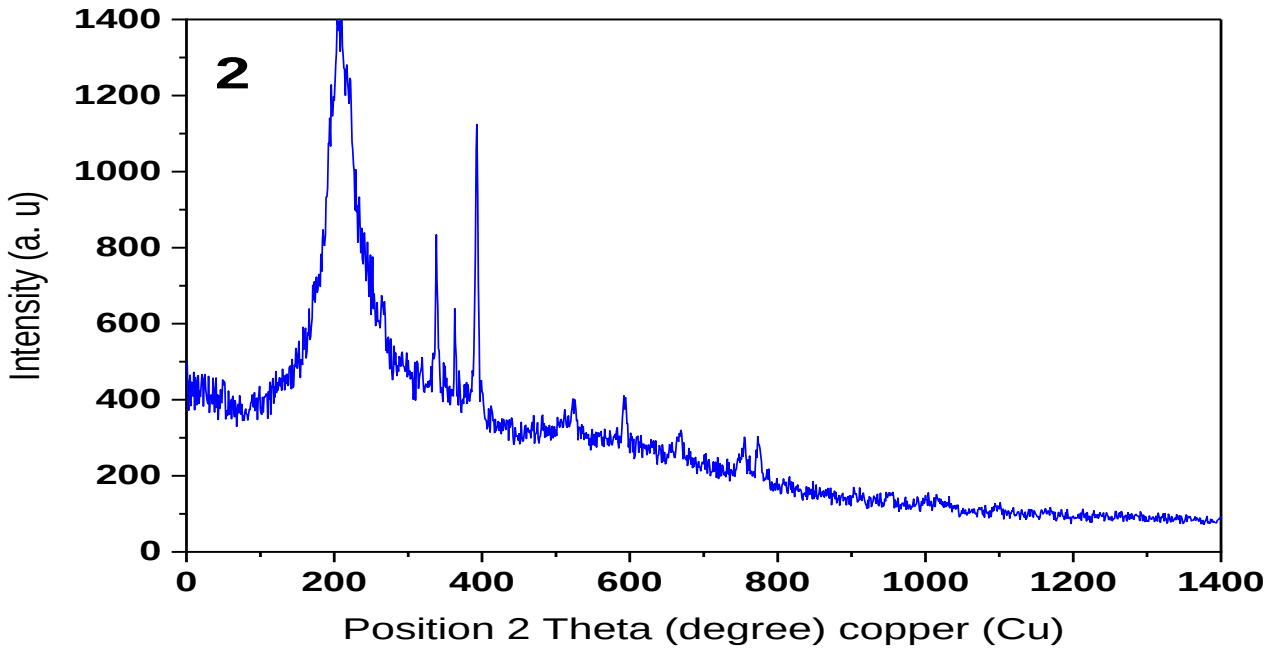

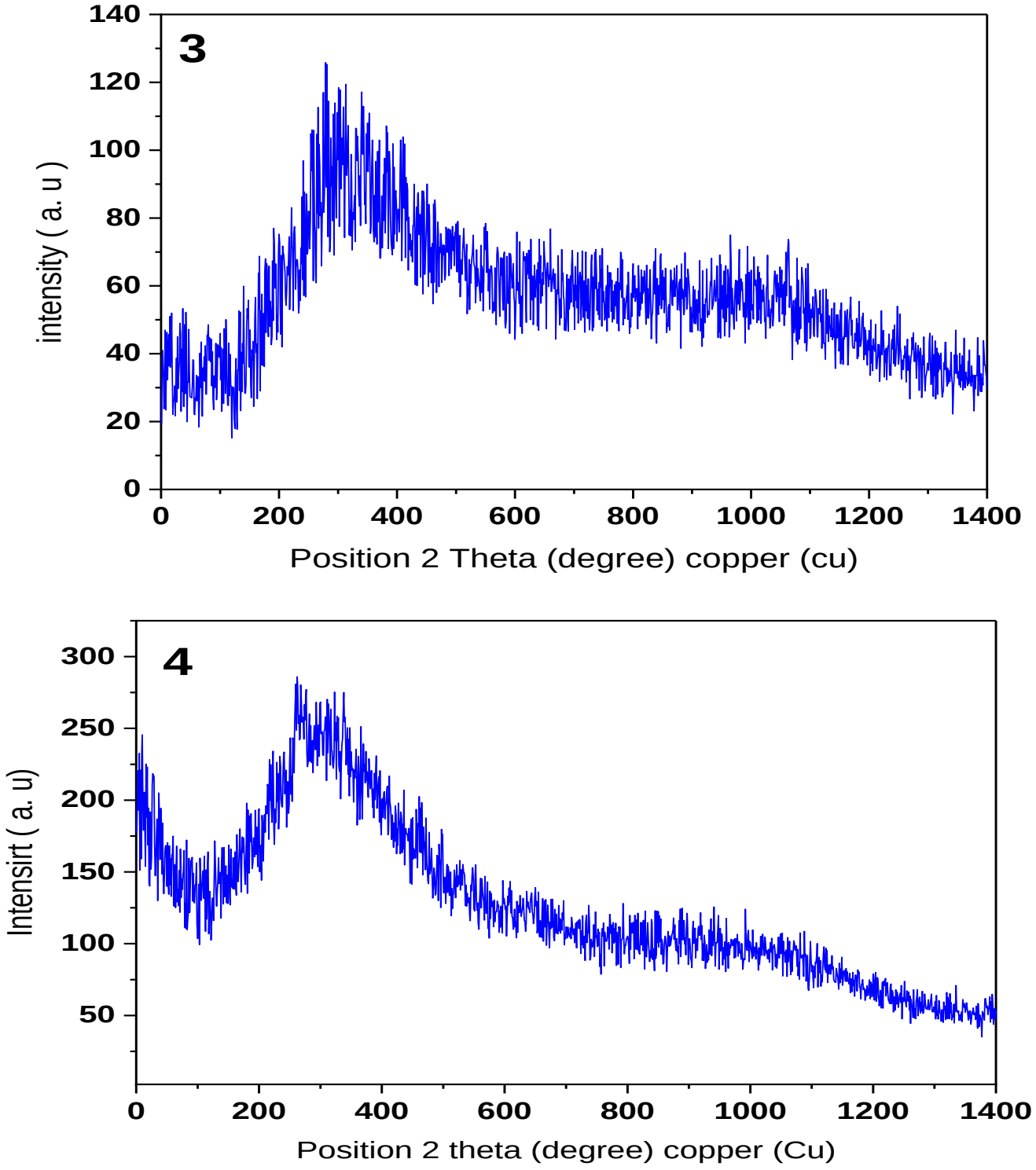

Figure (3-8): XRD patterns of (1) POM hexamolybedate, (2) chitosan, (3)the as-prepared nanostructure prior to loading with TMZ and (4) the as-prepared nanostructure after loading with TMZ.

3.1.3 Scanning Electron Microscopy (SEM)

3.1.3.1 Scanning Electron Microscopy (SEM) and EDX analysis of the POM-DA as-prepared nanostructures prior and after loading with TMZ.

The morphology of the as-prepared nanostructures of POM-DA before and after loading with TMZ were investigated via SEM. As can be seen from Fig. (3-9), which shows the SEM micrographs of the POM-DA nanostructure, the nanostructure itself consists of hierarchical microsphere structures with a size of about 1 μm constructed from a multitude of nano petals of thicknesses ranging from 20 to 40 nm and widths of 300-500 nm. 3D hierarchical structures were formed from the central connection of these nano petals.

The loading of TMZ onto the hierarchical microsphere structures resulted in different morphological (shape and size) structures compared to POM-DA. As can be seen from Fig. (3-10) nanosphere particles with diameters ranging from 20 to 45 nm are formed upon loading with TMZ. These considerable changes in both morphology and size can be attributed to the TMZ loaded onto the surface of POM-DA nanostructure.

These findings are consistent with the XRD results, which showed a change to a smaller particle size upon loading of TMZ compared to the naked POM-DA nanostructures.

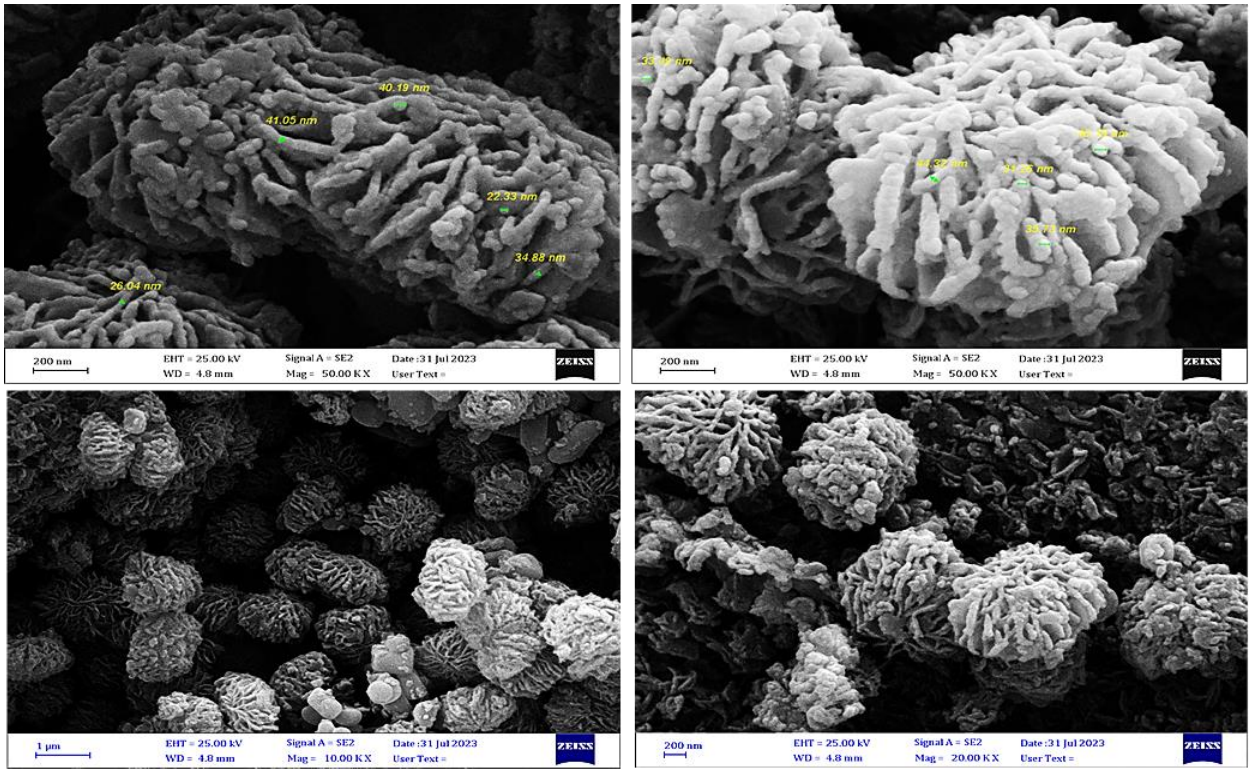

Figure (3-9) SEM images of the POM-DA as-prepared nanostructures prior to loading with TMZ.

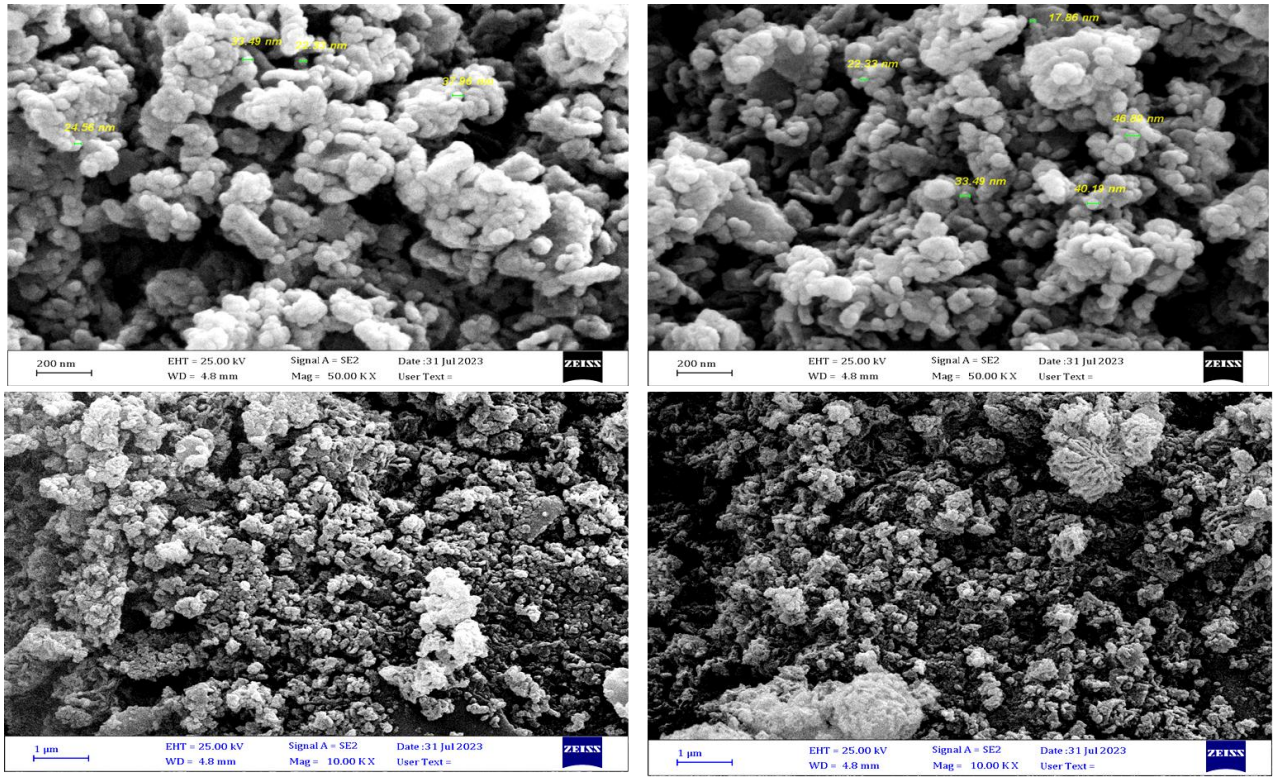

Figure (3-10) SEM images of POM-DA as-prepared nanostructures after loading with TMZ.

The elemental compositions of the POM-DA as-prepared nanocomposite prior and after loading were confirmed by energy dispersive X-ray (EDX) analysis as shown in fig. (3-11). The finding result explain the presence of most important basic element with different intensities, The fig. (3-11.1) shows wight percentage of POM-DA prior to loading with TMZ as follow: the Molybdenum (44.6 %), Carbon (40.9 %), Oxygen (11.2 %) and Nitrogen (3.3 %). While the fig. (3-11. 2) shows wight percentage of POM-DA after loading with TMZ as follows: Carbon (48.3 %), Molybdenum (38.5 %), Oxygen (11.6 %) and Nitrogen (1.6 %). These percentages confirm the successful association of nano-composite with TMZ drug.

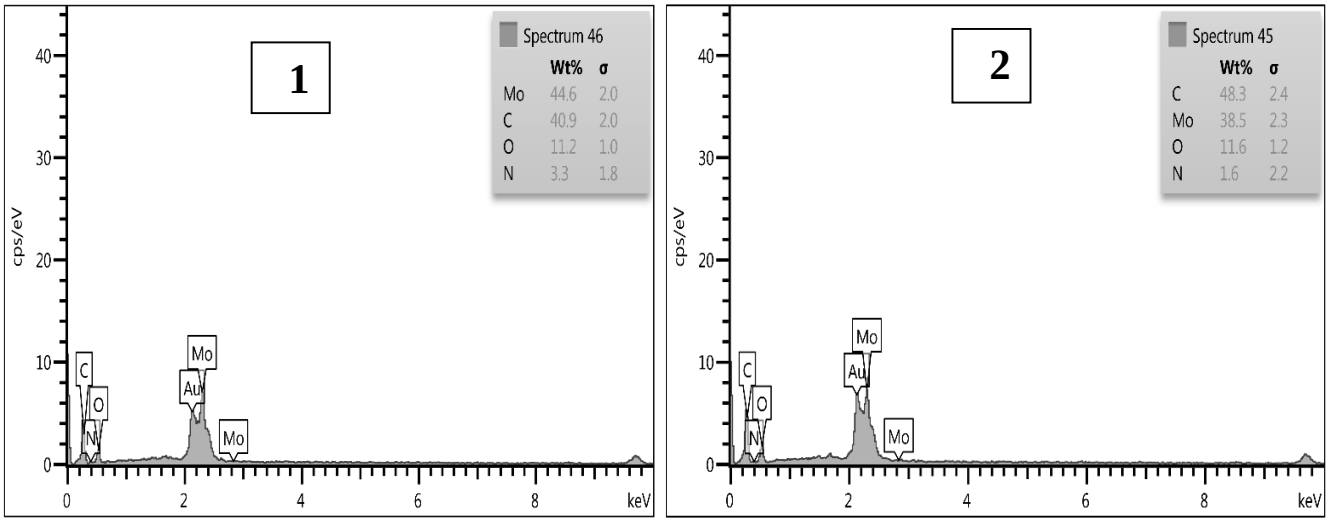

Figure (3-11) the EDX analysis of the (1) POM-DA as-prepared nanostructures prior to loading with TMZ (2) POM-DA as-prepared nanostructures after loading with TMZ.

3.1.3.2 Scanning Electron Microscopy (SEM)and EDX analysis of the as-prepared nanostructures POM-Chitosan

The morphology of the as-prepared nanostructures of POM-chitosan before and after loading with TMZ were investigated via SEM. As can be shown in Fig. (3-12), which demonstrate the SEM micrographs of the POM-chitosan nanostructure, the nanostructure itself consists of hierarchical microsphere structures with a size of about 1 μm constructed from a multitude of nanoplates of thicknesses ranging from 20 to 113 nm and widths of

200-500 nm 3D hierarchical structures were formed from the central connection of these nanoplates. The loading of TMZ onto the hierarchical microsphere structures resulted in totally different morphological (shape and size) structures compared to POM-Chitosan. As can be seen from Fig. (3-13), nanosphere particles with diameters ranging from 13 to 42 nm are formed upon loading with TMZ. These considerable changes in both morphology and size can be attributed to the TMZ loaded onto the surface of POM-Chitosan nanostructure. These findings are consistent with the XRD results, which showed a change to a smaller particle size upon loading of TMZ compared to the naked POM-Chitosan nanostructures.

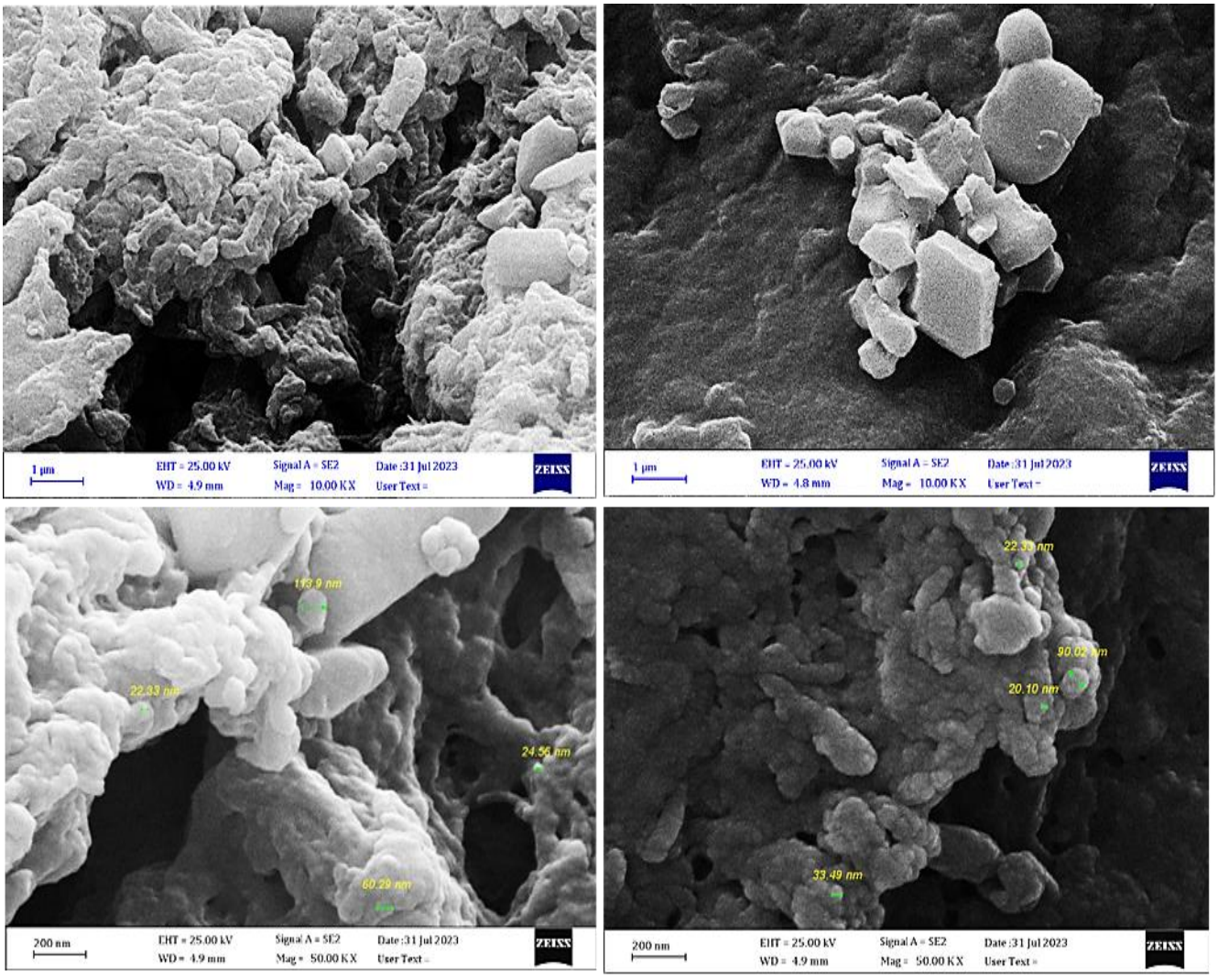

Figure (3-12) SEM images of the POM-Chitosan as-prepared nanostructures prior to loading with TMZ.

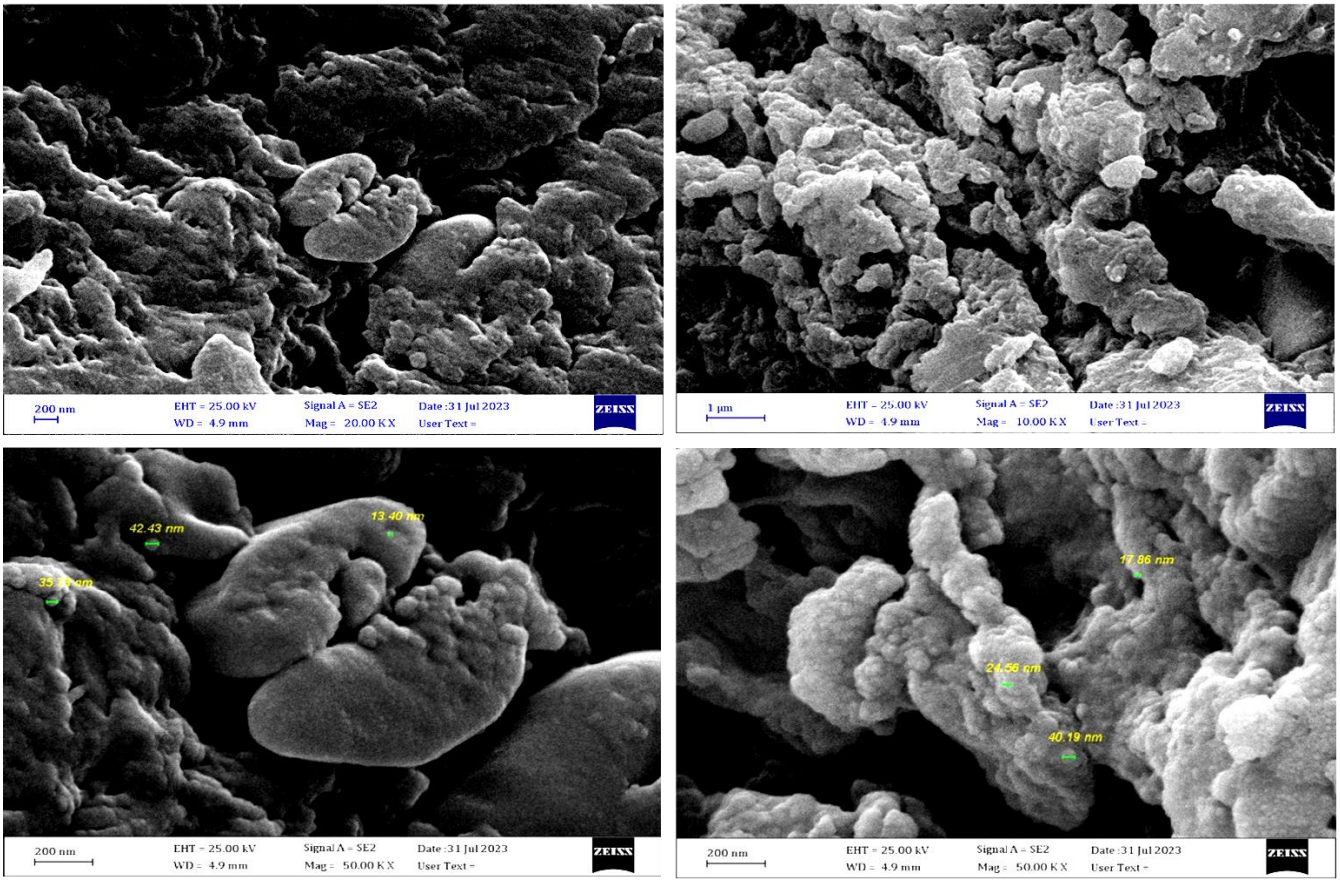

Figure (3-13) SEM images of the POM -Chitosan as-prepared nanostructures after loading with TMZ.

The elemental compositions of the POM-DA nanocomposite, both before and after loading, were verified using energy dispersive X-ray (EDX) analysis, as shown in Fig. (3-14). The results indicate that the presence of key elements at varying intensities. Fig. (3-14 .1) illustrates the weight percentages of POM-DA prior to loading with TMZ: Molybdenum (47.2%), Carbon (31.4%), Oxygen (19.9 %), and Nitrogen (1.5 %).

Conversely, Fig. (3-14 .2) displays the weight percentages of POM-DA after loading with TMZ: Molybdenum (52.4 %), Carbon (28.3 %), Oxygen (17.3 %), and Nitrogen (2.0 %). These percentages validate the successful incorporation of the nanocomposite with the TMZ drug.

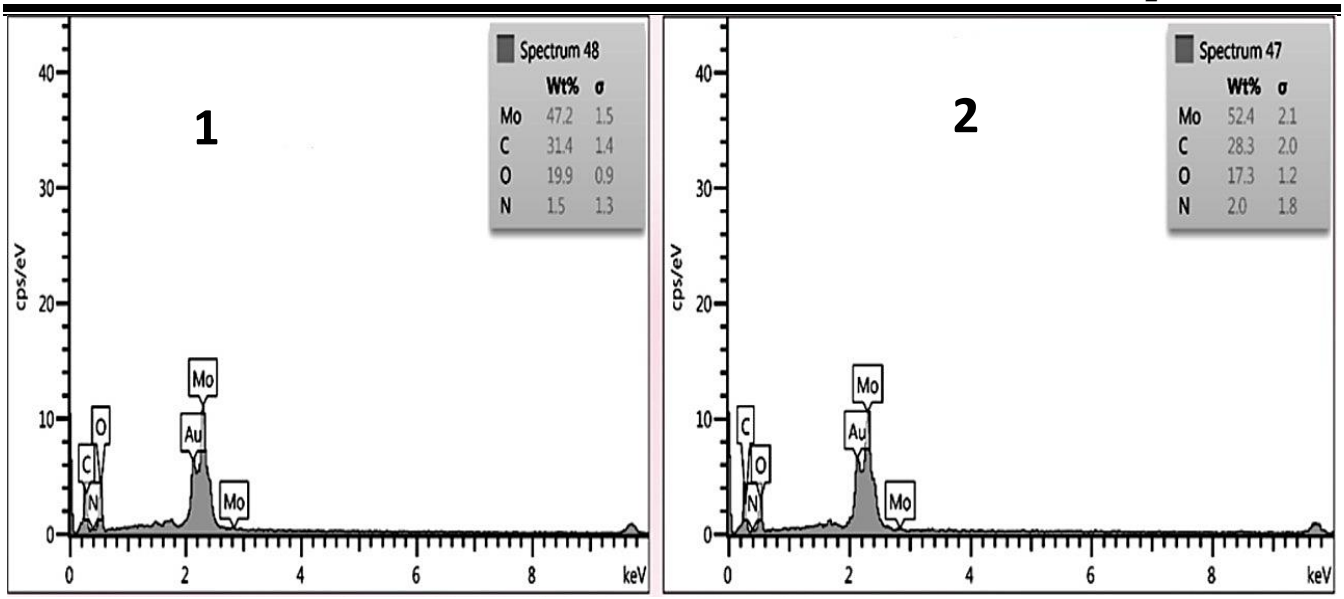

Figure (3-14) the EDX analysis of the (1) POM-Chitosan as-prepared nanostructures prior to loading with TMZ (2) POM- Chitosan as-prepared nanostructures after loading with TMZ.

3.1.4 Atomic Force Microscopy (AFM)

3.1.4.1 Atomic Force Microscopy (AFM) of the POM-DA as-prepared nano-structures prior and after loaded with TMZ.

AFM analysis of the POM-DA nano-composite, The fig. (3-15.A), explained the presence of different shapes of blocks on the surface. The images indicated that the surface was rough, with a peak-to-valley roughness (Rt) value of 22.00 nm, an average roughness (Ra) of 2.254 nm, and an RMS roughness (Rq) value of 2.791 nm. This roughness is attributed to the clustering of nanoparticles, causing uneven distribution and surface irregularities. The AFM results demonstrate that the POM-DA nanocomposite exhibits a rough surface texture, and this roughness is primarily caused by the agglomeration of nanoparticles within the composite structure.

While POM-DA nano-composite after loaded with TMZ as in fig. (3-15.B) showed the presence of blocks of different a peak-to- valley roughness (Rt) value of 38.15nm, average roughness (Ra) of 2.370 nm and RMS roughness (Rq) value of 3.147 nm. These values

show an increase in roughness due to increase in rate of agglomeration which indicates to successful association of the nano-composite with the TMZ drug.

Table (3-3) demonstrated the major surface characteristics of the as-prepared nanostructures POM-DA prior and after loaded with TMZ.

Surface characteristics	POM-DA prior to loading with TMZ	POM-DA after to loading with TMZ
peak-to- valley roughness (Rt)	22.00 nm	38.15 nm
average roughness (Ra)	2.254 nm	2.370 nm
RMS roughness (Rq)	2.791 nm	3.147 nm

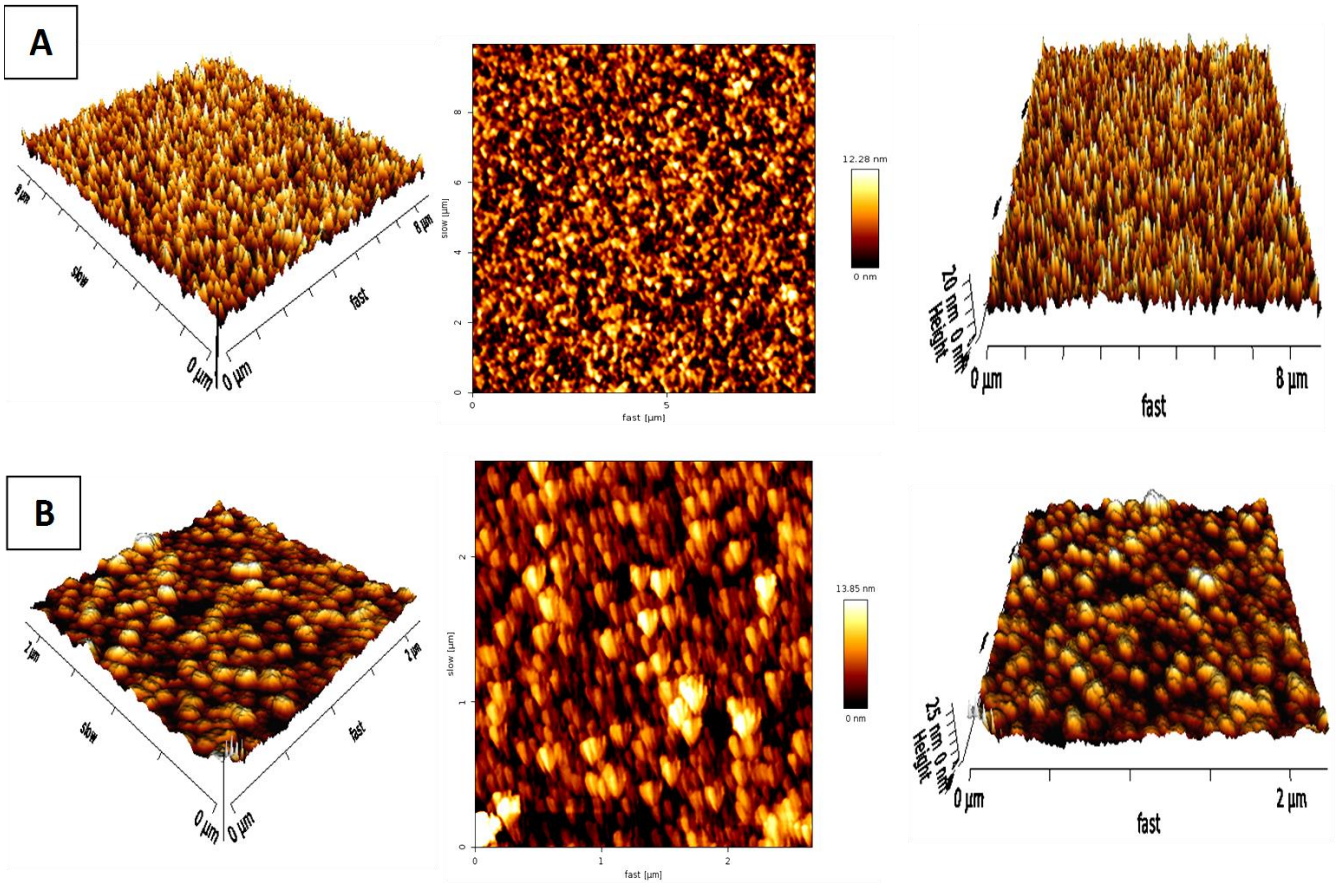

Figure (3-15) AFM images of (A) the POM-DA as-prepared nanostructure before loading with TMZ (B) The POM-DA as-prepared nanostructure after loading with TMZ.

3.1.4.2 Atomic Force Microscopy (AFM) of the as-prepared nanostructures POM-Chitosan prior and after loaded with TMZ.

The AFM analysis of the POM-Chitosan nanocomposite, shown in Fig. (3-16.A), revealed the presence of blocks with different shapes on the surface. The images indicated that the surface was rough, with a peak-to-valley roughness (Rt) value of 14.55 nm, an average roughness (Ra) of 1.607 nm, and an RMS roughness (Rq) value of 2.012 nm. This roughness is attributed to the clustering of nanoparticles, causing uneven distribution and surface irregularities. The AFM results demonstrate that the POM-chitosan nanocomposite exhibits a rough surface texture, and this roughness is primarily caused by the agglomeration of nanoparticles within the composite structure.

While POM-chitosan nano-composite after loaded with TMZ as in Fig. (3-16.B) showed the presence of blocks of different a peak-to- valley roughness (Rt) value of 21.86 nm, average roughness (Ra) of 2.257 nm and RMS roughness (Rq) value of 2.863 nm. These values show an increase in roughness due to increase in rate of agglomeration which indicates to successful association of the nano-composite with the TMZ drug.

Table (3-4) demonstrated the major surface characteristics of the as-prepared nanostructures POM-Chitosan prior and after loaded with TMZ

Surface characteristics	POM-Chitosan prior to loading with TMZ	POM-Chitosan after to loading with TMZ
peak-to- valley roughness (Rt)	**14.55 nm**	**21.86 nm**
average roughness (Ra)	**1.607 nm**	**2.257 nm**
RMS roughness (Rq)	**2.012 nm**	**2.863 nm**

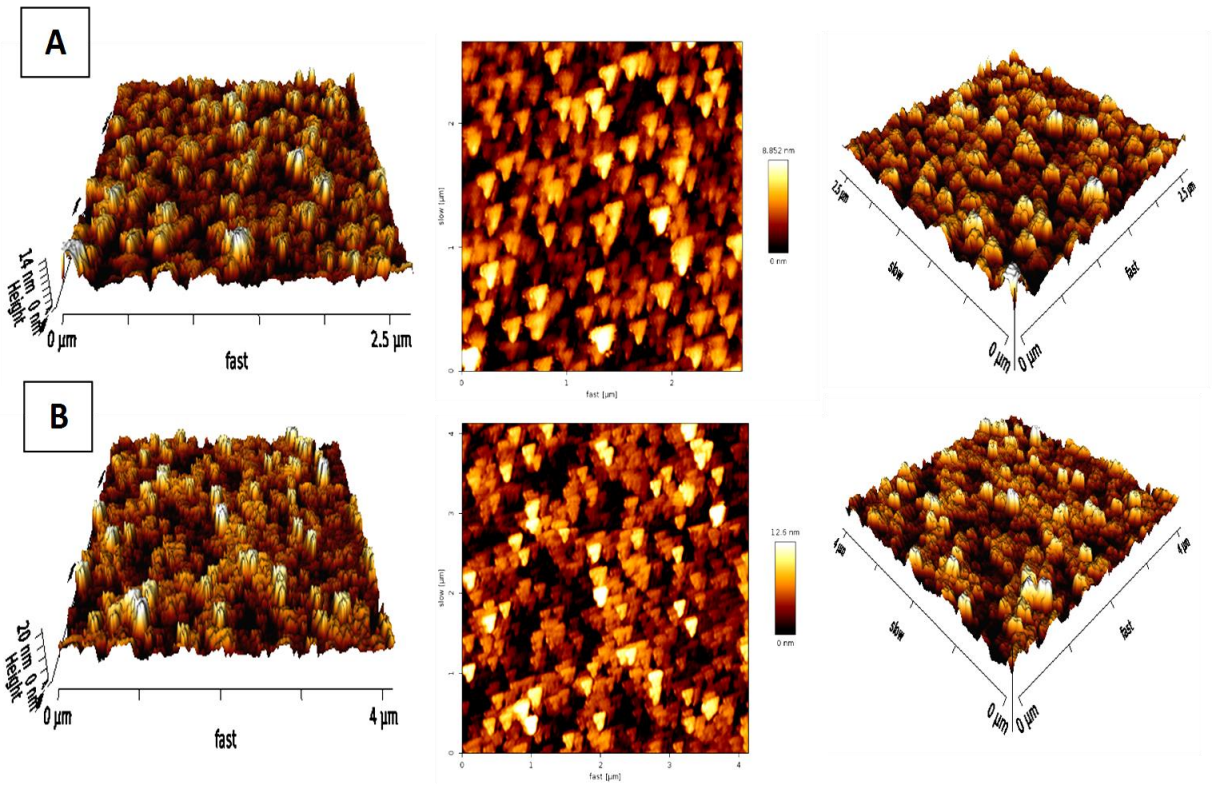

Figure (3-16) AFM images of (A) the POM-chitosan as-prepared nanostructure before loading with TMZ (B) The POM-chitosan as-prepared nanostructure after loading with TMZ.

3.1.5 X-Ray Photoelectron Spectroscopy (XPS)

3.1.5.1 X-Ray Photoelectron Spectroscopy (XPS) for POM-DA as-prepared nano-structure prior to and after loading with TMZ

XPS spectroscopy was performed to identify the elemental composition of the nanocomposites, the results of which are presented in Fig. (3-17) These confirm the presence of C, N, and Mo, with peaks corresponding to C1s (BE = 289 eV), N1s (BE = 404 eV), and Mo3d5/2 (BE = 237 eV). The C1s and the N1s signals can be attributed to the carbon and amido in DA (and TMZ in (2)), while the Mo3d can be attributed to POM Lindqvist-type hexamolybdate. It can clearly be seen that the N1s band comprises two peaks: the first, at 404 eV, can be assigned to alkylamines, whilst the second, at higher binding energy, can be attributed to protonation of the amine groups in DA, confirming

the existence of electrostatic interactions between POM and DA [77] . XPS results again confirm the successful complexation of DA with POM Lindqvist-type hexamolybdate**.**

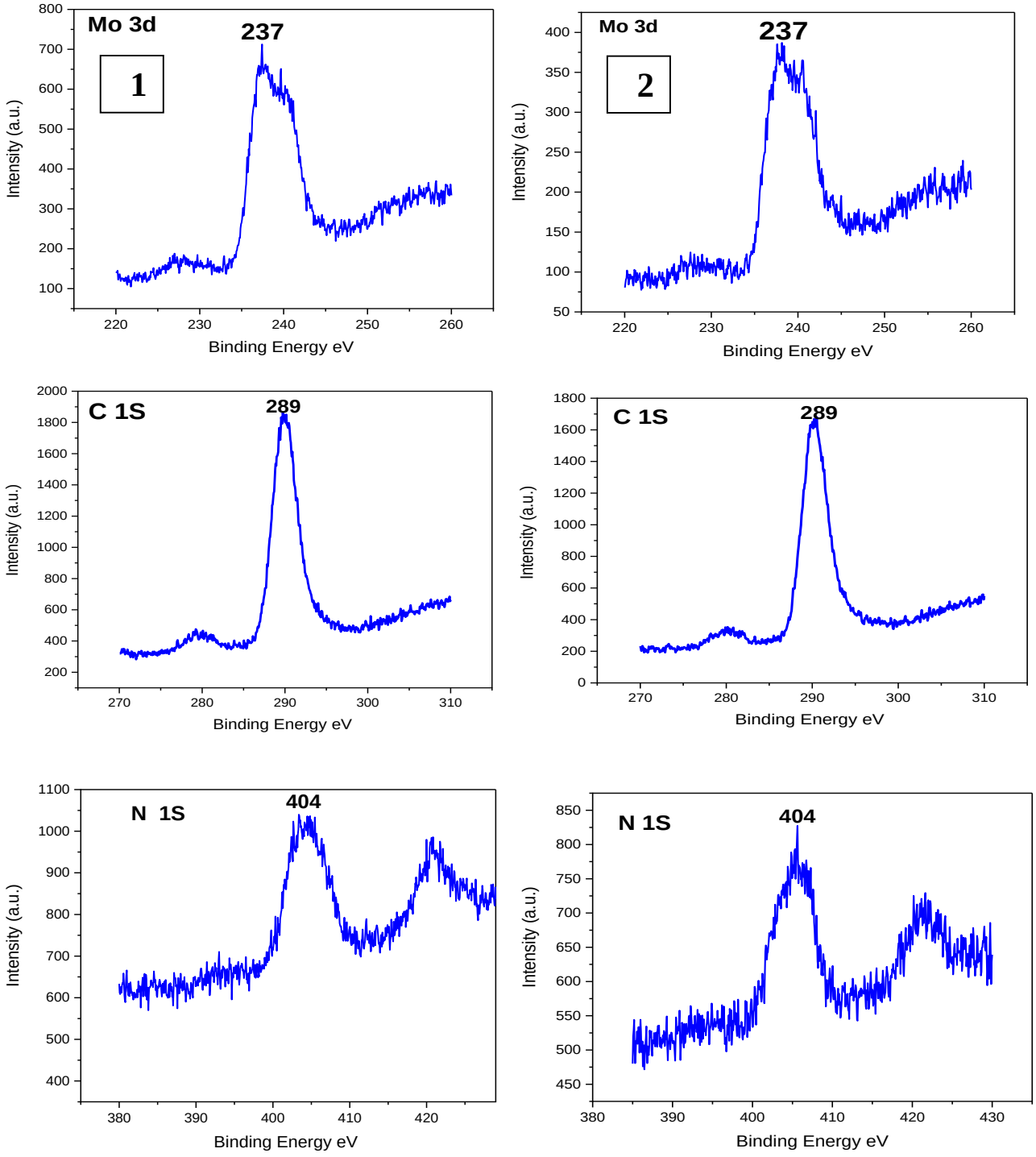

Figure (3-17) shows X-Ray photoelectron spectra of: (1) the as-prepared POM-DA nanostructure prior to loading with TMZ; and (2) the as-prepared POM-DA nanostructure after loading with TMZ.

3.1.5.2 X-Ray Photoelectron Spectroscopy (XPS) for POM-Chitosan as-prepared nano-structure prior to and after loading with TMZ

X-ray photoelectron spectroscopy (XPS) was employed to determine the elemental composition of the nanocomposites. The findings are depicted in Fig. (3-18). The XPS analysis verified the presence of carbon (C), nitrogen (N), and molybdenum (Mo), as evidenced by the respective peaks observed. The C1s peak was measured at a binding energy (BE) of 290 eV, indicating the presence of carbon in Chitosan (and TMZ in (2)). The N1s peak appeared at a BE of 404 eV, representing the amido groups in Chitosan. Moreover, the Mo3d peak at a BE of 237 eV confirmed the existence of POM Lindqvist-type hexamolybdate. Notably, the N1s band exhibited two distinct peaks: the first one, observed at 404 eV, was associated with alkylamines, while the second peak at a higher binding energy indicated the protonation of the amine groups in chitosan. This finding further supported the presence of electrostatic interactions between POM and chitosan. XPS results again confirm the successful complexation of chitosan with POM Lindqvist-type hexamolybdate**.**

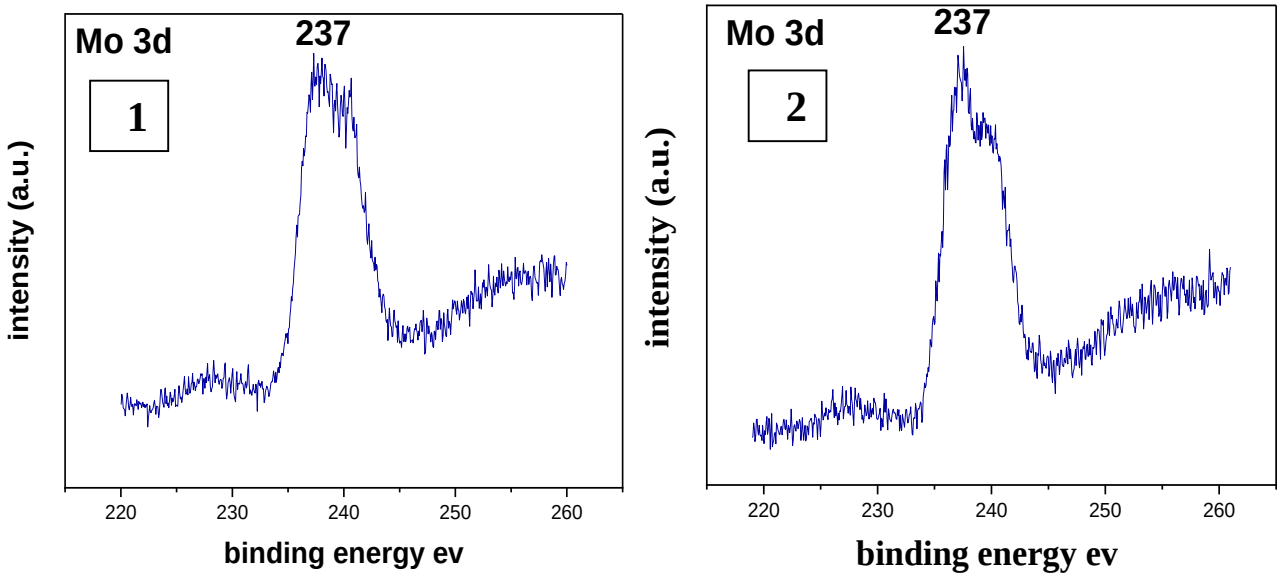

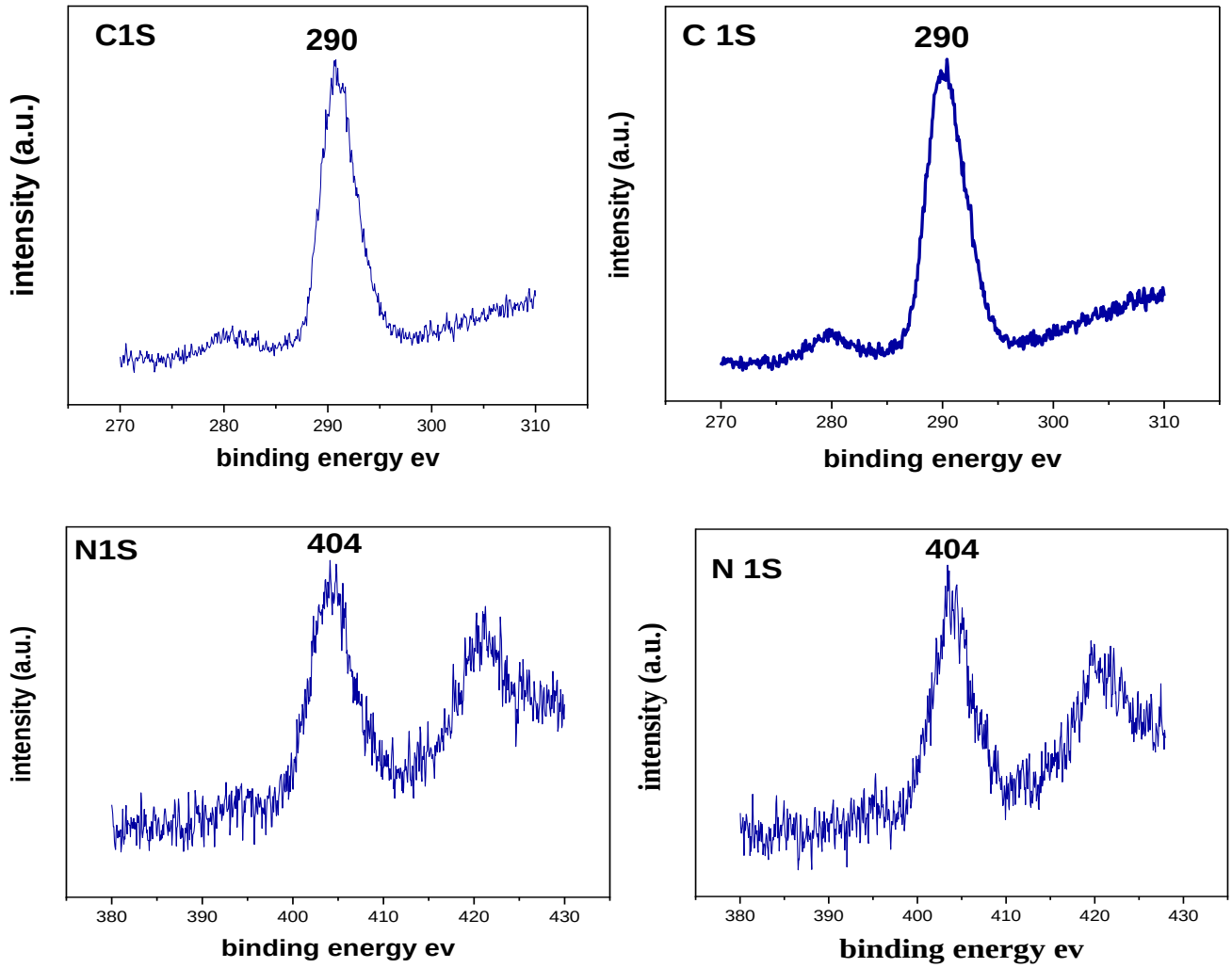

Figure (3-18) shows X-Ray photoelectron spectra of: (1) the as-prepared POM-Chitosan nanostructure prior to loading with TMZ; and (2) the as-prepared POM-Chitosan nanostructure after loading with TMZ.

3.2 Calibration curve of Temozolomide

The calibration curve of Temozolomide was done by preparing ten sequential concentrations. This drug solution was read its absorbance for these concentrations at the wavelength (λ_{max}) 328 nm in HPLC technique. That shows in the Fig.(3-19).

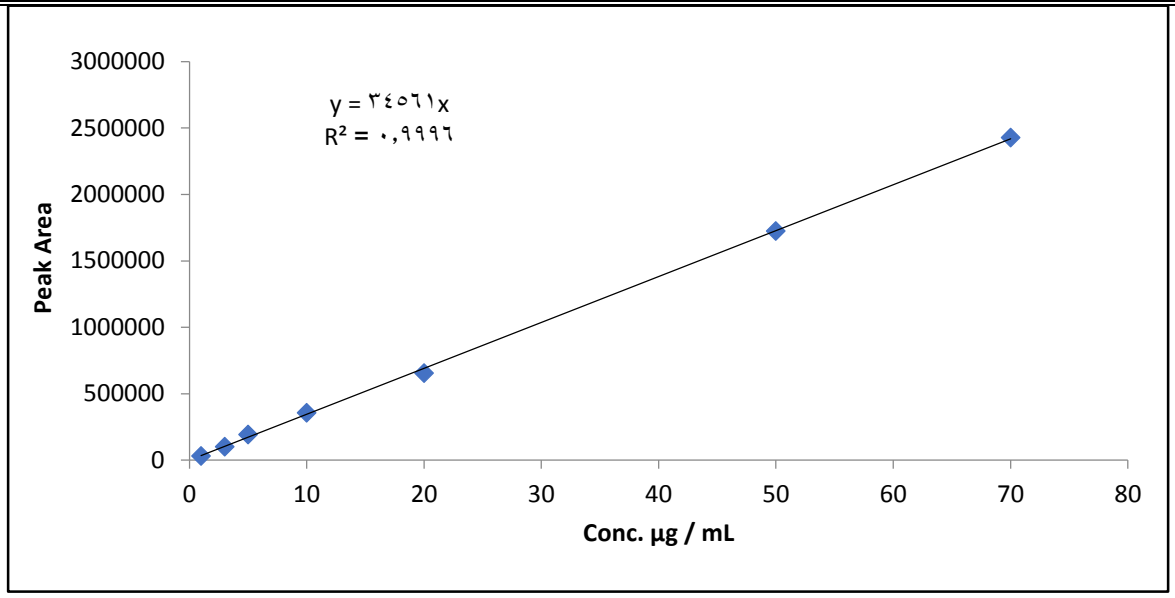

Figure (3-19) HPLC Calibration curve of Temozolomide.

3.3 Optimization of HPLC

The mobile phase comprises a mixture of acetonitrile and water with flow rate of 1ml/min was selected from preliminary studies. The concentration of mobile phase components acetonitrile and water, and flow rate were selected independent variable, whereas peak area and retention time were chosen as response for experimental design. The experimental runs with many center points obtained from the design matrix were subjected to laboratory experiment in order to generate the response variables as summarized in Table (3-5).

Statistical analysis was performed using ANOVA to compute the significant difference in the mobile phase composition obtained from the design matrix. The response surface methodology was employed to analyze the effect of independent variables on the responses.

Table (3-5) Chromatographic conditions.

Column	C18
Mobile phase	Acetonitrile 60:40 Water HPLC
Detector (Wavelength)	328 nm
Flow rate mL/min	1.0
Column temperature	37°C
Injection volume	20 µL
Run time	5 or 10 min
pH	2.8 and 7.4
Rang	(1-70) µg/mL
Slope	Y = 34561

HPLC measurement was done for four nano composite that loaded with TMZ drug, the best result given by two compound A and B which shows in table (3-6). It can be clearly seen that POM-DA nano-composite showed the highest loading percentage of 38% indicating a high loading efficiency.

Table (3-6) Result of drug loading.

NO.	Drug	Nano particles	% of loading
1	Temozolomide	A (POM-DA)	**38 %**
2	Temozolomide	B (POM-Chitosan)	**21 %**

3.4 Release behavior of TMZ loaded onto as-prepared nanostructures

3.4.1 Release behavior of TMZ loaded onto POM-DA as-prepared nanostructures

In this study, the potential of the nanostructures to act as carriers in oral drug delivery were explored by studying the loading and release behavior of TMZ in media of different pHs. Upon loading TMZ onto the nanostructures, a color change from dark red to red was clearly seen which indicating the successful loading of TMZ.

The amount of TMZ loaded onto the POM-DA nanostructures was determined via HPLC and was found to be about 38% (by weight), which represents a high loading efficiency. This could be attributed to the large relative surface area (smaller particle size compared to POM-DA prior to loading) of the nanostructures. The utilization of pH changes within the gastrointestinal (GI) tract is one of the most interesting methods in the design of oral delivery protocols for drugs in which two pH changes are chosen, the first mimicking the acidic conditions of the stomach (pH 1–3), and the second the more basic conditions of the intestines (pH 5–8). Fig. (3-20) shows the release profile of TMZ at pH 2.8 and pH 7.4 over 24 h, from which it can clearly be seen that release was pH dependent, at pH 7.4 the release of TMZ reaches 97% in 24 h, where in the first four hours the amount released shows a dramatic increase, at up to 90%, which is then followed by a more sustained release over the following 20 h.

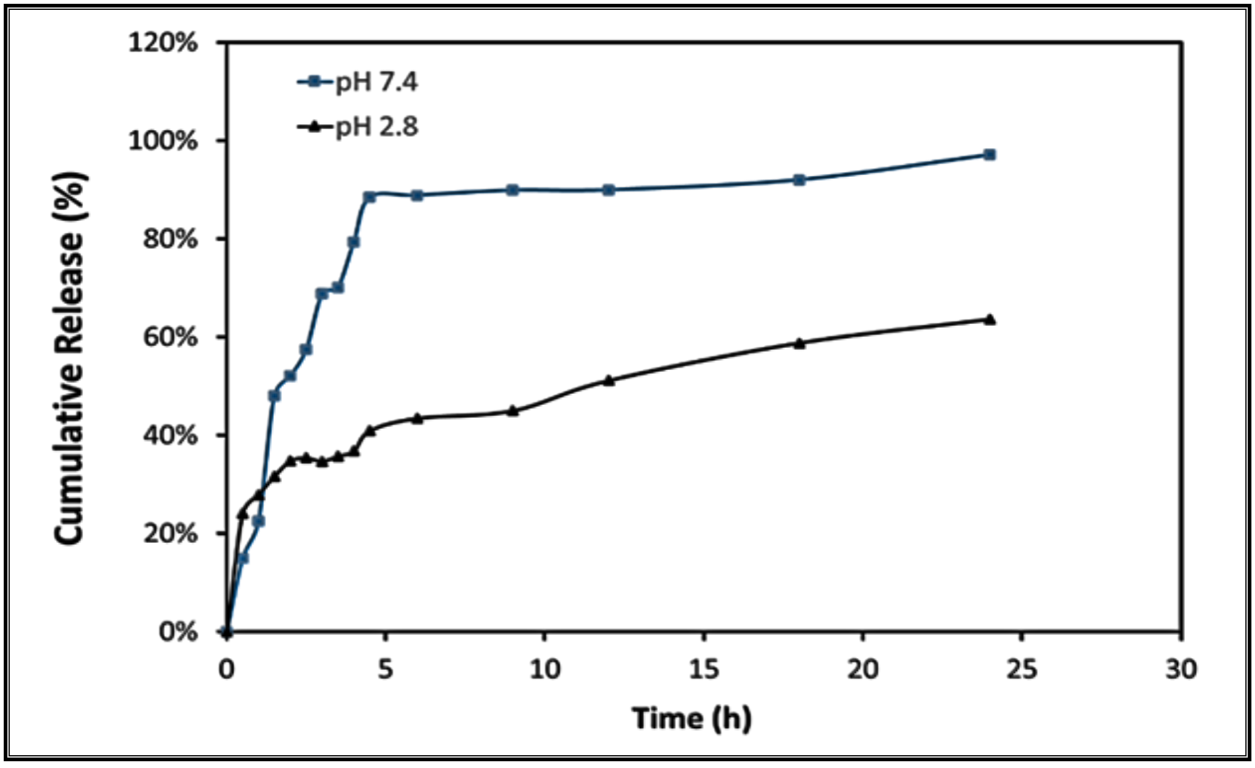

Figure (3-20) Release behavior of TMZ loaded onto nanostructures at pH 7.4 (blue) and pH 2.8 (black).

On the other hand, at pH 2.8 the total amount of TMZ released over 24 h was only 64%. An 'eruption' release of up to 25% was seen in the first 30 minutes at both pH 7.4 and 2.8, which can be attributed to the physisorption of TMZ onto the dispersed POM-DA nanostructure powder. Compared to the pH 7.4 release profile, the amount of TMZ released at pH 2.8 in the first hour was relatively small, at up to 30%, indicating that the absorption of TMZ is favored at lower pH. Thus, it can clearly be concluded that the release behavior of TMZ from POM-DA nanostructures was pH-responsive. The above results clearly demonstrate the potential use of POM-DA nanostructures as nanocarriers for the oral delivery of TMZ in the therapy for certain cancers.

3.4.2 Release behavior of TMZ loaded onto POM-Chitosan as-prepared nanostructures

In this study, the potential of the nanostructures to act as carriers in oral drug delivery were explored by studying the loading and release behavior of TMZ in media of different pHs. Upon loading of TMZ onto the nanostructures, a color change from pale yellow to green was clearly seen, indicating the successful loading of TMZ. The amount of TMZ loaded onto the POM-chitosan nanostructures was determined via HPLC and was found to be about 21% (by weight), which represents a high loading efficiency. This could be attributed to the large relative surface area (smaller particle size compared to POM-chitosan prior to loading) of the nanostructures. The employment of pH changes within the gastrointestinal (GI) tract is one of the most interesting methods in the design of oral delivery protocols for drugs in which two pH changes are chosen, the first mimicking the acidic conditions of the stomach (pH 1–3), and the second the more basic conditions of the intestines (pH 5–8). The release profile of TMZ at pH 2.8 and pH 7.4 over 24 h, from which it can clearly be seen that release was pH dependent. As can be seen from Fig. (3-21) , at pH 7.4 the release of TMZ reaches 97% in 24 h, where in the first ten hours the amount released shows a dramatic increase, at up to 90%, which is then followed by a more sustained release over the following 14 h.

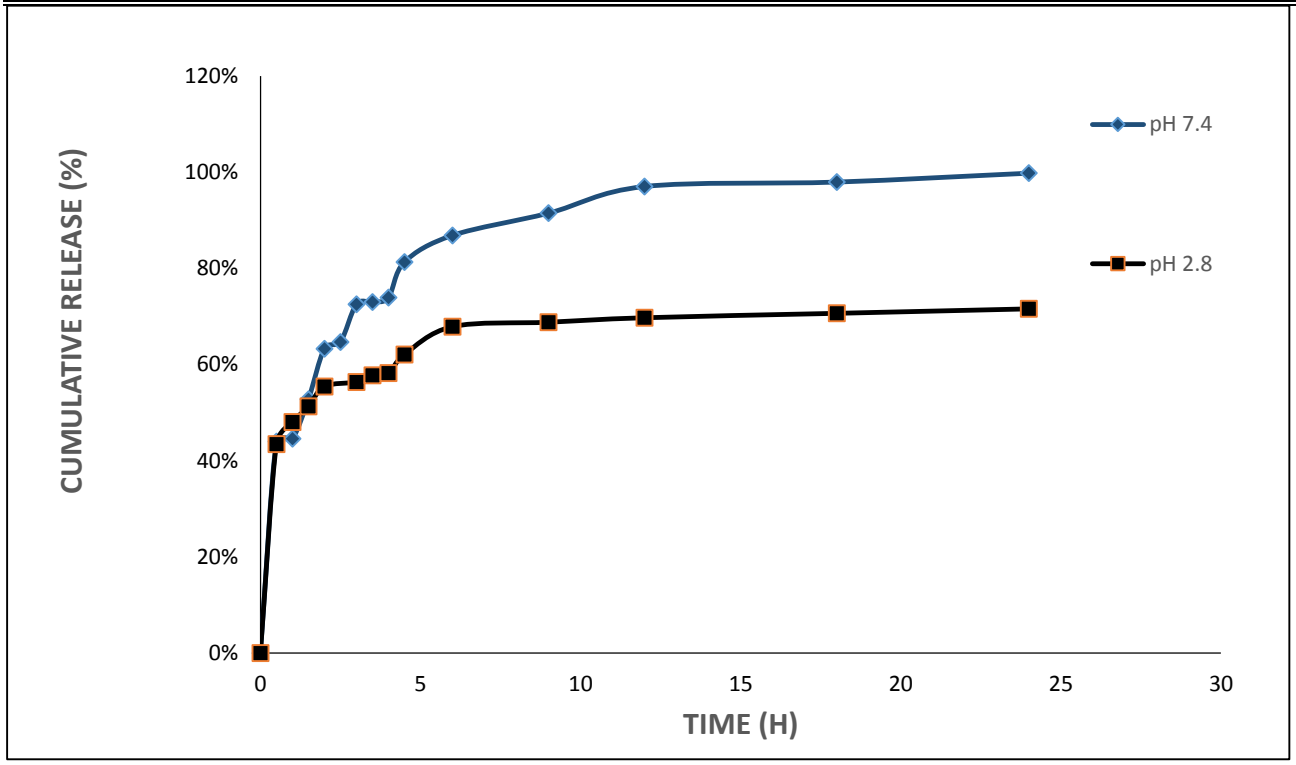

Figure (3-21) Release behavior of TMZ loaded onto nanostructures at pH 7.4 (blue) and pH 2.8 (black).

On the other hand, at pH 2.8 the total amount of TMZ released over 24 h was only 73%. An 'eruption' release of up to 45% was seen in the first 60 minutes at both pH 7.4 and 2.8, which can be attributed to the physisorption of TMZ onto the dispersed POM-chitosan nanostructure powder. Compared to the pH 7.4 release profile, the amount of TMZ released at pH 2.8 in the first four hours was relatively smaller, at up to 50%, indicating that the absorption of TMZ is favored at lower pH. Thus, it can clearly be concluded that the release behavior of TMZ from POM-Chitosan nanostructures was pH-responsive. The above results clearly demonstrate the potential use of POM-Chitosan nanostructures as nanocarriers for the oral delivery of TMZ in the therapy for certain cancers.

3.5 Conclusion

1. Nanocarriers from POM coated with dopamine and Chitosan were effectively synthesized using a self-assembly method. The primary goal is the development and innovation of these nanocarriers for oral drug delivery.
2. These nanocarriers were loaded with TMZ (Temozolomide) with a loading efficiency of 21% for POM-chitosan nano-composite and 38% for POM-DA nano-composite.
3. The nanocarriers were fully characterized using various techniques: XRD analysis provided information about the crystal structure and arrangement. FTIR analysis helped determine and confirm the chemical structure of the nanocomposite by identifying the functional groups present. XPS analysis was used to provide information about the composition of the nanocomposite by identifying the elements within. AFM provided information about the size, shape, and surface roughness of the nanocomposite. SEM analysis was used to determine the structural features and surface morphology of the nanocomposite.
4. The oral formulation of TMZ loaded into the nanocarriers exhibited pH-dependent release behavior. The release rate was faster at pH 7.4 compared to pH 2.8 in both POM-DA and POM-Chitosan nanocomposite, demonstrating the ability of the nanocarriers to control TMZ release based on pH media changes. The POM-DA nanocomposite has favorable release behavior than POM-Chitosan nanocomposite due to amount of release in POM-DA nanocomposite at pH 2.8 below 60% while the amount of release in POM-Chitosan nanocomposite at pH 2.8 about 70%. The pH-dependent release behavior of the nanocomposites makes them a promising method for oral drug delivery of TMZ.
5. The successful production and characterization of the POM-Chitosan and POM-DA nanocomposites loaded with TMZ, along with their pH-dependent release behavior, show the potential of these nanocomposites as effective carriers for oral drug delivery.
6. These results provide new possibilities for enhancing the delivery of TMZ, maximizing therapeutic efficiency, and minimizing the side effects.

3.6 Future Works

1 .Further characterization for 3D hierarchical nanostructures using various techniques such as transmission electron microscope (TEM), Zeta potentials, and Confocal laser scanning microscopy (CLSM).

2 .Preparation of 3D hierarchical nanostructures using various methodologies like the Microwave technique.

3 .Use another type of POM instead of the hexamolybedate, or another coated instead Chitosan and dopamine.

4. Using other medicines, such as (Paclitaxel, Docetaxel).

5. Assess the potential of POM-DA and POM-Chitosan nano-composite for environmental applications like water purification, heavy metal removal and pollutant degradation.

References

References

[1] S. Mohammed, H. Ali, L. Majeed, A. Muqdam, and M. Ali, "Synthesis and Investigation of Hybrid Polyoxometalate (POM)-Dopamine Nano-Structures as Drug Delivery System," 2016.

[2] J. Jeevanandam, A. Barhoum, Y. S. Chan, A. Dufresne, and M. K. Danquah, "Review on nanoparticles and nanostructured materials: History, sources, toxicity and regulations," *Beilstein J. Nanotechnol.*, vol. 9, no. 1, pp. 1050–1074, 2018, doi: 10.3762/bjnano.9.98.

[3] J. K. Patra *et al.*, "Nano based drug delivery systems: Recent developments and future prospects," *J. Nanobiotechnology*, vol. 16, no. 1, pp. 1–33, 2018, doi: 10.1186/s12951-018-0392-8.

[4] D. Lombardo, P. Calandra, L. Pasqua, and S. Magazù, "Self-assembly of organic nanomaterials and biomaterials: The bottom-up approach for functional nanostructures formation and advanced applications," *Materials (Basel).*, vol. 13, no. 5, 2020, doi: 10.3390/ma13051048.

[5] Y. Gong *et al.*, "Fabrication of pH-and temperature-directed supramolecular materials from 1D fibers to exclusively 2D planar structures using an ionic self-assembly approach," *J. Mater. Chem. C*, vol. 3, no. 14, pp. 3273–3279, 2015.

[6] D. C. Ferreira Soares, S. C. Domingues, D. B. Viana, and M. L. Tebaldi, "Polymer-hybrid nanoparticles: Current advances in biomedical applications," *Biomed. Pharmacother.*, vol. 131, no. August, p. 110695, 2020, doi: 10.1016/j.biopha.2020.110695.

[7] I. Khan, K. Saeed, and I. Khan, "Nanoparticles: Properties, applications and toxicities," *Arab. J. Chem.*, vol. 12, no. 7, pp. 908–931, 2019, doi: 10.1016/j.arabjc.2017.05.011.

[8] S. Sim and N. K. Wong, "Nanotechnology and its use in imaging and drug delivery (Review)," *Biomed. Reports*, vol. 14, no. 5, 2021, doi: 10.3892/br.2021.1418.

[9] D. A. Newfang, G. T. Johnson, and R. D. Harbison, "Nanoparticles," *Hamilt. Hardy's Ind. Toxicol. Sixth Ed.*, vol. 5, no. June, pp. 1025–1028, 2015, doi: 10.1002/9781118834015.ch97.

[10] M. Ghorbanpour, K. Manika, and A. Varma, *Nanoscience and plant-soil systems*. Springer, 2017.

[11] J. K. Patel, D. J. Patel, and V. M. Pandya, "An Overview: Nanoparticles," *Int. J. Pharm. Sci. Nanotechnol.*, vol. 1, no. 3, pp. 215–220, 1970, doi: 10.37285/ijpsn.2008.1.3.3.

[12] E. V. Balaji and A. T. Selvan, "Nanopharmacology: A Novel Approach in Therapeutics," *Asian J. Res. Pharm. Sci.*, vol. 9, no. 1, p. 9, 2019, doi: 10.5958/2231-5659.2019.00003.1.

[13] S. A. Özkan, A. Dedeoğlu, N. Karadaş Bakirhan, and Y. Özkan, "Nanocarriers used most in drug delivery and drug release: Nanohydrogel, chitosan, graphene, and solid lipid," *Turkish J. Pharm. Sci.*, vol. 16, no. 4, pp. 481–492, 2019, doi: 10.4274/tjps.galenos.2019.48751.

[14] F. Allhoff, "The coming era of nanomedicine," *Am. J. Bioeth.*, vol. 9, no. 10, pp. 3–11, 2009, doi: 10.1080/15265160902985027.

[15] E. M. MODAN and A. G. PLĂIAȘU, "Advantages and Disadvantages of Chemical Methods in the Elaboration of Nanomaterials," *Ann. "Dunarea Jos" Univ. Galati. Fascicle IX, Metall. Mater. Sci.*, vol. 43, no. 1, pp. 53–60, 2020, doi: 10.35219/mms.2020.1.08.

[16] R. Thiruvengadathan, V. Korampally, A. Ghosh, N. Chanda, K. Gangopadhyay, and S. Gangopadhyay, "Nanomaterial processing using self-assembly-bottom-up chemical and biological approaches," *Reports Prog. Phys.*, vol. 76, no. 6, 2013, doi: 10.1088/0034-4885/76/6/066501.

References

[17] N. Baig, I. Kammakakam, W. Falath, and I. Kammakakam, "Nanomaterials: A review of synthesis methods, properties, recent progress, and challenges," *Mater. Adv.*, vol. 2, no. 6, pp. 1821–1871, 2021, doi: 10.1039/d0ma00807a.

[18] S. Zeghoud, D. Chandran, I. Ben Amor, H. Hemmami, P. Mohankumar, and T. Bin Emran, "Nanotechnology and nanomaterials in the treatment and diagnosis of cancer: Correspondence," *Ann. Med. Surg.*, vol. 85, no. 5, pp. 2258–2260, 2023, doi: 10.1097/ms9.0000000000000677.

[19] R. K. Thapa and J. O. Kim, "Nanomedicine-based commercial formulations: current developments and future prospects," *J. Pharm. Investig.*, vol. 53, no. 1, pp. 19–33, 2023, doi: 10.1007/s40005-022-00607-6.

[20] H. H. Hakimovich, "American Journal of Technology and Applied Sciences NANOTECHNOLOGY ADVANCEMENTS : FROM MATERIALS American Journal of Technology and Applied Sciences," vol. 14, pp. 16–20, 2023.

[21] M. Doroudian, R. MacLoughlin, F. Poynton, A. Prina-Mello, and S. C. Donnelly, "Nanotechnology based therapeutics for lung disease," *Thorax*, vol. 74, no. 10, pp. 965–976, 2019, doi: 10.1136/thoraxjnl-2019-213037.

[22] F. U. Din *et al.*, "Effective use of nanocarriers as drug delivery systems for the treatment of selected tumors," *Int. J. Nanomedicine*, vol. 12, pp. 7291–7309, 2017, doi: 10.2147/IJN.S146315.

[23] V. Chandrakala, V. Aruna, and G. Angajala, "Review on metal nanoparticles as nanocarriers: current challenges and perspectives in drug delivery systems," *Emergent Mater.*, vol. 5, no. 6, pp. 1593–1615, 2022, doi: 10.1007/s42247-021-00335-x.

[24] V. Bhardwaj, A. Kaushik, Z. M. Khatib, M. Nair, and A. J. McGoron, "Recalcitrant issues and new frontiers in nano-pharmacology," *Front. Pharmacol.*, vol. 10, no. November, pp. 1–9, 2019, doi: 10.3389/fphar.2019.01369.

[25] S. Z. Alshawwa, A. A. Kassem, R. M. Farid, S. K. Mostafa, and G. S. Labib, "Nanocarrier Drug Delivery Systems: Characterization, Limitations, Future Perspectives and Implementation of Artificial Intelligence," *Pharmaceutics*, vol. 14, no. 4, 2022, doi: 10.3390/pharmaceutics14040883.

[26] W. Zhao, Y. Zhao, Q. Wang, T. Liu, J. Sun, and R. Zhang, "Remote Light-Responsive Nanocarriers for Controlled Drug Delivery: Advances and Perspectives," *Small*, vol. 15, no. 45, pp. 1–34, 2019, doi: 10.1002/smll.201903060.

[27] S. Dünnhaupt, O. Kammona, C. Waldner, C. Kiparissides, and A. Bernkop-Schnürch, "Nano-carrier systems: Strategies to overcome the mucus gel barrier," *Eur. J. Pharm. Biopharm.*, vol. 96, pp. 447–453, 2015, doi: 10.1016/j.ejpb.2015.01.022.

[28] B. Kumar, K. Jalodia, P. Kumar, and H. K. Gautam, "Recent advances in nanoparticle-mediated drug delivery," *J. Drug Deliv. Sci. Technol.*, vol. 41, pp. 260–268, 2017.

[29] A. Maroni, A. Melocchi, L. Zema, A. Foppoli, and A. Gazzaniga, "Retentive drug delivery systems based on shape memory materials," *J. Appl. Polym. Sci.*, vol. 137, no. 25, pp. 1–10, 2020, doi: 10.1002/app.48798.

[30] A. Haleem, M. Javaid, R. P. Singh, S. Rab, and R. Suman, "Applications of nanotechnology in medical field: a brief review," *Glob. Heal. J.*, vol. 7, no. 2, pp. 70–77, 2023, doi: 10.1016/j.glohj.2023.02.008.

[31] B. K. Lee, Y. H. Yun, and K. Park, "Smart nanoparticles for drug delivery: Boundaries and opportunities," *Chem. Eng. Sci.*, vol. 125, pp. 158–164, 2015.

[32] D. Ramadon, M. T. C. McCrudden, A. J. Courtenay, and R. F. Donnelly, "Enhancement strategies for transdermal drug delivery systems: current trends and applications," *Drug Deliv. Transl. Res.*, vol. 12, no. 4, pp. 758–791, 2022, doi: 10.1007/s13346-021-00909-6.

[33] A. Mansour, M. Romani, A. B. Acharya, B. Rahman, E. Verron, and Z. Badran, "Drug Delivery Systems in Regenerative Medicine: An Updated Review," *Pharmaceutics*, vol. 15, no. 2, pp. 1–23, 2023, doi: 10.3390/pharmaceutics15020695.

[34] C. Li *et al.*, "Recent progress in drug delivery," *Acta Pharm. Sin. B*, vol. 9, no. 6, pp. 1145–1162, 2019, doi: 10.1016/j.apsb.2019.08.003.

[35] A. Tewabe, A. Abate, M. Tamrie, A. Seyfu, and E. A. Siraj, "Targeted drug delivery — from magic bullet to nanomedicine: Principles, challenges, and future perspectives," *J. Multidiscip. Healthc.*, vol. 14, no. July, pp. 1711–1724, 2021, doi: 10.2147/JMDH.S313968.

[36] S. Bhattacharya, P. Rodriques, and B. Prajapati, "Introductory Chapter: Advanced Drug Delivery Systems," in *Advanced Drug Delivery Systems*, IntechOpen, 2023.

[37] D. Paolino, P. Sinha, M. Fresta, and M. Ferrari, "Drug delivery systems," *Encycl. Med. devices Instrum.*, 2006.

[38] B. P. Panda, R. Krishnamoorthy, S. K. Bhattamisra, N. K. H. Shivashekaregowda, L. Bin Seng, and S. Patnaik, "Fabrication of second generation smarter PLGA based nanocrystal carriers for improvement of drug delivery and therapeutic efficacy of gliclazide in type-2 diabetes rat model," *Sci. Rep.*, vol. 9, no. 1, p. 17331, 2019.

[39] H. Park, A. Otte, and K. Park, "Evolution of drug delivery systems: From 1950 to 2020 and beyond," *J. Control. Release*, vol. 342, no. November 2021, pp. 53–65, 2022, doi: 10.1016/j.jconrel.2021.12.030.

[40] Y. H. Yun, B. K. Lee, and K. Park, "Controlled Drug Delivery: Historical perspective for the next generation," *J. Control. Release*, vol. 219, pp. 2–7, 2015, doi: 10.1016/j.jconrel.2015.10.005.

[41] Y. H. Bae and K. Park, "Advanced drug delivery 2020 and beyond: Perspectives on

the future," *Adv. Drug Deliv. Rev.*, vol. 158, pp. 4–16, 2020, doi: 10.1016/j.addr.2020.06.018.

[42] O. Tacar, P. Sriamornsak, and C. R. Dass, "Doxorubicin: An update on anticancer molecular action, toxicity and novel drug delivery systems," *J. Pharm. Pharmacol.*, vol. 65, no. 2, pp. 157–170, 2013, doi: 10.1111/j.2042-7158.2012.01567.x.

[43] S. Sur, A. Rathore, V. Dave, K. R. Reddy, R. S. Chouhan, and V. Sadhu, "Recent developments in functionalized polymer nanoparticles for efficient drug delivery system," *Nano-Structures and Nano-Objects*, vol. 20, 2019, doi: 10.1016/j.nanoso.2019.100397.

[44] Y. K. Sung and S. W. Kim, "Recent advances in polymeric drug delivery systems," *Biomater. Res.*, vol. 24, no. 1, p. 12, 2020.

[45] M. Farzan, R. Roth, J. Schoelkopf, J. Huwyler, and M. Puchkov, "The processes behind drug loading and release in porous drug delivery systems," *Eur. J. Pharm. Biopharm.*, 2023.

[46] K. C. de Castro, J. M. Costa, and M. G. N. Campos, "Drug-loaded polymeric nanoparticles: a review," *Int. J. Polym. Mater. Polym. Biomater.*, vol. 71, no. 1, pp. 1–13, 2022, doi: 10.1080/00914037.2020.1798436.

[47] A. L. Ruiz, A. Ramirez, and K. McEnnis, "Single and Multiple Stimuli-Responsive Polymer Particles for Controlled Drug Delivery," *Pharmaceutics*, vol. 14, no. 2, 2022, doi: 10.3390/pharmaceutics14020421.

[48] N. Kamaly, B. Yameen, J. Wu, and O. C. Farokhzad, "Degradable controlled-release polymers and polymeric nanoparticles: Mechanisms of controlling drug release," *Chem. Rev.*, vol. 116, no. 4, pp. 2602–2663, 2016, doi: 10.1021/acs.chemrev.5b00346.

[49] F. Directions, "Controlled Drug Delivery Systems : Current Status and," *Molecules*,

vol. 26, p. 5905, 2021.

[50] A. J. Gavasane, "Synthetic Biodegradable Polymers Used in Controlled Drug Delivery System: An Overview," *Clin. Pharmacol. Biopharm.*, vol. 3, no. 2, 2014, doi: 10.4172/2167-065x.1000121.

[51] Z. Hami, "A brief review on advantages of nano-based drug delivery systems," *Ann. Mil. Heal. Sci. Res.*, vol. 19, no. 1, 2021.

[52] T. H. Baryakova, B. H. Pogostin, R. Langer, and K. J. McHugh, "Overcoming barriers to patient adherence: the case for developing innovative drug delivery systems," *Nat. Rev. Drug Discov.*, vol. 22, no. 5, pp. 387–409, 2023.

[53] M. Sowjanya, S. Debnath, P. Lavanya, R. Thejovathi, and M. N. Babu, "Polymers used in the Designing of Controlled Drug Delivery System," *Res. J. Pharm. Technol.*, vol. 10, no. 3, p. 903, 2017, doi: 10.5958/0974-360x.2017.00168.8.

[54] Y. Cui, H. Zhu, J. Cai, and H. Qiu, "Self-regulated co-assembly of soft and hard nanoparticles," *Nat. Commun.*, vol. 12, no. 1, pp. 1–7, 2021, doi: 10.1038/s41467-021-25995-5.

[55] L. T. Varma *et al.*, "Recent Advances in Self-Assembled Nanoparticles for Drug Delivery," *Curr. Drug Deliv.*, vol. 17, no. 4, pp. 279–291, 2020, doi: 10.2174/1567201817666200210122340.

[56] J. Pan and Z. Cui, "Self-Assembled Nanoparticles: Exciting Platforms for Vaccination," *Biotechnol. J.*, vol. 15, no. 12, pp. 1–14, 2020, doi: 10.1002/biot.202000087.

[57] D. Fujita *et al.*, "Self-Assembly of M30L60 Icosidodecahedron," *Chem*, vol. 1, no. 1, pp. 91–101, 2016, doi: 10.1016/j.chempr.2016.06.007.

[58] J. P. Quiñones, H. Peniche, and C. Peniche, "Chitosan based self-assembled nanoparticles in drug delivery," *Polymers (Basel).*, vol. 10, no. 3, pp. 1–32, 2018,

doi: 10.3390/polym10030235.

[59] S. Yadav, A. K. Sharma, and P. Kumar, "Nanoscale Self-Assembly for Therapeutic Delivery," *Front. Bioeng. Biotechnol.*, vol. 8, no. February, pp. 1–24, 2020, doi: 10.3389/fbioe.2020.00127.

[60] E. V. Amadi and A. Venkataraman, "Nanoscale self-assembly : concepts , applications and challenges," 2022.

[61] H. T. Feng, J. W. Y. Lam, and B. Z. Tang, "Self-assembly of AIEgens," *Coord. Chem. Rev.*, vol. 406, p. 213142, 2020, doi: 10.1016/j.ccr.2019.213142.

[62] H. Zhang, L. Y. Guo, J. Jiao, X. Xin, D. Sun, and S. Yuan, *Ionic self-assembly of polyoxometalate-dopamine hybrid nanoflowers with excellent catalytic activity for dyes*, vol. 5, no. 2. 2017. doi: 10.1021/acssuschemeng.6b01805.

[63] Y. F. Song and R. Tsunashima, "Recent advances on polyoxometalate-based molecular and composite materials," *Chem. Soc. Rev.*, vol. 41, no. 22, pp. 7384–7402, 2012, doi: 10.1039/c2cs35143a.

[64] N. I. Gumerova and A. Rompel, "Synthesis, structures and applications of electron-rich polyoxometalates," *Nat. Rev. Chem.*, vol. 2, no. 2, 2018, doi: 10.1038/s41570-018-0112.

[65] J. M. Cameron, D. J. Wales, and G. N. Newton, "Shining a light on the photo-sensitisation of organic-inorganic hybrid polyoxometalates," *Dalt. Trans.*, vol. 47, no. 15, pp. 5120–5136, 2018, doi: 10.1039/c8dt00400e.

[66] G. Geisberger, S. Paulus, E. B. Gyenge, C. Maake, and G. R. Patzke, "Targeted delivery of polyoxometalate nanocomposites," *Small*, vol. 7, no. 19, pp. 2808–2814, 2011, doi: 10.1002/smll.201101264.

[67] T. M. Authier, "Applications of Polyoxometalates in Medicine and their Putative Mechanisms of Action," pp. 1–35, 2015.

[68] G. Fiorani *et al.*, "Chitosan-Polyoxometalate Nanocomposites: Synthesis, Characterization and Application as Antimicrobial Agents," *J. Clust. Sci.*, vol. 25, no. 3, pp. 839–854, 2014, doi: 10.1007/s10876-013-0685-x.

[69] A. Al-Yasari, H. F. Alesary, H. Alghurabi, M. M. M. Ali Alali, L. M. Ahmed, and R. Alasadi, "Methotrexate pH-responsive release from nanostructures of dopamine and polyoxometalate," *Biochem. Cell. Arch.*, vol. 19, no. 2, pp. 3675–3680, 2019, doi: 10.35124/bca.2019.19.2.3675.

[70] L. Fu *et al.*, "Polyoxometalate-Based Organic-Inorganic Hybrids as Antitumor Drugs," *Small*, vol. 11, no. 24, pp. 2938–2945, 2015, doi: 10.1002/smll.201500232.

[71] S. K. Petrovskii, E. V Grachova, and K. Y. Monakhov, "Bioorthogonal chemistry of polyoxometalates–challenges and prospects," *Chem. Sci.*, 2024.

[72] O. S. Panteleieva *et al.*, "Anion-π stacks of Lindqvist superoctahedra [Mo6O19] 2− supported by caffeinium and theophyllinium cations," *Inorganica Chim. Acta*, vol. 537, p. 120945, 2022.

[73] X. Su, Y. Wei, N. Ma, H. Zhang, and L. Yan, "Theoretical insight into oxidation of anilines to azobenzenes catalyzed by hexamolybdate: outer-sphere electron and proton transfer," *J. Phys. Chem. C*, vol. 127, no. 8, pp. 4124–4131, 2023.

[74] R. Tajgardoon, A. Zarnegaryan, and D. Elhamifar, "A Lindqvist type hexamolybdate [Mo6O19]-modified graphene oxide hybrid catalyst: Highly efficient for the synthesis of benzimidazoles," *J. Photochem. Photobiol. A Chem.*, vol. 430, p. 113960, 2022.

[75] C. Wang, C.-Y. Zhu, M. Zhang, Y. Geng, Y.-G. Li, and Z.-M. Su, "An intriguing window opened by a metallic two-dimensional Lindqvist-cobaltporphyrin organic framework as an electrochemical catalyst for the CO 2 reduction reaction," *J. Mater. Chem. A*, vol. 8, no. 29, pp. 14807–14814, 2020.

[76] A. V. Anyushin, A. Kondinski, and T. N. Parac-Vogt, "Hybrid polyoxometalates as post-functionalization platforms: From fundamentals to emerging applications," *Chem. Soc. Rev.*, vol. 49, no. 2, pp. 382–432, 2020, doi: 10.1039/c8cs00854j.

[77] H. Li *et al.*, "Self-assembly of hierarchical nanostructures from dopamine and polyoxometalate for oral drug delivery," *Chem. - A Eur. J.*, vol. 20, no. 2, pp. 499–504, 2014, doi: 10.1002/chem.201302660.

[78] Y. Feng *et al.*, "Fabrication and characterization of multilayer films based on Keggin-type polyoxometalate and chitosan," *Mater. Lett.*, vol. 60, no. 13–14, pp. 1588–1593, 2006, doi: 10.1016/j.matlet.2005.11.069.

[79] S. Latif *et al.*, "Dopamine in Parkinson's disease," *Clin. Chim. acta*, vol. 522, pp. 114–126, 2021.

[80] M. R. Post and D. Sulzer, "The chemical tools for imaging dopamine release," *Cell Chem. Biol.*, vol. 28, no. 6, pp. 748–764, 2021, doi: 10.1016/j.chembiol.2021.04.005.

[81] R. Franco, I. Reyes-Resina, and G. Navarro, "Dopamine in health and disease: Much more than a neurotransmitter," *Biomedicines*, vol. 9, no. 2, pp. 1–13, 2021, doi: 10.3390/biomedicines9020109.

[82] J. Liebscher, "Chemistry of Polydopamine – Scope, Variation, and Limitation," *European J. Org. Chem.*, vol. 2019, no. 31–32, pp. 4976–4994, 2019, doi: 10.1002/ejoc.201900445.

[83] S. Lakard, I. A. Pavel, and B. Lakard, "Electrochemical biosensing of dopamine neurotransmitter: A review," *Biosensors*, vol. 11, no. 6, 2021, doi: 10.3390/bios11060179.

[84] R. Cools, "Chemistry of the Adaptive Mind: Lessons from Dopamine," *Neuron*, vol. 104, no. 1, pp. 113–131, 2019, doi: 10.1016/j.neuron.2019.09.035.

[85] X. Tan *et al.*, "Poly-dopamine, poly-levodopa, and poly-norepinephrine coatings: Comparison of physico-chemical and biological properties with focus on the application for blood-contacting devices," *Bioact. Mater.*, vol. 6, no. 1, pp. 285–296, 2021.

[86] Z. Khan, R. Shanker, D. Um, A. Jaiswal, and H. Ko, "Bioinspired Polydopamine and Composites for Biomedical Applications," *Electr. Conduct. Polym. Polym. Compos.*, pp. 1–29, 2018, doi: 10.1002/9783527807918.ch1.

[87] N. A. Negm, H. H. H. Hefni, A. A. A. Abd-Elaal, E. A. Badr, and M. T. H. Abou Kana, "Advancement on modification of chitosan biopolymer and its potential applications," *Int. J. Biol. Macromol.*, vol. 152, pp. 681–702, 2020, doi: 10.1016/j.ijbiomac.2020.02.196.

[88] S. (Gabriel) Kou, L. M. Peters, and M. R. Mucalo, *Chitosan: A review of sources and preparation methods*, vol. 169. 2021. doi: 10.1016/j.ijbiomac.2020.12.005.

[89] W. Wang *et al.*, "Molecular Sciences Chitosan Derivatives and Their Application in Biomedicine," *Int J Mol Sci*, vol. 21, p. 487, 2020, [Online]. Available: www.mdpi.com/journal/ijms

[90] I. Aranaz *et al.*, "Chitosan: An overview of its properties and applications," *Polymers (Basel).*, vol. 13, no. 19, 2021, doi: 10.3390/polym13193256.

[91] G. Cavallaro, S. Micciulla, L. Chiappisi, and G. Lazzara, "Chitosan-based smart hybrid materials: A physico-chemical perspective," *J. Mater. Chem. B*, vol. 9, no. 3, pp. 594–611, 2021.

[92] A. Ali and S. Ahmed, "A review on chitosan and its nanocomposites in drug delivery," *Int. J. Biol. Macromol.*, vol. 109, pp. 273–286, 2018, doi: 10.1016/j.ijbiomac.2017.12.078.

[93] S. Begum, N. Y. Yuhana, N. Md Saleh, N. H. N. Kamarudin, and A. B. Sulong,

"Review of chitosan composite as a heavy metal adsorbent: Material preparation and properties," *Carbohydr. Polym.*, vol. 259, no. January, p. 117613, 2021, doi: 10.1016/j.carbpol.2021.117613.

[94] M. Azmana, S. Mahmood, A. R. Hilles, A. Rahman, M. A. Bin Arifin, and S. Ahmed, "A review on chitosan and chitosan-based bionanocomposites: Promising material for combatting global issues and its applications," *Int. J. Biol. Macromol.*, vol. 185, no. June, pp. 832–848, 2021, doi: 10.1016/j.ijbiomac.2021.07.023.

[95] R. Stupp, M. Gander, S. Leyvraz, and E. Newlands, "Current and future developments in the use of temozolomide for the treatment of brain tumours," *Lancet Oncol.*, vol. 2, no. 9, pp. 552–560, 2001, doi: 10.1016/S1470-2045(01)00489-2.

[96] J. R. Wesolowski, P. Rajdev, and S. K. Mukherji, "Temozolomide (Temodar)," *Am. J. Neuroradiol.*, vol. 31, no. 8, pp. 1383–1384, 2010, doi: 10.3174/ajnr.A2170.

[97] Ł. Jedynak, M. Puchalska, M. Zezula, M. Łaszcz, W. Łuniewski, and J. Zagrodzka, "Stability of sample solution as a crucial point during HPLC determination of chemical purity of temozolomide drug substance," *J. Pharm. Biomed. Anal.*, vol. 83, pp. 19–27, 2013, doi: 10.1016/j.jpba.2013.04.032.

[98] A. Khan, S. S. Imam, M. Aqil, Y. Sultana, A. Ali, and K. Khan, "Design of experiment based validated stability indicating RP-HPLC method of temozolomide in bulk and pharmaceutical dosage forms," *Beni-Suef Univ. J. Basic Appl. Sci.*, vol. 5, no. 4, pp. 402–408, 2016, doi: 10.1016/j.bjbas.2015.11.011.

[99] A. Thomas, M. Tanaka, J. Trepel, W. C. Reinhold, V. N. Rajapakse, and Y. Pommier, "Temozolomide in the era of precision medicine," *Cancer Res.*, vol. 77, no. 4, pp. 823–826, 2017, doi: 10.1158/0008-5472.CAN-16-2983.

[100] J. Zhang, M. F.G. Stevens, and T. D. Bradshaw, "Temozolomide: Mechanisms of Action, Repair and Resistance," *Curr. Mol. Pharmacol.*, vol. 5, no. 1, pp. 102–114,

2011, doi: 10.2174/1874467211205010102.

[101] K. M. Hotchkiss and J. H. Sampson, "Temozolomide treatment outcomes and immunotherapy efficacy in brain tumor," *J. Neurooncol.*, vol. 151, no. 1, pp. 55–62, 2021, doi: 10.1007/s11060-020-03598-2.

[102] J. A. P. Dutra, M. T. Luiz, A. G. Tavares Junior, L. D. Di Filippo, S. G. Carvalho, and M. Chorilli, "Temozolomide: An overview of biological properties, drug delivery nanosystems, and analytical methods," *Curr. Pharm. Des.*, vol. 28, no. 25, pp. 2073–2088, 2022.

[103] P. Purification, *Protein purification: principles, high-resolution methods, and applications*, vol. 36, no. 01. 1998. doi: 10.5860/choice.36-0330.

[104] O. Coskun, "Separation Tecniques: CHROMATOGRAPHY," *North. Clin. Istanbul*, vol. 3, no. 2, pp. 156–160, 2016, doi: 10.14744/nci.2016.32757.

[105] A. Ahmad Dar, P. L. Sangwan, and A. Kumar, *Chromatography: An important tool for drug discovery*, vol. 43, no. 1. 2020. doi: 10.1002/jssc.201900656.

[106] R. Basharat *et al.*, "Ultra Performance Liquid Chromatography (Mini-Review).," *Orient. J. Chem.*, vol. 37, no. 4, 2021.

[107] M. M. Abdulbari and I. M. Sh, "Simultaneous determination and validation of Chlorpheniramine Maleate, Acetaminophen, Phenylpropanolamine Hydrochloride and Caffeine in tablet dosage form by using reverse phase high performance liquid chromatography (RP-HPLC)," *Int. J. Pharm. Pharm. Sci.*, vol. 5, no. SUPPL 3, pp. 666–670, 2013.

[108] M. Wan *et al.*, "Preparation and performance of a poly (ethyleneimine) embedded N-acetyl-L-phenylalanine mixed-mode stationary phase for HPLC," *Microchem. J.*, vol. 157, p. 105021, 2020.

[109] V. David, S. C. Moldoveanu, and T. Galaon, "Derivatization procedures and their

analytical performances for HPLC determination in bioanalysis," *Biomed. Chromatogr.*, vol. 35, no. 1, p. e5008, 2021.

[110] A. H. Ali, "High-performance liquid chromatography (HPLC): a review," *Ann. Adv. Chem*, vol. 6, pp. 10–20, 2022.

[111] J. F. F. Anderson *et al.*, "Development and validation of an isocratic HPLC method for simultaneous determination of quaternary mixtures of antihypertensive drugs in pharmaceutical formulations," *Acta Chromatogr.*, vol. 29, no. 1, pp. 95–110, 2017, doi: 10.1556/1326.2017.29.1.9.

[112] T. J. Wenzel, "Douglas A. Skoog, Donald M. West, F. James Holler, and Stanley R. Crouch: Fundamentals of analytical chemistry, international ed." Springer, 2013.

[113] A. Kounnoun *et al.*, "Development of a new HPLC method for rapid histamine quantification in fish and fishery products without sample clean-up," *Eur. Food Res. Technol.*, vol. 248, no. 6, pp. 1679–1689, 2022.

[114] G. Campmajó, R. Saez-Vigo, J. Saurina, and O. Núñez, "High-performance liquid chromatography with fluorescence detection fingerprinting combined with chemometrics for nut classification and the detection and quantitation of almond-based product adulterations," *Food Control*, vol. 114, p. 107265, 2020.

[115] T. Revision, "Stock Solution," no. 314, p. 8778, 2015.

[116] S. M. Hussein, M. M. M. A. A. Ali, and L. M. Ahmed, "Hybrid phosphotungstic acid -dopamine (PTA-DA) like-flower nanostructure synthesis as a furosemide drug delivery system and kinetic study of drug releasing," *Egypt. J. Chem.*, vol. 64, no. 10, pp. 5547–5553, 2021, doi: 10.21608/ejchem.2021.75210.3692.

[117] M. K. Jalil and A. I. Mohammed, "Synthesis of Hybrid Organic-Inorganic Polyoxometalates- based Materials for Optoelectronic Applications," 2023.

[118] C. Platelet and R. P. Stem, "Characterization and Formulation of the Bivalve

Anodonta ’ s Composite Scaffold,” vol. 8, no. 6, pp. 718–724, 2015.

[119] H. A. Ahad, C. Haranath, K. Tarun, S. Rao, D. Rahul, and P. S. Raghav, “TEMOZOLOMIDE AFLOAT MICROSPHERES FOR CARCINOMA OF THE BRAIN: FABRICATION AND CHARACTERIZATION”.

[120] H. Zhang, L.-Y. Guo, J. Jiao, X. Xin, D. Sun, and S. Yuan, “Ionic self-assembly of polyoxometalate–dopamine hybrid nanoflowers with excellent catalytic activity for dyes,” *ACS Sustain. Chem. Eng.*, vol. 5, no. 2, pp. 1358–1367, 2017.

[121] S. M. H. Ali, M. M. M. A. Alali, and L. M. Ahmed, “Flower-like hierarchical nanostructures synthesis of polyoxometalate-dopamine and loading furosemide on its surface and aging them using microwave technique,” *AIP Conf. Proc.*, vol. 2547, no. December 2022, 2022, doi: 10.1063/5.0113440.

الخلاصة

في العقود الأخيرة، تم تحقيق تقدم كبير في مجال توصيل الأدوية من خلال إنشاء مركبات إطلاق خاضعة للرقابة، مما أدى إلى تقدم طبي كبير. لقد حظيت الهياكل النانوية باهتمام كبير نظرًا لخصائصها المميزة وامكانية استخدامها في مجالات واسعة. ان إحدى هذه الفئات من الهياكل النانوية هي بولي أوكسوميتالات (POMs)، وهي عبارة عن مجموعات نانوية أنيونية سالبة الشحنة تتكون من ذرات المعدن والأكسجين. تتميز هذه POMs بإمكانية التحكم بها بدقة من حيث الحجم والشكل. تساهم هذه الخصائص، جنبًا إلى جنب مع شحنتها السالبة، في استقرارها مما يجعلها هياكل متعددة الاستخدامات. تناولت هذه الدراسة التجميع الذاتي للمركبات النانوية الهجينة العضوية وغير العضوية باستخدام بولي أوكسوميتالات (POM) (هيكساموليبدات) من نوع ليندكفيست مع الدوبامين / الكيتوسان لتكوين هياكل نانوية ثلاثية الأبعاد جديدة. تم بعد ذلك فحص هذه المركبات النانوية للتأكد من ملاءمتها كحاملات نانوية للعلاج الكيميائي التيموزولومايد TMZ. تمت دراسة إطلاق TMZ من الناقل النانوي في ظل ظروف مختلفة للأس الهيدروجيني.

تتكون هذه الدراسة من جزئين عمليين. يركز الجزء الأول على تصنيع الهياكل النانوية المصممة خصيصًا لتحميل دواء TMZ. تم تحديد كمية الدواء المحملة على البنية النانوية المجهزة لـ POM-Chitosan باستخدام جهاز HPLC في أوقات تحميل مختلفة. بينما الجزء الثاني من الدراسة يتضمن عملية إطلاق عقار TMZ من الهياكل النانوية. يتم فحص عملية الإطلاق هذه في وجود محلولين بقيم pH مختلفة. تشمل هذه المحاليل محلول ملحي بالفوسفات (PBS) مع درجة حموضة 7.4 وجلايسين-حمض الهيدروكلوريك مع درجة حموضة 2.8. تم تحليل خصائص السطح والحجم والتركيب الكيميائي وهوية الهياكل النانوية باستخدام تقنيات مثل HPLC وFTIR وXRD وSEMو AFMوXPS. أظهرت الناقلات النانوية سلوكًا مثيرًا للاهتمام يعتمد على الاس الهيدروجيني، مما يشير إلى إمكانية تطبيقها في أنظمة توصيل الأدوية. أخيرًا، أظهرت هذه الدراسة نجاحا في تحضير ناقلات نانوية جديدة من الدوبامين/الكيتوسان وPOM محملة بـ TMZ عبر التجميع الذاتي كوسيلة لتوصيل الدواء عن طريق الفم.

جامعة كربلاء

كلية العلوم

قسم الكيمياء

كيتوسان و دوبامين / هكسامولبيدات كتراكيب نانوية جديدة كأنظمة توصيل دوائي

رسالة مقدمة الى

مجلس كلية العلوم- جامعة كربلاء

وهي جزء من متطلبات نيل درجة الماجستير في علوم الكيمياء

كتبت بواسطة

مريم راضي كاظم

بكلوريوس علوم كيمياء (2017) / جامعة كربلاء

بأشراف

أ.م.د. احمد هادي عبد الأمير

أ.م.د. احسان مهدي شهيد

يوليو 2024 م **محرم 1446 هـ**